January 2015

# Analysis of Carbon Policies for Electricity Networks with High Penetration of Green Generation

Felipe Feijoo
*University of South Florida*, felipefeijoo@gmail.com

# Analysis of Carbon Policies for Electricity Networks with High Penetration of Green Generation

by

Felipe A. Feijoo

A dissertation submitted in partial fulfillment
of the requirements for the degree of
Doctor of Philosophy
Department of Industrial and Management Systems Engineering
College of Engineering
University of South Florida

Major Professor: Tapas K. Das, Ph.D.
Alex Savachkin, Ph.D.
Bo Zeng, Ph.D.
Lingling Fan, Ph.D.
Andrei Barbos, Ph.D.

Date of Approval:
June 20, 2015

Keywords: Bi-level programming, Pareto Analysis, cap-and-trade, smartgrids, microgrids

## Dedication

To all of you that have supported and helped me in my life. To my family and friends.

## Acknowledgment

I want to acknowledge my mentor, Dr. Tapas K. Das, for his continuous support, guidance, and friendship. Also, I want to recognize Dr. Jaime Bustos, who inspired me to pursue this extraordinary experience. Finally, I want to acknowledge the significant contribution of my doctoral committee.

## Table of Contents

## List of Tables

## List of Figures

## Abstract

In recent decades, climate change has become one of the most crucial challenges for humanity. Climate change has a direct correlation with global warming, caused mainly by the green house gas emissions (GHG). The Environmental Protection Agency in the U.S. (EPA) attributes carbon dioxide to account for approximately 82% of the GHG emissions. Unfortunately, the energy sector is the main producer of carbon dioxide, with China and the U.S. as the highest emitters. Therefore, there is a strong (positive) correlation between energy production, global warming, and climate change. Stringent carbon emissions reduction targets have been established in order to reduce the impacts of GHG. Achieving these emissions reduction goals will require implementation of policies like as cap-and-trade and carbon taxes, together with transformation of the electricity grid into a smarter system with high green energy penetration. However, the consideration of policies solely in view of carbon emissions reduction may adversely impact other market outcomes such as electricity prices and consumption.

In this dissertation, a two-layer mathematical-statistical framework is presented, that serves to develop carbon policies to reduce emissions level while minimizing the negative impacts on other market outcomes. The bottom layer of the two layer model comprises a bi-level optimization problem. The top layer comprises a statistical model and a Pareto analysis. Two related but different problems are studied under this methodology. The first problem looks into the design of cap-and-trade policies for deregulated electricity markets that satisfy the interest of different market constituents. Via the second problem, it is demonstrated how the framework can be used to obtain levels of carbon emissions reduction while minimizing the negative impact on electricity demand and maximizing green penetration from microgrids. In the aforementioned

studies, forecasts for electricity prices and production cost are considered. This, this dissertation also presents anew forecast model that can be easily integrated in the two-layer framework.

It is demonstrated in this dissertation that the proposed framework can be utilized by policy-makers, power companies, consumers, and market regulators in developing emissions policy decisions, bidding strategies, market regulations, and electricity dispatch strategies.

# Chapter 1: Introduction

Greenhouse gas emissions (GHG) are the major contributor to the current global warming. There are numerous examples of the negative effects of the increasing worldwide temperature. For instance, the northern region of Chile, known for being the driest place in the world, suffered heavy floods during the dry season in 2015, a phenomena extremely rare in the region. Other examples of global warming include the raising of sea levels, warming of the earth at high northern-southern latitudes, and the melting of the polar ice caps.

To reduce the negative impacts of global warming, there has been a worldwide commitment to achieve reduction of GHG emissions. For instance, in 2005 the European Union (EU) launched its first emission trading mechanism (EU ETS) that attempted to cut GHG emissions by 21% by 2020 from 2005 levels. Also, according to the European Commission [1], the budget for 2014 through 2020 associated to climate-related projects and policies was set at 20% as a minimum. In the U.S., also different mechanisms have been implemented. Carbon taxes, renewable portfolio standards, and cap-and-trade programs (e.g., RGGI) are some examples. Several researchers have studied the impact of these policies in electricity markets. For instance, the authors in [2] developed a study to assess the implications that the state of Maryland would have by joining the regional green house gas initiative (RGGI). The impacts of cap-and-trade and network characteristics in an oligopoly market were studied in [3]. Allowances distribution mechanisms (e.g., grand-fathering or auction-based among others) have been shown to have an important role in the success of these carbon reduction initiatives. Some of these $CO_2$ auction based allowances allocation mechanisms were studied in [4]. Nevertheless, the current literature does not consider the impact of carbon

emissions into the society, or social cost of carbon (SCC), when analyzing environmental policies. The societal impact of carbon emissions is explained in detail in the Appendix C.

In a recent effort, the Environmental Protection Agency (EPA) in the U.S. has set carbon emissions reduction targets for each state with an overall goal of achieving 30% reduction below 2005 levels by 2030. Stringent carbon emissions targets will require implementation of the above mentioned carbon policies together with high green penetration via distributed energy resources (e.g., microgrids or solar and wind farms). However, consideration of these policies solely in view of carbon emissions reduction may adversely impact electricity price and consumption. Therefore, implementation of well-designed policies along with the transformation of the current electricity grids to a smarter system with improved technology and efficiency, known as smart grids, is likely to be needed. However, the constant changes in the electricity grid increases the complexity of maintaining a reliable system.

The optimal control of smartgrid operations in order to ensure an efficient and reliable grid operation was emphasized in [5]. In the smart grid context, microgrids are expected to have a predominant role. Microgrid electricity production is associated with high uncertainty since most of its generation capacity depends on weather characteristics. Also, technical problems such as power quality, voltage stability, and protection are associated to distributed generation [6]. Hence, a large deployment of microgrids with distributed generation is likely to affect smartgrid functionalities such as frequency control and allocation of reserves [7]. To address some of the microgrid issues, the incorporation of efficient, reliable and large scale energy storage facilities is vital to deployment [8]. Also, the efficiency of microgrid operation strongly depends on the scheduling process of these energy storage facilities [9]. Different studies have explored the operation strategies of microgrids via energy management models (EMS). The authors in [10] presented an economic analysis of EMSs for microgrids. They concluded that an appropriate battery capacity should be determined on the basis of both battery efficiency and power supply. A combined environmental and economic dispatch model for smartgrids with energy storage devices

and high penetration of renewable energy was presented in [8]. The proposed multi-objective energy management system (EMS) aims at minimizing both the operation cost and environmental impacts of large scale smartgrids. A similar study on environmental-economic dispatch from microgrids was presented in [11]. A microgrid-based planning model considering the power system reliability and economic criteria has recently appeared in [12]. The paper also studies the investment and operation cost of microgrids and concluded that they are able to reduce load shedding and improve system economics. The scenario for competition between microgrids and a large central generation unit is analyzed via a bi-level model in [13]. A linear programming cost minimization model for the high level system design and corresponding unit commitment of generators and storage within a microgrid was presented in [14]. The results broadly indicate that a microgrid can offer an economic proposition, although it is necessarily slightly more expensive than regular grid-connected decentralized generation. Game theory has been identified in the study as a suitable tool to analyze aspects of this situation. In this thesis, this aspect is studied by developing a bi-level optimization model (leader-follower game) for obtaining equilibrium operational strategies for microgrids and the optimal dispatch of electricity by the smartgrid when environmental constraints are implemented (see Appendix D).

Literature related to environmental policies for energy generation studies the impact of such policies considering economic and environmental effects. In this dissertation, the Appendix C presents a published paper entitled *Design of Pareto Optimal $CO_2$ Cap-and-Trade Policies for Deregulated Electricity Markets*. In this manuscript, the analysis of cap-and-trade policies is extended to policy design. The design considers important policies parameters (e.g., penalty, cap size, and cap reduction) and includes the societal impact of carbon emissions, known as the social cost of carbon (SCC). The designs also balance the different interest of market participant. Hence, these policies are likely to achieve emissions reduction and, for example, minimize the increase of electricity prices.

As explained earlier in this section, integration of green energy (via microgrids or DERs) with carbon policies will be needed to achieve targets for emissions reduction. Most microgrid models in the open literature consider the main grid (smartgrid) as a buffer for electricity to buy from and sell to, as necessary. However, with the expected growth of community microgrids and the resulting increase in the percentage of total electricity demand supplied by the microgrids, the above buffer assumption will increasingly be inappropriate. Also, none of the papers in the open literature, to our knowledge, integrate carbon emissions control considerations in the microgrid models. In this dissertation, the Appendix D presents a second published paper entitled *Emissions Control via Carbon Policies and Microgrid Generation: A Bilevel Model and Pareto Analysis*. This research considers the joint operation of the community microgrids and the parent smartgrid in the presence of carbon emissions cap and the social cost of carbon. Also, it is shown how the methodology presented in the Appendix C can be used to obtain levels of emissions reduction that will sustain market demand and green energy penetration from microgrids. The mathematical model presented here assumes accurate forecast of electricity prices, but no forecast model is introduced. Therefore, Chapter 4 of this thesis presents such a LMP forecast model, called K-SVR. The main advantages of K-SVR are that it provides accurate LMP forecasts (that are comparable with other studies) and significantly improves the computational efficiency. The K-SVR model could be easily incorporated in the two-layer framework discussed in the Appendices C and D.

## 1.1 Research Contributions

The research contributions of the articles presented in Appendices C and D are presented next.

1. Develop an economic model for optimal operation of community microgrids with green generation and storage capacities in an islanded mode under carbon emissions considerations.

2. Build a comprehensive economic model that integrates operational strategies of microgrids and the grid under a carbon emissions control regime.

3. Develop policies for emissions control and green penetration by balancing multiple objectives of emissions reduction, green penetration, and electricity consumption using a Pareto analysis.

4. Develop a model to analyze the impact of a $CO_2$ cap-and-trade program in a restructured power market considering stochastic fuel price variations and the social cost of carbon.

5. Obtain Pareto designs for cap-and-trade policies to be used as a decision support framework for policymakers and market participants.

6. Consider the societal impact of carbon emissions as an emissions control strategy to determine generators bidding behavior and microgrids operation.

7. Develops and accurate and computational-efficient forecast model for electricity prices in real time (and day-ahead) markets.

## 1.2 Methods

In this section, the modeling methods used in this dissertation are summarized. The research described in Appendices C and D are based on a mathematical-statistical framework. This framework presents two layers. The bottom layer involves the behavior of the market participants under different market conditions, e.g., different types of cap-and-trade policies, or the inclusion of SCC or not. The behavior of market participants is modeled using a bi-level optimization model. The top layer involves an analysis of variance (ANOVA) for different levels of, for example, policy parameters, SCC, and green energy from microgrids. The ANOVA results are used to formulate regression equations for the network performance measures. Thereafter, a Pareto analysis is developed by solving a multi-objective optimization model that consider the regressions equations derived from the ANOVA analysis. The two-layer model is given as follows.

$$\text{Top layer}\begin{cases} \text{Optimize } \ f(X) \end{cases}$$
$$\text{Bottom layer}\begin{cases} \text{Maximize } \ g_i(\alpha_i,\omega_i), \ \ \forall i \in I \\ s.t. \text{ Maximize } \ W(Q,\Theta) \\ \quad s.t. \text{ Network and policy constraints.} \end{cases} \tag{1.1}$$

In the top layer, $f(X)$ represents the objective function of the multi-objective optimization model. The bottom layer is formulated, for each player $i \in I = \{1,2,\cdots,n\}$, as a bi-level optimization model, where $g_i(\alpha_i,\omega_i)$ denotes the profit of the player $i$. $W(Q,\Theta)$ denotes the social welfare objective function for the DC optimal power flow (OPF) problem. Further details are presented in Appendix C. The different methodologies utilized in both the bottom and top layer are summarized next.

- Bi-level Programming:

  Bi-level optimization models have been widely studied in the literature [e.g., 16, 17] , and used for modeling the electricity markets [e.g., 18–20]. Bi-level models include two mathematical programs, where one serves as a constraint for the other. A generic description of the bi-level model can be presented as follows.

$$\begin{aligned} &\underset{x_i}{\text{Max}}\ f_i(x,y) \\ &s.t \ \ d_i(x_i,y) \geq 0, \ \ g_i(x_i,y) = 0, \\ &y = \underset{y}{\text{Min}}\, F(x,y) \\ &\quad s.t \ \ D(x,y) \geq 0, \ \ G(x,y) = 0. \end{aligned} \tag{1.2}$$

  For the lower level problem, with a convex objective function and non-empty feasible set, the first order necessary conditions for a solution to be optimal are given (under some regularity conditions) by the *Karush Kuhn Tucker* (KKT) conditions as follows.

$$\begin{aligned} &\nabla_y F(x,y) - \nabla_y D(x,y)^t \delta + \nabla_y G(x,y)^t \gamma = 0, \\ &G(x,y) = 0, D(x,y) \geq 0, D(x,y)^t \perp \delta, \delta \geq 0, \end{aligned} \tag{1.3}$$

where $\delta$ and $\eta$ are the vector of dual variables for inequality and equality constraints, respectively. $D(x,y)^t \perp \delta$ represent the orthogonality conditions, which is often stated as the complementarity slackness constraint in the primal-dual relationship denoted by $D(x,y)^t \delta = 0$. Replacing the lower level problem in (1.2) by the set of conditions in (1.3) yields what is known as a mathematical program with equilibrium constraints (MPEC), as given below.

$$\begin{aligned} &\underset{x_i}{\text{Max}}\ f_i(x,y) \\ &s.t\ \ d_i(x_i,y) \geq 0, \quad g_i(x_i,y) = 0, \\ &\nabla_y F(x,y) - \nabla_y D(x,y)^t \delta + \nabla_y G(x,y)^t \gamma = 0, \\ &G(x,y) = 0,\ \ D(x,y) \geq 0,\ \ D(x,y)^t \perp \delta,\ \ \delta \geq 0. \end{aligned} \tag{1.4}$$

Further details on the MPEC models can be found in [21], [22], and [23].

The equilibrium among market participant is found by solving an Equilibrium Program with Equilibrium Constraint (EPEC). An EPEC is defined as a game, $EPEC = (MPEC)_1^n$, among competing generators. Typically MPECs have non-convex feasible sets (due to the complementarity constraints), therefore the resulting games are likely to have non-convex feasible strategy sets. Since a global equilibrium for this type of games is difficult to identify, the authors in [24] define a *local Nash equilibrium* as follows. The vector $(x^*, y^*, \delta^*, \gamma^*)$ is called a *local Nash Equilibrium* for the game $EPEC = (MPEC)_1^n$ if, for each player $i$, $(x_i^*, y^*, \delta^*, \gamma^*)$ is a local optimal solution for the MPEC (1.4) when $(x_{-i}) = (x_{-i}^*)$. Hence, the local Nash equilibrium is comprised of stationary points of the MPEC (1.4) for each player $i$ in the game $EPEC = (MPEC)_1^n$.

Literature presents different strategies to solve EPECs, of which linear and nonlinear complementarity (CP/NCP) formulation [25] and diagonalization methods [26, 27] are the most discussed. In this thesis (Appendix C), we consider a diagonalization method as described in [28].

- Multi-objective Optimization:

  Multi-objective optimization (MOO) has tremendous significance in modeling real-world problems with conflicting objectives. In a complex system with multiple performance measures and the set of significant design factors that affect them, the conflict appears when a set of factor values (levels) that are optimal for a particular performance measure may not be optimal for other measures. In the context of environmental (carbon levels) and economic activity, C&T and network parameters that minimizes $CO_2$ emissions may not yield lowest electricity prices, when both reduced emissions and lower prices may be among the priorities. Therefore, a solution that can consider different priorities simultaneously must be considered. Multi-objective optimization models, that yield Pareto fronts, are an example of such approaches.

  A Pareto front is a set of points representing factor level combinations where all points are Pareto efficient. A Pareto efficient point indicates that no measure of performance can be further improved without worsening one or more of the other performance measures. Similarly, for any point outside of the Pareto front, by moving the point onto the front, one or more measures can be improved without worsening the others. In this thesis, the evolutionary algorithm NSGA-II genetic algorithm [30] is used to solve the MOO models and obtain the Pareto envelope. NSGA-II algorithm, as many others, uses the concept of domination, e.i., two solutions are compared on the basis of whether one dominates the other or not. Hence, the Pareto front (compound of non-dominated solutions) can be formally defined as follow.

**Definition:** A solution $x1$ is said to dominate another solution $x2$ ($x1 \preceq x2$) if the solution x1 is no worse than x2 in all objectives, and the solution x1 is strictly better than x2 in at least one objective.

$$\textbf{x1} \preceq \textbf{x2} \ \textbf{iff}$$

$$1) f_i(x1) \leq f_i(x2) \ \ \forall i \in 1,...,M.$$

$$2) \exists j \in 1,...,M \ \text{ for which } \ f_j(x1) < f_j(x2).$$

- Analysis of Variance (ANOVA):

  Analysis of variance (ANOVA) is a widely used statistical approach to determine factors of a system that significantly impact its output measures [29]. The results of ANOVA yields a response surface equation for each output (performance) measure, which can then be optimized to obtain factor levels. Relevant factors that might impact performance of an electricity network are policy parameters (cap size, cap reduction rate, SCC, taxes, and penalties) and network parameters (e.g., demand-price sensitivity, line capacities, and social cost of carbon). A factorial experimental design (e.g., a $3^k$ experiment, with $k$ factors each at 3 levels) with the relevant $k$ factors yields the necessary factor combinations for the ANOVA.

  The designed experiment and ANOVA results are used in the top layer of the mathematical-statistical framework. For each factor combination, the bottom layer of the two-layer model is solved, which yields the network performance measures (e.g., $CO_2$ emissions, consumption level, and marginal electricity price). Once every factor combination is considered by the bottom layer, ANOVA is performed for each performance measure, and the corresponding response surface equation is obtained. A complete explanation of how ANOVA analysis is utilized in the two-layer model can be found in Appendix C.

# Chapter 2: Design of Pareto Optimal $CO_2$ Cap and Trade Policies for Deregulated Electricity Networks

The complete presentation of the article *Design of Pareto Optimal $CO_2$ Cap and Trade Policies for Deregulated Electricity Networks* (published in Applied Energy) can be found in the Appendix C. This paper fully describes a two-layer mathematical-statistical framework (discussed earlier) that is used to develop Pareto designs of Cap-and-Trade policies for emissions reduction.

## 2.1 Abstract

Among the $CO_2$ emission reduction programs, cap-and-trade (C&T) is one of the most used policies. Economic studies have shown that C&T policies for electricity networks, while reducing emissions, will likely increase price and decrease consumption of electricity. This paper presents a two layer mathematical−statistical model to develop Pareto optimal designs for $CO_2$ cap-and-trade policies. The bottom layer finds, for a given C&T policy, equilibrium bidding strategies of the competing generators while maximizing social welfare via a DC optimal power flow (DC-OPF) model. We refer to this layer as policy evaluation. The top layer (called policy optimization) involves design of Pareto optimal C&T policies over a planning horizon. The performance measures that are considered for the purpose of design are social welfare and the corresponding system marginal price (MP), $CO_2$ emissions, and electricity consumption level.

# Chapter 3: Emissions Control via Carbon Policies and Microgrid Generation: A Bilevel Model and Pareto Analysis

The complete presentation of the article *Emissions Control via Carbon Policies and Microgrid Generation: A Bilevel Model and Pareto Analysis* (accepted for publication in Energy) can be found in the Appendix D. This paper presents a bi-level optimization model that finds the optimal operation strategies of cooperative community microgrids in a smart grid under carbon emissions control. The potential of microgrid generation in emissions reduction is accounted by applying the framework described in Appendix C.

## 3.1 Abstract

Economic models are needed to analyze the impact of policies adopted for controlling carbon emissions and increasing distributed renewable generation in microgrids (green penetration). The impacts are manifested in performance measures like emissions, electricity prices, and electricity consumption. This paper presents an economic model comprising bi-level optimization and Pareto analysis. In the bi-level framework, the upper level models the operation of the microgrids and the lower level deals with electricity dispatch in the grid. The economic model is applied on a sample network in two steps. In step1, the bi-level model yields operational strategies for the microgrids and the corresponding values of the grid performance measures. In step2, a statistical analysis of variance combined with Pareto optimization attains guidelines for setting policies for emissions reduction and green penetration without adversely impacting electricity prices and demand. We

conclude that renewable generation from microgrids can significantly reduce the negative impacts of the policies. Our economic model is novel as it 1) integrates operational strategies of microgrids and the grid under an emissions control regime, 2) explicitly considers social cost of carbon in the electricity dispatch, and 3) balances multiple objectives of emissions reduction, green penetration, and electricity consumption using a Pareto analysis.

### 3.2 Stochastic Microgrid Operational Model

The microgrid operational model (also refer to as an energy management system, EMS) presented in Appendix D minimizes a community microgrid's operation cost. The cost includes production and maintenance cost of green generators (levelized cost), the cost of trading power with the smartgrid, and the battery storage cost. This model assumes deterministic forecasts for wind and solar weather data (average values for historical data is considered). Here, a stochastic version of the operational model is presented. Also, the model considers the option of investment capacity. To keep notation simple, the model is presented for a single time period.

Uncertainty for wind and solar weather data is modeled via scenarios. Each scenario $w \in \Omega$ has a probability $prob(w)$. The model is presented in constraints (3.1)-(3.14). The objective function (3.1) minimizes the expected operational cost and the investment capacity decisions. The investment decision can be interpreted as the first stage variables. The production level variables correspond to the second stage, which depend on the scenario realization. Constraint (4.3) shows how the investment capacity allows higher production for microgrid $m$ and production type (wind and solar) $i$. Constraint 3.6 limits the investment cost to a defined investment budget for each microgrid. Detail explanation of the microgrid operational model is presented in Appendix D. Finally, a budget constraint is introduced in constraint (3.6).

Note that each scenario corresponds to a possible realization of weather data. Therefore, for each realization (scenario), the electricity dispatch (DC-OPF) needs to be obtained. Hence, each

scenario is solved independently in a lower level model. Each lower level model can replaced by its $KKT$ optimality conditions. The lower level model is presented in Appendix ]D.

$$\underset{P}{\text{Min}} \quad \sum_{m\in M}\sum_{i\in Gm}\sum_{w\in\Omega} prob(w)[OM_i(P^w_{im}) + STC_iY^w_{im} + \mu^w_m(P^w_{gm} - \hat{P}^w_{mg}) + BSC_m(P^w_{sm})] + \sum_{m\in M}\sum_{i\in Gm} C_{im}X_{im} \tag{3.1}$$

$$s.t. \sum_{i\in Gm} P^w_{im} + P^w_{gm} + \beta^{out}_m P^{w,out}_{bm} = \sum_{l\in m} P^w_{lm} + P^{w,in}_{bm} + \hat{P}^w_{mg} \quad \forall m, w, \tag{3.2}$$

$$P^{w,out}_{bm} \le \beta_m P^{w,h-1}_{sm} \qquad \forall m \in M, w, \tag{3.3}$$

$$P^w_{sm} = \beta_m P^{w,h-1}_{sm} - P^{w,out}_{bm} + \beta^{in}_m P^{w,in}_{bm} \quad \forall m \in M, w, \tag{3.4}$$

$$Y^w_{im}P^{w,min}_{im} \le P^w_{im} \le P^{w,max}_{im}Y^w_{im} + X_{im} \quad \forall i \in Gm, m \in M, w, \tag{3.5}$$

$$\sum_i C_{im}X_{im} \le B_m \qquad \forall m \in M, w, \tag{3.6}$$

$$\hat{P}^w_{mg} \le \sum_i P^w_{im} + \beta_m P^{h-1}_{sm} \qquad \forall m \in M, w, \tag{3.7}$$

$$P^w_{sm} \le P^{max}_{sm} \quad \forall m \in M, w, \tag{3.8}$$

$$P^{w,out}_{bm} \le \beta_m P^{max}_{sm} Y^w_{dm} \quad \forall m \in M, w, \tag{3.9}$$

$$P^{w,in}_{bm} \le \beta_m P^{max}_{sm} Y^w_{cm} \quad \forall m \in M, w, \tag{3.10}$$

$$Y^w_{dm} + Y^w_{cm} \le 1 \quad \forall m \in M, w, \tag{3.11}$$

$$\hat{P}^w_{mg} \le (P^{max}_{sm} + \sum_{i\in m} P^{w,max}_{im})Y^w_{mg} \quad \forall m \in M, w, \tag{3.12}$$

$$P^w_{gm} \le (P^{max}_{sm} + \sum_{l\in m} P^w_{lm})Y^w_{gm} \quad \forall m \in M, w, \tag{3.13}$$

$$Y^w_{gm} + Y^w_{mg} \le 1 \quad \forall m \in M, w. \tag{3.14}$$

# Chapter 4: Computationally Efficient LMP Forecast Model for Real Time Electricity Markets

## 4.1 Introduction

This chapter presents a forecast model for electricity prices. Accurate and fast price forecasting is needed to take intelligent and correct operational decisions at different levels (production and distribution), especially in real time markets. Appendix D presents an operational model for microgrids and the parent smartgrid. The referred operational model assumes forecasted prices for future hours, which are accurate for microgrid generation. In this chapter, the forecasting model presented attempts to fill the assumption previously mentioned, as it is shown that result obtained are precise, stable, and computationally efficient. The data used for modeling and testing purposes is publicly available and represent the PJM real time market for time periods 2005-2006 and 2011-2012.

## 4.2 Motivation and Literature Review

Forecast of the electricity prices (LMPs) is of critical significance to all participants in deregulated electric power markets. The task of forecasting is complex as LMPs can vary widely owing to changes in weather, demand spikes, network outages, changes in generation mix, and competitive bidding strategies of the generators. Imprecise estimation of LMPs can lead to inappropriate quantity bidding strategies by the generators, over/under supply of planned generation, rise in

cost of meeting demand, and increase in real time operational challenges. Hence, it is imperative to have a methodology to precisely predict real time (and day ahead) LMPs. Real time market is a spot market in which current locational marginal prices (LMPs) are calculated at five-minute intervals based on actual grid operating conditions. The independent system operator (ISO) is in charge of the settlement of the real (and day ahead) markets and obtains the planned electricity dispatch as well as the corresponding LMPs.

LMPs tend to have a non-stationary mean and variance as well as seasonal and non-seasonal peaks. These characteristics make the forecasting of LMPs difficult. Literature shows that several different modeling approaches have been used to forecast electricity prices. Zareipour et al. [31] used univariate and multivariate ARIMA models for the hourly prices in Ontario energy system. The model did not predict well the prices that were either very high or low. Several other models achieving varying degrees of success were developed and presented to the literature. A subset of these models are cited here. Zhang [32] and Tan [33] used wavelet transform combined with ARIMA models to predict prices in Australian and Spanish markets, respectively. Artificial neural networks (ANN) combined with similar days method have also been proposed by Mandal in [34] and [35]. Vahidinasab [36] combined ANN with fuzzy c-means. Recurrent neural network models were used by Hong [37] and Mandal [38]. A number of researchers have used support vector machine (SVM) models. Examples include price forecasting for Australian electricity market, as presented in [39] and [40], which use a combination of SVM and neural networks models. A two-stage hybrid network of self-organized map (SOD) and SVM was used by Fan [41] for the New England electricity market. Swief [42] combined SVM with principal component analysis (PCA) and k nearest neighbor method (knn) for forecasting in the PJM market. LMP forecasting models have also used support vector regression methods (e.g., Pai [43]).

Other hybrid methods include Li [44], which combined fuzzy inference systems and least squares estimation. Amjady [45] in his forecasting model incorporated feature selection technique and cascaded neuro-evolutionary algorithm. A mixed model for load and price forecasting where

a load forecast is used to forecast price was presented by Amjady [46]. Arabali [47] considered Gauss-Markov process to represent the stochastic dynamics of the electricity price.

As stated to earlier, electricity price is highly non-stationary and non-linear, and linear prediction models (e.g., ARIMA and linear regression) are insufficient. Hence, many non-linear models have been developed using artificial and fuzzy neural networks. But, it has been shown that though NN learns training data well, it may encounter large prediction errors in the test phase due to the time dependence of electricity prices [45], [46]. Feature selection algorithms have been proposed to address this issue. However, the training and testing time associated with these algorithms using neural networks and feature selection mechanisms may significantly increase as the data size increases. Also, for feature selection, it has been shown that the combinations of good individual features do not necessarily lead to a good classification performance [48].

In this paper, we present a simpler alternative hybrid approach for LMP forecasting that would be useful in real time markets. The approach first uses a clustering model to form clusters of similar prices. The cluster information is then fitted with a SVM model, which is used to classify the future electricity prices. Thereafter, for each cluster, we develop a local SVR model that yields the price forecast. We developed and implemented our hybrid model using publicly available data from the Pennsylvania-New Jersey-Maryland (PJM) market for the years 2005-2006 and 2011-2012.

The rest of the paper is organized as follows. Section 4.3 presents a description and statistical analysis of the PJM data. Section 4.4 presents the basics of the support vector machine models, which is followed by the details of the proposed hybrid model (K-SVR). Section 4.5 describes the performance measures that are used to evaluate forecasting accuracy. The forecast results and a comparative analysis with the results from other methods in the literature are presented in Section 4.6. Concluding remarks are placed in Section 4.7.

### 4.3 Description of Data Set from PJM

PJM interconnection is a regional transmission organization (RTO), and is one of the largest competitive wholesale electricity markets in the U.S. We have used LMP data from PJM for the years 2005-2006 for training and testing purposes as did other previous researchers (e.g., [34] and [49]). Subsequently, we used the data from 2011 to train our model and test it using 2012 data.

The data for 2005-2006 comprises hourly LMP and hourly demand of electricity. Whereas, the data set for 2011-2012 contains hourly LMP and its predictors: demand (abbreviated later as Dem), wind energy, index hour, relative humidity (RH), temperature (Temp), and dew point (DP). Table 4.1 shows the correlation matrix between the LMP and the predictors for 2011-2012. Clearly demand has the highest correlation with LMP, whereas dew point has almost none. Wind energy and relative humidity have negative correlations.

Table 4.1: Correlation matrix.

| | LMP | Hour | Dem. | Wind | Temp. | DP | RH |
|---|---|---|---|---|---|---|---|
| LMP | 1 | | | | | | |
| Hour | 0.267 | 1 | | | | | |
| Dem. | 0.687 | 0.457 | 1 | | | | |
| Wind | -0.162 | -0.011 | -0.243 | 1 | | | |
| Temp | 0.156 | 0.145 | 0.329 | -0.305 | 1 | | |
| DP | 0.056 | 0.004 | 0.203 | -0.334 | 0.887 | 1 | |
| RH | -0.212 | -0.307 | -0.285 | -0.056 | -0.268 | 0.195 | 1 |

The scatter plot for LMP and demand (for period 2011-2012) is presented in Figure 4.1. The high positive correlation coefficient (0.687)is evident as higher demand increases the price of electricity. The relationship appears to be somewhat quadratic. Similar trend was observed in the data set for 2005-2006 (see Figure 4.2), where the correlation between demand (or load) and LMP even higher (0.799).

Figure 4.3 shows the autocorrelation function (ACF) for LMP prices during the year 2005. The ACF for a series gives correlations between the series $x_t$ and lagged values of the series

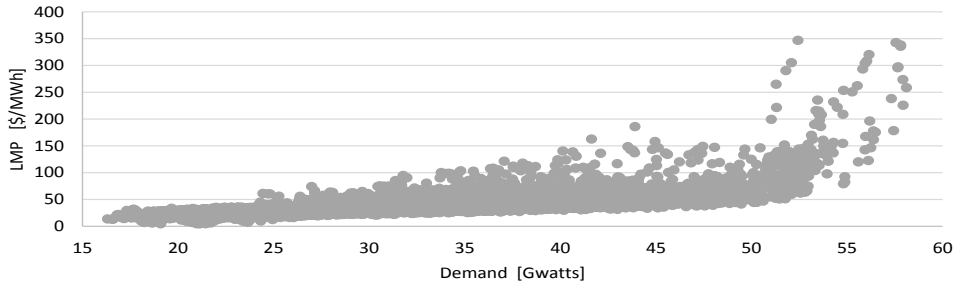


Figure 4.1: Scatter plot for LMP and electricity demand for period 2011-2012.

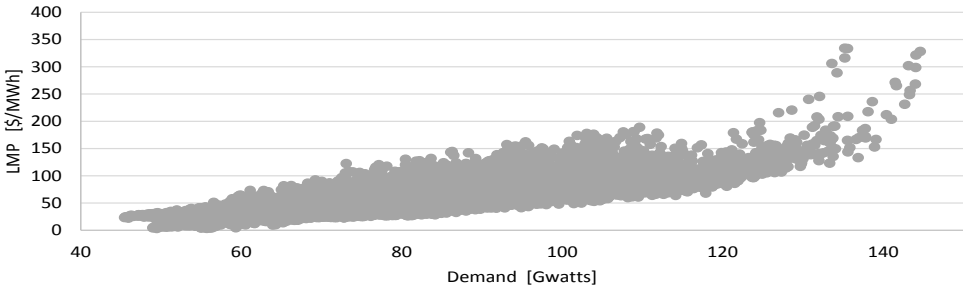


Figure 4.2: Scatter plot for LMP and electricity demand for period 2005-2006.

$x_{t-1}, x_{t-2}, x_{t-3}, \ldots$.It can be noticed that there appears to be a significant positive correlation up to the lagged value $x_{t-4}$, and also a seasonality of 24 periods.

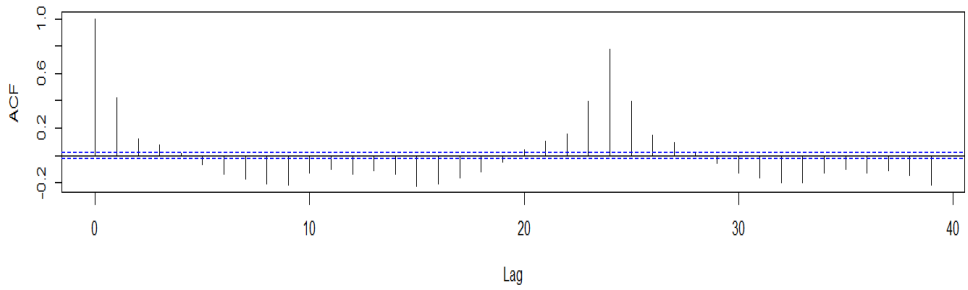


Figure 4.3: Autocorrelation function for LMP.

The seasonality is confirmed by the partial autocorrelation plot (PACF) shown in Figure 4.4. The PACF is the amount of correlation between a variable and a lag of itself that is not explained by correlations at all lower lag levels. It can be seen that the lag period $t-24$ has a high correlation with the LMP at time $t$.

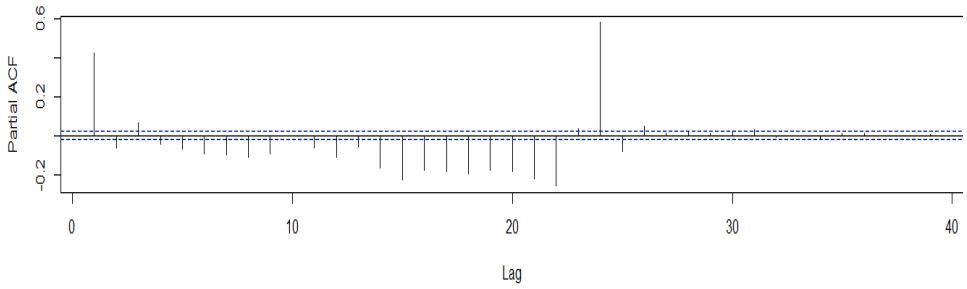


Figure 4.4: Partial autocorrelation function for LMP.

The information obtained from the ACF and PACF should not be surprising due to the natural seasonality pattern of electricity prices. Table 4.2 shows some descriptive statistics of both data sets. Clearly, the years 2005-2006 have a higher variability than 2011-2012. Also, the mean LMP for the 2005-2006 period is considerably higher.

Table 4.2: Variability in the data sets.

| | LMP2005 | LMP2006 | LMP2011 | LMP2012 |
|---|---|---|---|---|
| Mean | 57.89 | 48.09 | 42.51 | 32.79 |
| Standard Deviation | 30.04 | 23.42 | 20.48 | 13.29 |
| Variance | 902.52 | 548.55 | 419.5 | 176.63 |

## 4.4 Forecasting Model

In this section, we first provide a brief description of the SVR model and, thereafter, present a detailed description of our proposed hybrid forecasting model (K-SVR).

### 4.4.1 SVR

Support vector machines, the basis for support vector regression (SVR) models, are founded on the duality theory of optimization. If a data set is not linearly separable, SVR maps the data points to a higher dimensional space via a kernel function, and builds a regression model in this kernel

induced space [50]. The epsilon-SVR finds a line (linear function $f(x)$) connecting all the points allowing a predefined error tube (+- epsilon). SVR introduces a penalty (C) for being outside of the error tube. However, once the data points are close enough (in some epsilon-tube) the error is ignored. Given a set of data points $D = \{(x_i, y_i)\}_{i=i}^{n}$ (where $x$ is the input vector and $y$ the target value), SVR finds the $w$ and $b$ of linear function $y = f(x) = w\phi(x) + b$ by solving the following optimization model via duality theory.

$$\text{Min } \frac{1}{2}\|w\|^2 + C\sum_i (\xi_i - \hat{\xi}_i) \tag{4.1}$$

$$s.t.\ \ w^2\phi(x_i) + b - y_i \leq \varepsilon + \hat{\xi}_i \ \ \forall i \tag{4.2}$$

$$y_i - w^T\phi(x_i) - b \leq \varepsilon + \xi_i \ \ \forall i \tag{4.3}$$

In the above optimization model, the input data in the induced high dimensional space is given by $\phi(x_i)$, $w$ is a vector perpendicular to the plane, $b$ is a variable scanning the space, $\xi_i$ is a positive slack variable (point above the hyper-plane), and $\hat{\xi}_i$ is a negative slack variable (point below the hyper-plane).

### 4.4.2 LMP Forecasting

LMPs can be forecasted using information of LMP time series and other variables such us electricity demand, temperature, wind energy, and fuel prices, among others. There are many research papers in the open literature that have focused on developing forecast models for wind speed, solar irradiance, and LMPs utilizing feature selection and data selection techniques. For large data sets, feature selection techniques (e.g., backward and forward selection, stepwise selection) may become computationally challenging. In K-SVR, we propose a computationally simpler feature selection method that uses information derived from the autocorrelation and partial

autocorrelation functions. That is, if the LMP forecast for time $t+1$ is desired, then features (previous LMPs) for all significant lags in the ACF plot and the features with seasonal information from the PACF plot are utilized. This approach is similar to that used for ARIMA model. However, ARIMA models themselves are unsuitable for predicting LMPs as they assume stationary mean and variance. Hence, we adopt SVR approach that does not require the stationary assumption.

The SVR model can thus be viewed in the form of a regression model as follows. Let $l$ denote the number of significant lags from the ACF plot, and $s$ denote the lag for seasonal trend observed from PACF plot. Then we can write that

$$\hat{Y}_{t+1} = \sum_{i=0}^{l-1} \beta_i Y_{t-i} + \beta Y_{t-(s-1)} + \sum_{j=1}^{P} \sum_{i=0}^{l-1} \beta_{ij} X_{t-i}^{j}, \tag{4.4}$$

where $Y_t$ represents the LMP value at time $t$, $X_t$ represent covariates other than LMP at time $t$, and $P$ represent the number of such covariates. Before deriving the SVR models, the LMP training data is classified into $K$ clusters of different prices. For each price cluster, we develop a separate SVR model. The forecast for time $t+1$ is obtained from one of these $K$ SVR models. If current time is $t$, for which actual LMP is known, the forecast for the next $t+\tau$ periods is obtained as follows. The expected LMP for the period $t+1$ is assigned to one of the $K$ clusters using a SVM model. Then the SVR model for the corresponding cluster is used to obtain the LMP forecast for period $t+1$. The forecast for period $t+1$ is considered as the actual LMP for forecasting for period $t+2$. This process continues till period $t+\tau$. A depiction of the proposed model is shown in Figure 4.5.

A step by step summary of the training and testing of the model by forecasting price at time $t+\tau$ is given as follows.

1. Perform K-means using the historical data in order to identify the clusters.

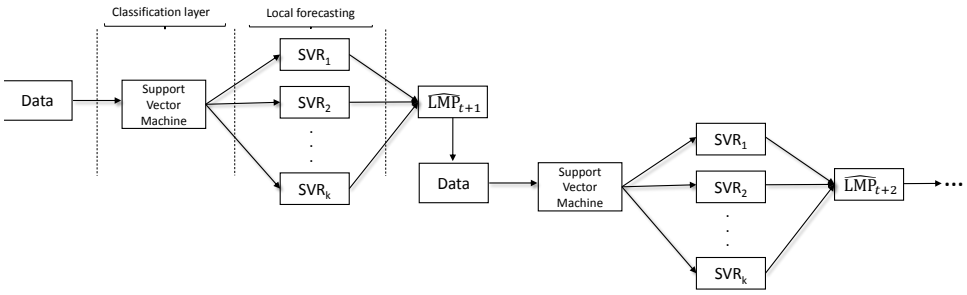


Figure 4.5: Schematic of K-SVR model.

2. Choose the number of clusters beyond which the decrease in the sum of square within the clusters is below a chosen threshold.

3. For each cluster, train a SVR model for prediction.

4. Train a SVM model for classification using information of all $K$ clusters.

   Given the trained SVM and SVR models, consider a forecast period $t+h$. Set $h=1$.

5. Classify the LMP for $t+h$ as belonging to one of the $K$ clusters.

6. Obtain the prediction for period $t+h$ using the SVR model for the cluster found in step 1.

7. Use the forecasted value for $t+h$ to predict LMP for $t+h+1$.

8. Set $h=h+1$. Repeat steps 1 through 3 till $h=\tau$.

## 4.5 Measures of Forecast Performance

The mean percentage error (MAPE) is among the most common measure used to evaluate forecast performance. MAPE is defined as average of the absolute value of the error forecast (real minus predicted) over the real value. We refer to this as MAPE1. Some authors have redefined the concept of MAPE due to the highly volatile nature of electricity prices [34]. We will refer to this as MAPE2. In the expressions for MAPE1 and MAPE2 ,given bellow, $LMP^r$ and $LMP^f$ are used to denote real and forecasted values, respectively.

$$\text{MAPE1} = \frac{1}{N}\sum_{i=1}^{N}\frac{\left|LMP_i^r - LMP_i^f\right|}{LMP_i^r},$$

$$\text{MAPE2} = \frac{1}{N}\sum_{i=1}^{N}\frac{\left|LMP_i^r - LMP_i^f\right|}{LMP_i^a},$$

where

$$LMP_i^a = \frac{1}{N}\sum_{i=1}^{N} LMP_i^r.$$

Other performance measures that are also presented in the literature are the forecast mean square error (FMSE) and the mean absolute error (MAE), which are given as

$$\text{FMSE} = \sqrt{\frac{1}{N}\sum_{i=1}^{N}(LMP_i^r - LMP_i^f)^2},$$

$$\text{MAE} = \frac{1}{N}\sum_{i=1}^{N}\left|LMP_i^r - LMP_i^f\right|.$$

### 4.6 Results and Comparison

We first tested our model, developed using PJM data from 2005, on the data for 2006. We then repeated the process using data from 2011 and 2012. Results from our model were compared with those obtained using the same data sets by other models in the open literature. While implementing our model, we chose a relatively small value for the number of clusters $K$=3, which was based on a plot of sum of squares within clusters from the 2005 data (see Figure 4.6). The figure shows that beyond $K$=3, the reduction of the sum of squares is small. Also, if a higher values of $K$ is chosen,

fewer price data points will be assigned to each cluster. This is likely to lower the performance of the prediction models or result in over-fitting. The values chosen for parameters $l$ and $s$ were 4 and 24, based on ACF and PACF plots (see Figures 4.3 and 4.4), respectively. The kernel function chosen for the SVM/SVR models is the radial basis function.

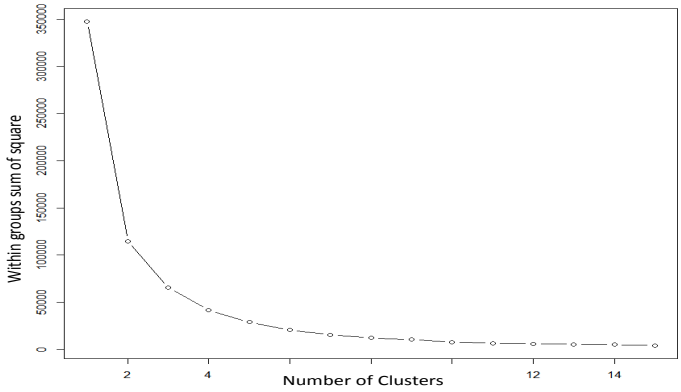


Figure 4.6: Sum of square within clusters.

### 4.6.1 Model Validation Using PJM Market Data-2006

For validation, we tested our model using data from 2006. Several other models in the literature have used data from 2006 for testing. For the purpose of comparison, we chose data from the same days of the year 2006, as considered by other models. We obtained all four measures of LMP forecast performance, which are presented in Table 4.3. The average values over all the days to which our model was implemented (see the last row), indicate a mean absolute deviation from real LMPs by \$2.47/MWh with standard deviation of \$3.17/MWh, which represents an average forecast error of 5.17-5.18%.

Table 4.4 shows a comparison of the performance of our model (K-SVR) with those obtained from selected models in the literature. The first model that we had selected for comparison can be found in [34], which has been used as a benchmark in many previous studies. This model (henceforth referred to as SD+NN) uses similar days (SD) to perform a forecast, which is then

Table 4.3: LMP forecast errors for K-SVR model.

| Test Days | MAE [$/MWh] | FMSE [$/MWh] | MAPE1 [%] | MAPE2 [%] |
|---|---|---|---|---|
| 20-Jan | 2.06 | 2.55 | 5.17 | 5.15 |
| 10-Feb | 2.68 | 3.31 | 4.86 | 4.89 |
| 5-March | 2.54 | 3.25 | 5.55 | 5.54 |
| 7-Apr | 2.41 | 2.98 | 4.46 | 4.57 |
| 13-May | 1.63 | 1.85 | 5.26 | 4.71 |
| February 1-7 | 2.94 | 4.49 | 5.31 | 5.85 |
| February 22-28 | 2.98 | 3.74 | 5.59 | 5.59 |
| Average | 2.47 | 3.17 | 5.17 | 5.18 |

improved using neural networks (NN). Note from Table 4.4 that, for each of the test days, K-SVR outperformed SD+NN, for which only MAPE2 values were made available in [34]. Results indicate an error reduction of up to 49%.

The second model with which K-SVR was compared was proposed in [49]. This model comprises a pre-processor coupled with a hybrid neuro-evolutionary system (HNES). The pre-processor selects the input features of the HNES according to MRMR (maximum relevance minimum redundancy) principle. The HNES is composed of three neural networks (NN) and evolutionary Algorithms (EA) arranged in a cascaded structure, supported by auxiliary predictors from ARIMA and batch NN models. As seen from Table 4.4, the HNES model outperforms K-SVR per MAPE2 by 15% on average. However, the complex structure of the HNES model demands a much higher computational time of about 30 minutes [49] compared to K-SVR that takes approximately 1 minute, using a similar computer CPU. Though superior in performance (per MAPE2) to K-SVR, the high computational effort needed by HNES may make it unattractive for use in real time electricity markets that are often settled every five minutes (as in PJM).

In addition to the mean forecast error, the variance of the forecast error has also been used as a measure of performance of the models in the literature. Table 4.5 shows the variance of the forecast errors (using MAPE2) for the test days considered earlier. K-SVR has lower error variances than SD+NN for all of the test days and weeks, which indicates a higher stability of prediction. Also, K-

Table 4.4: MAPE for LMP forecast result for test days.

| Test Days | SD+NN [34] (MAPE2) | HNES [49] (MAPE2) | K-SVR (MAPE1) | K-SVR (MAPE2) |
|---|---|---|---|---|
| 20-Jan | 6.93 | 4.98 | 5.17 | 5.15 |
| 10-Feb | 7.96 | 4.10 | 4.86 | 4.89 |
| 5-March | 7.88 | 4.45 | 5.55 | 5.54 |
| 7-Apr | 9.02 | 4.67 | 4.46 | 4.57 |
| 13-May | 6.91 | 4.05 | 5.26 | 4.71 |
| February 1-7 | 7.66 | 4.62 | 5.31 | 5.85 |
| February 22-28 | 8.88 | 4.66 | 5.59 | 5.59 |
| Average | 7.89 | 4.50 | 5.17 | 5.18 |

SVR has a lower error variance for most of the test days compared to HNES and CNEA (cascaded neuro-evolutionary algorithm) [45].

Table 4.5: Forecast error variance comparison.

| Test Days | K-SVR | SD+NN [34] | HNES [49] | CNEA [45] |
|---|---|---|---|---|
| 20-Jan | 0.0014 | 0.0034 | 0.0020 | 0.0031 |
| 10-Feb | 0.0014 | 0.0050 | 0.0012 | 0.0036 |
| 5-March | 0.0020 | 0.0061 | 0.0015 | 0.0042 |
| 7-Apr | 0.0011 | 0.0038 | 0.0018 | 0.0022 |
| 13-May | 0.0006 | 0.0049 | 0.0013 | 0.0027 |
| February 1-7 | 0.0045 | 0.0066 | 0.0016 | 0.0035 |
| February 22-28 | 0.0018 | 0.0047 | 0.0017 | 0.0035 |
| Average | 0.0018 | 0.0049 | 0.0016 | 0.0034 |

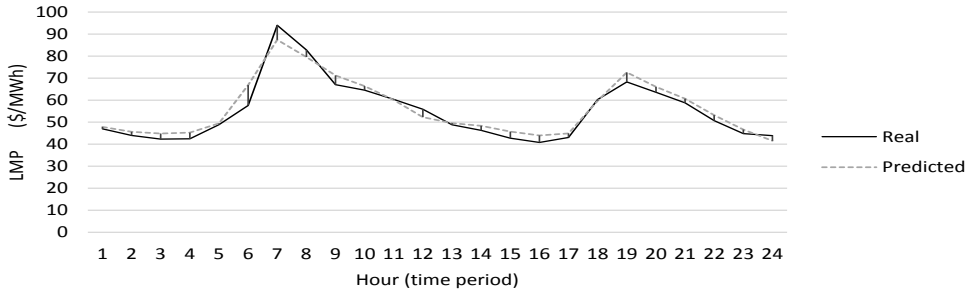


Figure 4.7: Real and forecast LMPs for February 20, 2006.

Table 4.6 presents further comparative performance outcomes for K-SVR with a number of other models studied in [51].

Table 4.6: MAPE comparison.

| | K-SVR | | Ref. [51] (MAPE1) | | | | |
|---|---|---|---|---|---|---|---|
| Test Weeks | MAPE1 | MAPE2 | ARIMA | MLP+LM | MLP + BFGS | MLP+BR | WT+NN+EA |
| Winter | 6.72 | 6.46 | 11.21 | 9.82 | 12.90 | 13.22 | 4.44 |
| Spring | 8.26 | 7.78 | 15.30 | 8.87 | 10.12 | 12.92 | 4.31 |
| Summer | 5.34 | 5.08 | 13.56 | 10.43 | 11.46 | 11.98 | 4.78 |
| Fall | 4.18 | 4.07 | 12.93 | 9.54 | 9.83 | 12.24 | 4.75 |
| Average | 6.12 | 5.84 | 13.25 | 9.66 | 11.07 | 12.59 | 4.57 |

The comparison was performed using data for one week from each of the four different seasons: winter (February 15-21), spring (May 15-21), summer (August 15-21), and fall (November 15-21). The models used for comparison are: ARIMA, multi-layer perceptron neural network (MLP) with Levenberg & Marquardt learning algorithm (LM); MLP with Broyden, Fletcher, Goldfarb, and Shanno learning algorithm (BFGS); MLP with Bayesian regularization learning algorithm (BR); and a hybrid model comprising wavelet transform (WT), neural networks (NN), and evolutionary algorithm (EA). The MAPE1 values for K-SVR are significantly better than all models except for WT+NN+EA. On average WT+NN+EA errors are 25% lower than K-SVR. However, as reported in [51], computational time needed by the WT+NN+EA model is between 16 and 35 minutes compared to up to one minute for K-SVR, when implemented on a comparable CPU.

It may also be noted that a study, presented in [52], implemented a number of models, such as ARMA, GARCH, FFNN (feed forward neural network), SVM (support vector machine), FIS (fuzzy inference system), LSE (least square estimation), and a combination of FIS and LSE, on data from PJM electricity market in 2004. Best MAPE1 value reported was about 9.6% and the computational time ranged from 80 to more than 10,000 seconds.

### 4.6.2 Model Validation Using PJM Market Data-2012

For further validation, we refitted our model (4.4) using data from the 2011 PJM market. We kept the values of the model parameters ($K$, $s$, and $l$) same as those obtained from 2005 data.

We then tested our model using data from 2012. To the best of our knowledge, no other models have used data from 2012, which reflects a more up to date condition of the PJM market. We have chosen six test periods, including a high peak scenario that occurred in June 21st, 2012. The values of MAPE1, MAE, and FMSE were first obtained using K-SVR considering LMP and demand as the only predictors. Results are presented in Table 4.7. The overall average values over all the test periods indicate a mean absolute deviation from observed LMPs of \$0.64/MWh with a standard deviation of \$0.836/MWh, representing a forecast error of approximately 1.2%. Also, note that the forecast error obtained for June 21st (peak day) was around 5.5%, which is significantly smaller when compared with the peak price predicting performance of other forecast models. For instance, see [45] where MAPE1 values are 20-25% for days (in 2006) with peak prices at or above \$150/MWh.

Hereafter, LMP predictions using K-SVR were obtained by extending the set of covariates beyond LMP and demand to include wind energy, temperature, dew point, and humidity. The results showed a drop in accuracy, where the MAPE1 values were consistently higher for all test periods, with an overall average of 1.727%. Further analysis of the negative impact of the additional covariates needs to be performed to better understand their influence on the LMP forecast. Similar observations were made in a related study [34], where demand and generator outages were found to be the most significant predictors of LMP. The relatively small forecast errors (MAPE1) obtained by K-SVR with 2012 data compared to 2006 may be attributed to both the inherent lower variability in the LMPs in 2012 (see Table 4.2) as well as the method used for selecting the number of clusters $K$ with low within cluster LMP variations.

## 4.7 Conclusions

With the proliferation of smart grids and distributed wind and solar energy resources, the variabilities in generation mix and the corresponding prices are likely to increase. This in turn

Table 4.7: K-SVR forecast accuracy for LMP in PJM 2012.

| Test period | MAPE1 | MAE | FMSE |
|---|---|---|---|
| 20-January | 0.289 | 0.109 | 0.161 |
| 5-March | 0.141 | 0.057 | 0.077 |
| 7-April | 0.115 | 0.029 | 0.035 |
| July 5-7 | 0.303 | 0.178 | 0.230 |
| 18-September | 0.665 | 0.234 | 0.402 |
| 21-June | 5.522 | 3.232 | 4.111 |
| Average | 1.172 | 0.640 | 0.836 |

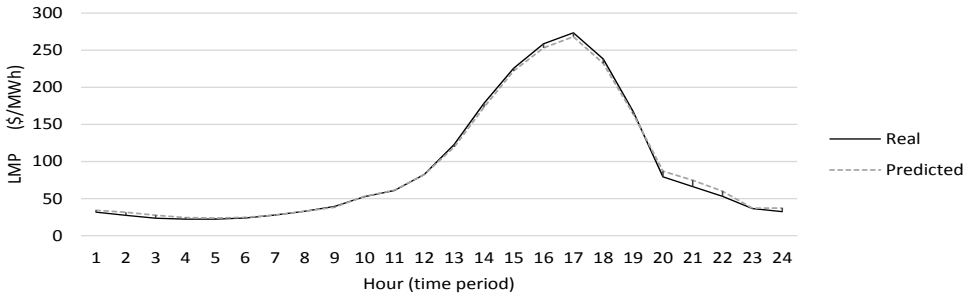


Figure 4.8: Real and forecast LMPs for June 21th.

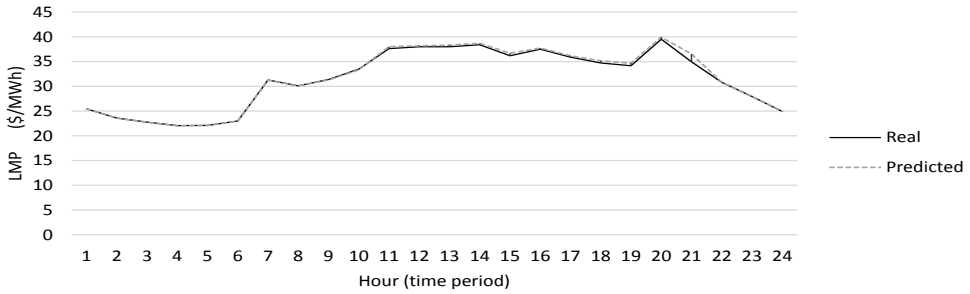


Figure 4.9: Real and forecast LMPs for September 18th.

will make prediction of LMPs in real time markets more challenging requiring faster models to process up to date data. Increase in the size of the restructured markets will also contribute to the need for models capable of faster processing of larger volume of data. These motivated our quest to develop an accurate LMP forecasting model that is fast enough to accommodate most up to date data on covariates. In order to reduce the impact of variability, we chose to first segregate the data into clusters with low within cluster variabilities and then apply the SVR on each cluster. Then we apply a SVM classification model to determine which cluster the future LMP is likely to belong.

The SVR of that cluster is then used to form the prediction. Our method is recursive, where, if the current time is $t$, prediction for hour $t+\tau$ uses the past data along with the predicted values for $t+1$ up to $t+\tau-1$. The choice of the use of SVR models is motivated by the inherent non-linearity of the relationship between LMP and its predictors, as well as the non-stationary nature of the mean and variance of LMP.

K-SVR was compared with other existing models including a classical model that most models in the literature are compared with and other more recent well performing ones. The results show that K-SVR model provides comparable forecast errors with reduced error variances, in most cases, while needing a significantly smaller computational time. The reduction in computational time in K-SVR is achieved primarily through elimination of the use of feature selection for all the model covariates for each prediction. K-SVR instead uses the information from ACF and PACF to pick the significant lag values (covariates) to build a prediction model. We have implemented K-SVR on a new data set (PJM 2012) which will provide a benchmark for future models. Contrary to our expectation, adding more explanatory covariates (wind energy, temperature, dew point, and humidity) did not result in an improved forecast performance. With increased green energy penetration and corresponding data availability, further studies should be designed to examine the influence of explanatory covariates.

# Chapter 5: Conclusions

Global warming is among the key issues that scientists and policy makers worldwide are deliberating on. The U.S. Energy Information Administration reports that in 2013 only 11% of the U.S. energy portfolio corresponded to renewable sources, whereas 32% of the total carbon emissions were produced in the power energy sector. To overcome global warming, the U.S. and European Union, among others, are currently increasing the use of renewable energy to reduce the reliance on fossil fuels energy based, as well as imposing stricter carbon policies. The development of a smart grid will help the integration of these renewable energy sources. Therefore, models capable to analyze the impact of carbon policies and the wide range of opportunities of renewable energy are highly needed. This thesis presents a compilation of two papers (both published in referred journals) that seek to address the problematic of both renewable energy integration and carbon emissions policy designs that will sustain adequate market demand for electricity needed to spur economic growth.

Among the CO2 emission reduction program, cap-and-trade (*C&T*) is one of the most popular policies. Economic studies have shown that *C&T* policies for electricity networks, while reducing emissions, will likely increase price and decrease consumption of electricity. Chapter 2 and Appendix C describe the details of the paper entitled *Design of Pareto Optimal CO2 Cap-and-Trade Policies for Deregulated Electricity Networks*. In this paper, it was demonstrated that a Pareto envelope generated by the proposed model can serve as a useful tool for policy makers to select alternative *C&T* policies while satisfying various interests of the electricity network

constituents. Results presented in the paper also examine the sensitivity of important factors affecting electricity markets such as social cost of carbon and demand-price sensitivity.

Carbon policies solely designed to reduce energy generation from fossil fuels sources (emissions level) may adversely affect electricity prices and consumption. Hence, new energy sources, such as DERs and microgrids, will play a predominant role to satisfy the projected increasing energy demand. Chapter 3 and Appendix D provide the details of the paper entitled *Emissions Control via Carbon Policies and Microgrid Generation: A Bilevel Model and Pareto Analysis*. The proposed model can be used by the microgrids operators to derive economic operational strategies for any given planning horizon. Operational strategies include decisions for green electricity production, storage/discharge of batteries, and trading of electricity with the smartgrid. The results from the model provide critical insights on how combinations of SCC, cap, and size of the community microgrids impact the electricity prices and the demand in the smartgrid. An example of such insights is that in the presence of emissions control (SCC and cap), higher green penetration by the microgrids reduces the average electricity cost and increases the demand in the smartgrid even in the peak hours. The model also allows the public (policy makers) to set targets for percent green penetration, emissions reduction, and market demand restoration, among others. A key limitation of the proposed model is that it does not consider the stochastic hourly variations of solar irradiance and wind speed, instead takes their average values. Also, the model considers solar and wind as the only possible sources of generation in the community microgrids. The model also ignores the ramp up/down constraints for conventional generators.

Finally, chapter 4 of this dissertation presents an accurate and computational efficient forecast model for electricity prices. Results from this model can be easily used in the microgrid-ISO bilevel model. Also, the forecast algorithm can be easily integrated into the two-layer mathematical-statistical framework described in Appendix C. Further testing needs to be done to analyze the capabilities of the model to forecast energy demand and wind-solar energy.

## References


[1] European Commission, 2013. An EU budget for low-carbon growth. Technical Report. Available at http://ec.europa.eu/clima/policies/finance/budget/docs/ pr_2012_03_15_en.pdf. Released on November 19, 2013. Accessed on December 12, 2013.

[2] Ruth, M. and Gabriel, S.A. and Palmer, K.L. and Burtraw, D. and Paul, A. and Chen, Y. and Hobbs, B.F. and Irani, D. and Michael, J. and Ross, K.M. and others. 2008. Economic and energy impacts from participation in the regional greenhouse gas initiative: A case study of the State of Maryland. *Energy Policy* **36** 2279–2289.

[3] Limpaitoon, T., Chen, Y., Oren, S., 2011. The impact of carbon cap and trade regulation on congested electricity market equilibrium. Journal of Regulatory Economics , 1–24.

[4] Nanduri, V., Otieno, W., 2011. Assessing the impact of different auction-based co2 allowance allocation mechanisms, in: Power and Energy Society General Meeting, 2011 IEEE, IEEE. pp. 1–7.

[5] W. Saad, Z. Han, H. V. Poor, T. Basar, Game-theoretic methods for the smart grid: an overview of microgrid systems, demand-side management, and smart grid communications, Signal Processing Magazine, IEEE 29 (5) (2012) 86–105.

[6] B. Tomoiag?, et al, Pareto optimal reconfiguration of power distribution systems using a genetic algorithm based on NSGA-II, Energies 6.3 (2013) 1439-1455.

[7] M. Bollen, F. Hassan, Integration of distributed generation in the power system, Vol. 80. John wiley & sons, 2011.

[8] A. Del Real, A. Arce, C. Bordons, Combined environmental and economic dispatch of smart grids using distributed model predictive control, International Journal of Electrical Power & Energy Systems 54 (0) (2014) 65 – 76.

[9] A. Chaouachi, R. M. Kamel, R. Andoulsi, K. Nagasaka, Multiobjective intelligent energy management for a microgrid, IEEE Transactions on Industrial Electronics 60 (4) (2013) 1688–1699.

[10] Y.-H. Chen, S.-Y. Lu, Y.-R. Chang, T.-T. Lee, M.-C. Hu, Economic analysis and optimal energy management models for microgrid systems: A case study in taiwan, Applied Energy.

[11] G.-C. Liao, Solve environmental economic dispatch of smart microgrid containing distributed generation system–using chaotic quantum genetic algorithm, International Journal of Electrical Power & Energy Systems 43 (1) (2012) 779–787.

[12] A. Khodaei, M. Shahidehpour, Microgrid-based co-optimization of generation and transmission planning in power systems, IEEE Transactions on Power Systems 28 (2) (2013) 1582–1590.

[13] G. E. Asimakopoulou, A. L. Dimeas, N. D. Hatziargyriou, Leader-follower strategies for energy management of multi-microgrids, IEEE Transactions on Smart Grid 4 (4) (2013) 1909–1916.

[14] A. Hawkes, M. Leach, Modelling high level system design and unit commitment for a microgrid, Applied energy 86 (7) (2009) 1253–1265.

[15] F. Feijoo, T. K. Das, Design of pareto optimal CO2 cap-and-trade policies for deregulated electricity networks, Applied Energy 119 (2014) 371–383.

[16] Dempe, S., 2003. Annotated bibliography on bilevel programming and mathematical programs with equilibrium constraints .

[17] Colson, B., Marcotte, P., Savard, G., 2007. An overview of bilevel optimization. Annals of operations research 153, 235–256.

[18] Fampa, M., Barroso, L., Candal, D., Simonetti, L., 2008. Bilevel optimization applied to strategic pricing in competitive electricity markets. Computational Optimization and Applications 39, 121–142.

[19] Hobbs, B., Metzler, C., Pang, J., 2000. Strategic gaming analysis for electric power systems: An mpec approach. Power Systems, IEEE Transactions on 15, 638–645.

[20] Gabriel, S., Leuthold, F., 2010. Solving discretely-constrained mpec problems with applications in electric power markets. Energy Economics 32, 3–14.

[21] Outrata, J., 1999. Optimality conditions for a class of mathematical programs with equilibrium constraints. Mathematics of Operations Research , 627–644.

[22] Scheel, H., Scholtes, S., 2000. Mathematical programs with complementarity constraints: Stationarity, optimality, and sensitivity. Mathematics of Operations Research , 1–22.

[23] Mordukhovich, B., 2005. Optimization and equilibrium problems with equilibrium constraints. Omega 33, 379–384.

[24] Hu, X., Ralph, D., 2007. Using epecs to model bilevel games in restructured electricity markets with locational prices. Operations research 55, 809–827.

[25] Ferris, M., Munson, T., 2000. Complementarity problems in gams and the path solver1. Journal of Economic Dynamics and Control 24, 165–188.

[26] Dafermos, S., 1983. An iterative scheme for variational inequalities. Mathematical Programming 26, 40–47.

[27] Pang, J., Chan, D., 1982. Iterative methods for variational and complementarity problems. Mathematical programming 24, 284–313.

[28] Su, C., Cottle, R., 2005. Equilibrium problems with equilibrium constraints: Stationarities, algorithms, and applications.

[29] Montgomery, D.C., Montgomery, D.C., Montgomery, D.C., 1984. Design and analysis of experiments. volume 7. Wiley New York.

[30] Deb, K., Pratap, A., Agarwal, S., Meyarivan, T., 2002. A fast and elitist multiobjective genetic algorithm: Nsga-ii. Evolutionary Computation, IEEE Transactions on 6, 182–197.

[31] H. Zareipour, C. A. Cañizares, K. Bhattacharya, J. Thomson, Application of public-domain market information to forecast ontario's wholesale electricity prices, Power Systems, IEEE Transactions on 21 (4) (2006) 1707–1717.

[32] J. Zhang, Z. Tan, S. Yang, Day-ahead electricity price forecasting by a new hybrid method, Computers & Industrial Engineering 63 (3) (2012) 695–701.

[33] Z. Tan, J. Zhang, J. Wang, J. Xu, Day-ahead electricity price forecasting using wavelet transform combined with arima and garch models, Applied Energy 87 (11) (2010) 3606–3610.

[34] P. Mandal, T. Senjyu, N. Urasaki, T. Funabashi, A. K. Srivastava, A novel approach to forecast electricity price for pjm using neural network and similar days method, Power Systems, IEEE Transactions on 22 (4) (2007) 2058–2065.

[35] P. Mandal, T. Senjyu, N. Urasaki, T. Funabashi, A. K. Srivastava, Short-term price forecasting for competitive electricity market, in: Power Symposium, 2006. NAPS 2006. 38th North American, IEEE, 2006, pp. 137–141.

[36] V. Vahidinasab, S. Jadid, A. Kazemi, Day-ahead price forecasting in restructured power systems using artificial neural networks, Electric Power Systems Research 78 (8) (2008) 1332–1342.

[37] Y. Y. Hong, C.-Y. Hsiao, Locational marginal price forecasting in deregulated electric markets using a recurrent neural network, in: Power Engineering Society Winter Meeting, 2001. IEEE, Vol. 2, IEEE, 2001, pp. 539–544.

[38] P. Mandal, A. K. Srivastava, T. Senjyu, M. Negnevitsky, A new recursive neural network algorithm to forecast electricity price for pjm day-ahead market, International Journal of Energy Research 34 (6) (2010) 507–522.

[39] D. Sansom, T. Downs, T. Saha, Support vector machine based electricity price forecasting for electricity markets utilising projected assessment of system adequacy data, in: The Sixth International Power Engineering Conference, Vol. 2, IPEC, 2003, pp. 783–788.

[40] D. C. Sansom, T. Downs, T. K. Saha, Evaluation of support vector machine based forecasting tool in electricity price forecasting for australian national electricity market participants, Journal of Electrical and Electronics Engineering, Australia 22 (3) (2003) 227–234.

[41] S. Fan, C. Mao, L. Chen, Next-day electricity-price forecasting using a hybrid network, IET generation, transmission & distribution 1 (1) (2007) 176–182.

[42] R. Swief, Y. Hegazy, T. Abdel-Salam, M. Bader, Support vector machines (svm) based short term electricity load-price forecasting, in: PowerTech, 2009 IEEE Bucharest, IEEE, 2009, pp. 1–5.

[43] P.-F. Pai, K.-P. Lin, C.-S. Lin, P.-T. Chang, Time series forecasting by a seasonal support vector regression model, Expert Systems with Applications 37 (6) (2010) 4261–4265.

[44] G. Li, C.-C. Liu, C. Mattson, J. Lawarree, Day-ahead electricity price forecasting in a grid environment, Power Systems, IEEE Transactions on 22 (1) (2007) 266–274.

[45] N. Amjady, F. Keynia, Day-ahead price forecasting of electricity markets by mutual information technique and cascaded neuro-evolutionary algorithm, Power Systems, IEEE Transactions on 24 (1) (2009) 306–318.

[46] N. Amjady, A. Daraeepour, Mixed price and load forecasting of electricity markets by a new iterative prediction method, Electric power systems research 79 (9) (2009) 1329–1336.

[47] A. Arabali, E. Chalko, M. Etezadi-Amoli, M. Fadali, Short-term electricity price forecasting, in: Power and Energy Society General Meeting (PES), 2013 IEEE, IEEE, 2013, pp. 1–5.

[48] N. Amjady, A. Daraeepour, Design of input vector for day-ahead price forecasting of electricity markets, Expert Systems with Applications 36 (10) (2009) 12281–12294.

[49] N. Amjady, F. Keynia, Application of a new hybrid neuro-evolutionary system for day-ahead price forecasting of electricity markets, Applied Soft Computing 10 (3) (2010) 784–792.

[50] H. Prem, N. S. Raghavan, A support vector machine based approach for forecasting of network weather services, Journal of Grid Computing 4 (1) (2006) 89–114.

[51] N. Amjady, F. Keynia, Day ahead price forecasting of electricity markets by a mixed data model and hybrid forecast method, International Journal of Electrical Power & Energy Systems 30 (9) (2008) 533–546.

[52] G. Li, C.-C. Liu, C. Mattson, J. Lawarree, Day-ahead electricity price forecasting in a grid environment, Power Systems, IEEE Transactions on 22 (1) (2007) 266–274.

# Appendices

## Appendix A: General Information About Appendices

Appendices include the copyright authorizations for the published material in the journal of Applied Energy and the journal Energy.

## Appendix B: Copyrights for Published Material

## Appendix B (continued)



**Jinyue Yan** <jinyue@kth.se> 12:34 PM (4 hours ago)
to me, F.Ogochi

Dear Author,
Thank you for your email. I can confirm - Elsevier journal authors retain the right to Use the article in full or in part to prepare other derivative works, including the article in a thesis or dissertation, with each work to include full acknowledgement of the article's original publication; see http://www.elsevier.com/about/policies/author-agreement/lightbox_scholarly-purposes for further permission.
best regards,

Professor J. Yan, Director of Future Energy Profile Royal Institute of Technology (KTH) and Malardalen University (MDU), Sweden

Editor-in-Chief of Applied Energy (IF: 5.261, 1.7 million downloads): http://www.journals.elsevier.com/applied-energy

Editor-in-Chief of Handbook of Clean Energy Systems: http://www.wiley.com/WileyCDA/WileyTitle/productCd-1118388585.html

ICAE2015: International Conference on Applied Energy, March 28-31, 2015, Abu Dhabi: www.applied-energy.org

ICAE2014 (Taipei, Taiwan), ICAE2013 (Pretoria, South Africa), ICAE2012 (Suzhou, China), ICAE 2011 (Perugia, Italy), ICAE2010 (Singapore), ICAE2009 (Hong Kong)

_____
From: Elsevier <stjournalsjhtp@elsevier.com> on behalf of Felipe Feijoo <felipefeijoo@mail.usf.edu>
Sent: Monday, April 20, 2015 01:13
To: Jinyue Yan
Subject: Applied Energy Enquiry: Authorization to use published paper in the appendixes of Thesis

The following enquiry was sent via the Elsevier website:

-- Sender --
First Name: Felipe
Last Name: Feijoo
Email: felipefeijoo@mail.usf.edu

## Appendix B (continued)



**Felipe Feijoo Palacios <felipefeijoo@mail.usf.edu>**

# Authorization request [150608-005230] [Reference: 150608-005230]

1 message

**EP Support** <support@elsevier.com> Tue, Jun 9, 2015 at 3:32 PM
Reply-To: EP Support <support@elsevier.com>
To: felipefeijoo@mail.usf.edu

**Subject**

Authorization request [150608-005230]

**Discussion**

**Response Via Email (Chricelda Red)** 09/06/2015 07.32 PM

Dear Dr. Feijoo,

Hope you are well and thank you for your e-mail.

I wish to inform that authors of an article accepted in to publish in Elsevier holds an Author rights, and I can confirm that including your paper in your thesis is included in your Author rights.

Please kindly see the list below of Author rights.

As an author, you retain rights for a large number of author uses, including use by your employing institute or company. These rights are retained and permitted without the need to obtain specific permission from Elsevier. These include:

- The right to make copies of the article for your own personal use, including for your own classroom teaching use.
- The right to make copies and distribute copies (including through e-mail) of the article to research colleagues, for the personal use by such colleagues (but not commercially or systematically, e.g. via an e-mail list or list serve).
- The right to post a pre-print version of the article on Internet web sites including electronic pre-print servers, and to retain indefinitely such version on such servers or sites (see also our information on electronic preprints for a more detailed discussion on these points.).
- The right to post a revised personal version of the text of the final article (to reflect changes made in the peer review process) on the author's personal or institutional web site or server, with a link to the journal home page (on elsevier.com).
- The right to present the article at a meeting or conference and to distribute copies of such paper or article to the delegates attending the meeting.
- For the author’s employer, if the article is a ‘work for hire’, made within the scope of the author’s employment, the right to use all or part of the information in (any version of) the article for other intra-company use (e.g. training).

## Appendix C: Published Material in Journal *Applied Energy*

# Appendix C (continued)

Applied Energy 119 (2014) 371–383

Contents lists available at ScienceDirect

Applied Energy

journal homepage: www.elsevier.com/locate/apenergy

## Design of Pareto optimal $CO_2$ cap-and-trade policies for deregulated electricity networks

Felipe Feijoo *[,1], Tapas K. Das [2]

*University of South Florida, 4202 E. Fowler Avenue, ENB118, Tampa, FL 33620, United States*

### HIGHLIGHTS

- A mathematical–statistical model for designing Pareto optimal $CO_2$ cap-and-trade policies.
- The model fills a gap in the current literature that primarily supports cap-and-trade policy evaluation but not policy design.
- Pareto optimal policies accommodate conflicting goals of the market constituents.
- Electricity demand-price sensitivity and social cost of carbon have significant influence on the cap-and-trade policies.
- Higher demand-price sensitivity increases the influence of penalty and social cost of carbon on reducing carbon emissions.

### ARTICLE INFO

*Article history:*
Received 15 August 2013
Received in revised form 2 January 2014
Accepted 4 January 2014

*Keywords:*
Electricity networks
Cap-and-trade
Game theory
MPEC/EPEC

### ABSTRACT

Among the $CO_2$ emission reduction programs, cap-and-trade (C&T) is one of the most used policies. Economic studies have shown that C&T policies for electricity networks, while reducing emissions, will likely increase price and decrease consumption of electricity. This paper presents a two layer mathematical–statistical model to develop Pareto optimal designs for $CO_2$ cap-and-trade policies. The bottom layer finds, for a given C&T policy, equilibrium bidding strategies of the competing generators while maximizing social welfare via a DC optimal power flow (DC-OPF) model. We refer to this layer as *policy evaluation*. The top layer (called *policy optimization*) involves design of Pareto optimal C&T policies over a planning horizon. The performance measures that are considered for the purpose of design are social welfare and the corresponding system marginal price (MP), $CO_2$ emissions, and electricity consumption level.



## 1. Introduction

A major part of the total $CO_2$ emissions come from the electricity production sector, e.g., 40% in the U.S. ([1]). In 2009, 70% of the electricity was produced from fossil fuel such as gas, coal, and petroleum ([2]). In 2005, the European Union Emissions Trading System (EU ETS) launched a cap-and-trade system that seeks to reduce the greenhouse gas (GHG) emissions by 21% by 2020 from the 2005 level. Currently, the EU ETS is the largest emission market in the world [3], and according to the European Commission [4], at least 20% of its budget for 2014–2020 will be spent on climate-related projects and policies. In the United States, as well as in the EU, different regulations have been discussed to cut $CO_2$ emissions such as carbon tax, renewable portfolio standards (RPS), and cap-and-trade programs (C&T). In the northeastern U.S., the Regional Greenhouse Gas Initiative (RGGI) has already implemented a C&T program through a nine state collaborative effort, which seeks to cut the $CO_2$ emissions by 10% by 2018. Recently the California Air Resources Board adopted a C&T program, held its first auction on November 2012, and started operation on January 2013. It is a part of California's historic climate change law (AB 32) that will reduce the carbon pollution to 1990 levels by 2020. Other countries who have already implemented C&T programs include New Zealand, Japan, The Netherlands, and Australia.

C&T policies implemented in the past for greenhouse gases had resulted in increase in cost for households, since the generators passed the emissions reduction costs to the consumers [5]. Linn [6] studied the economic impact of C&T policies for nitrogen oxides ($NO_x$) on deregulated firms. The study showed that the effect of reduction of $NO_x$ emissions may not increase electricity prices to a level which could fully compensate firms for their compliance costs, particularly for coal generators. This lead them to reduce their expected profit by as much as $25 billions. Chen et al. [7] developed a mathematical model to examine the ability of larger producers in an electricity market under $NO_x$ C&T policy to manip-

* Corresponding author. Tel.: +1 81 331 29776.
*E-mail addresses:* felipefeijoo@mail.usf.edu (F. Feijoo), das@usf.edu (T.K. Das).
[1] Industrial and Management Systems Engineering, University of South Florida, United States.
[2] Professor and Chair of Industrial and Management Systems Engineering, University of South Florida, United States.

0306-2619/$ - see front matter © 2014 Elsevier Ltd. All rights reserved.
http://dx.doi.org/10.1016/j.apenergy.2014.01.019

# Appendix C (continued)



ulate both the electricity and emission allowances markets. With regards to $CO_2$ cap-and-trade policies, Ruth et al. [8] examined the economic and energy impacts that the state of Maryland will have by joining the RGGI initiative. They identified several issues that are important to the acceptance and effectiveness of $CO_2$ C&T programs, such as rules for allowances distribution and subsidies for energy efficiency programs. Bird et al. [9] claimed that, while renewable energy will likely benefit from carbon cap-and-trade programs, C&T can also impact the ability of renewable energy generation to affect overall $CO_2$ emissions levels. They summarized the key issues for markets that are emerging under $CO_2$ C&T policies and also the policy design options to allow renewable energy generation to impact the emissions level. For further reading about economic impacts of $CO_2$ C&T, we refer the readers to Goettle and Fawcett [10] and Parmesano and Kury [11]. Linares et al. [12] have studied the impact of $CO_2$ C&T regulation and green certificates on power generation expansion model. They have shown that when a C&T policy is considered, locational marginal prices (LMPs) increase, emissions decrease, and installed green generation capacity increases. Limpaitoon et al. [2] studied the impact of C&T regulation and the interaction of demand elasticity, transmission network, market structure, and strategic behavior for an oligopoly electricity market (in the state of California). They concluded that GHG regulations will affect the system operations and market outcomes by increasing electricity prices (for both oligopoly and perfect competition scenarios), and reducing both GHG emissions and energy consumption. Their results also suggest that the interaction between $CO_2$ C&T regulations, market structure, and congestion might lead to potential abuses of market power and create more congestion, which will limit nuclear access to the market. This generates higher demand for emissions permit, which in turn increases permit prices. Fullerton and Metcalf [13] showed how certain environmental policies reduce profit under monopoly, raise prices, and reduce welfare profit. Rocha and Das [14] presented a game-theoretic model for developing joint bidding strategies in C&T allowances and electricity markets for competing generators. Rocha et al. [15] examined the impact of C&T policies on generation capacity investment.

Some of the current research concerning C&T policies is focused on the issue of development and analysis of allowance allocation mechanisms [16–18], and suggestions for policy effectiveness [8,9,19]. However, the open literature does not offer a methodology for design of $CO_2$ C&T policies that takes into account a range of conflicting measures of performance that appeal to different market stakeholders. For example, a consumer's concern is price increase [6,8,13], a generator's concern is profit/revenue reduction [2,13], and a policy maker's concerns include adequate emissions reduction and sustaining electricity consumption necessary to support economic growth [9,12,13]. There does not appear to be a consensus in the literature about economic impact that can be expected under C&T programs, neither is there an agreement about the choice of the C&T parameters and their values [20]. This paper attempts to fill the above gaps by presenting a 2-layer mathematical–statistical model to design Pareto optimal $CO_2$ C&T policies for deregulated electricity networks. This paper presents an elaborate sensitivity analysis of selected policy parameters (initial allowance cap, cap reduction rate, violation penalty) and network parameters (congestion, social cost of carbon, and demand-price sensitivity of the consumers).

In the bottom layer of the 2-layer model, the strategic bidding behavior of the competing generators is formulated as a bi-level mathematical model. The upper level model focuses on maximizing overall generator profit by bidding to the independent system operator (ISO) in the allowance and electricity markets. The lower level model focuses on social welfare maximization (or, social cost minimization) while meeting the network and policy constraints via a DC-OPF model. Each bi-level optimization problem is reformulated as an mathematical problem with equilibrium constraints (MPEC). Equilibrium bidding strategies among the competing generators are obtained by solving the set of MPECs as an equilibrium problem with equilibrium constraints (EPEC). Thus, the bottom layer of the 2-layer model essentially evaluates the impact of a given C&T policy on a network by obtaining the performance measures including electricity price, emissions level, and consumption level. The top layer model, using as input the results of the bottom layer model, develops regression equations for different network performance measures using the tools of analysis of variance (ANOVA). The regression equations relate the performance measures to the parameters of the C&T policy and the network. These equations are used in forming a multi-objective optimization model, solution of which yields the Pareto optimal $CO_2$ C&T policy designs.

The rest of the paper is organized as follow. In Section 2 we introduce the elements of a C&T policy and discuss social cost of carbon. Section 3 presents the complete 2-layer model-based methodology that obtains the Pareto optimal C&T policies. Section 4 demonstrates the application of our methodology on a sample network. Section 5 provides the concluding remarks.

## 2. Cap-and-trade and the social cost of carbon

Cap-and-trade is a market based mechanism that can be used to regulate the GHG emissions. The following are some of the primary features of a cap-and-trade mechanism.

- *Point of regulation*: Different approaches to regulate emissions in the electricity markets have been proposed and implemented. They range from regulating far upstream at the point of sale of fossil fuels to far downstream at the point of purchase of manufactured products and energy by ultimate consumers [21]. The upstream approach sets an emissions cap on producers of raw material that contains GHG (e.g., coal, gas, or petroleum), whereas the downstream approach regulates the direct producers of GHG [22].
- *Allowance distribution*: In an Emissions Trading System (ETS), one of the major concerns is how to distribute the allowances, as both the initial as well as the continuing distribution strategies have a significant influence on the final market equilibrium. Under a downstream regulation, several allowance allocation/distribution mechanisms have been studied in recent years. Most commonly discussed mechanisms in the literature are free allocation and auction based allocation [18,17]. Free allocation of allowances is often based either on historical emissions (known as *grandfathering*) or on energy input/product output (known as *benchmarking*) [23]. An allocation mechanism based on equal per capita cumulative emissions was presented in [24]. RGGI has implemented an auction based model with a combination of uniform and discriminatory pricing strategies. In the EU ETS, during the first and second trading periods, most of the allowances were given freely according to historical emissions. In the third trading period, free allowances allocation is scheduled to be progressively replaced by auctioning through 2020 [23].
- *Cap stringency*: This is a common feature in all C&T policies and refers to the rate of reduction of allowance cap. The cap reduction rate varies among markets due to network (market) intrinsic characteristics, policy decisions, external economic variables, and other C&T parameter values [25]. For instance, EU ETS implemented a 1.74% linear cap reduction for 2012–2020 and beyond ([26]), while RGGI implemented a fixed cap for 2009–2014 and a subsequent 2.5% reduction until 2018.

# Appendix C (continued)



- *Banking*: It allows generators to save allowances for future periods. Some markets also allow secondary trading of excess allowances at the end of each period. Banking rules could vary among different markets. EU ETS permitted allowance banking during phase I of its operation, but did not permit allowances to be carried over into phase II. From phase II and on, unlimited banking and borrowing is allowed [25]. The RGGI allows banking with no restrictions from current compliance periods into the future.
- *Penalty*: Fossil fuel generators must procure allowances commensurate with their emissions level or pay a penalty for any shortfall. EU ETS introduced a monetary penalty (40 euros during phase I and 100 euros for phase II), whereas California's policy require four additional allowances for each shortfall. IETA (International Emissions Trading Association) advises against using a non-compliance penalty by additional withdrawal of allowances. Instead, IETA recommends adopting a more traditional fixed monetary fine similar to those entered in the $SO_2$ and $NO_x$ emissions markets in the U.S. [27].

Other features of a cap-and-trade mechanism include initial cap size, safety value, revenue recycling and cost containment mechanisms [28,29].

In this paper, we consider a downstream regulation for C&T. The electricity generators are assume to acquire allowances by competing in an allowance market that is settled via discriminatory auction. The generators submit price-quantity bids that are arranged in a decreasing price order by the auctioneer. The price paid by each generator selected to received allowances is its own bid price [17]. As presented in our model in Section 3.2, the independent system operator (ISO) obtains the allowance allocation together with generation dispatch by incorporating the allowances auction model within the OPF model.

### 2.1. Social cost of carbon

The fiscal impact of $CO_2$ emissions on the environment and society is often referred to as the social cost of carbon (SCC). The most common means that are used to characterize SCC include marginal social cost of emissions and shadow prices of policies (e.g., cap-and-trade). Mandell [32] presents various definitions and estimates of SCC. The most common approach used in the literature defines the marginal social cost of carbon as "the cost to the society for each additional unit of carbon (in the form of $CO_2$) into the atmosphere." However, as the carbon remains in the atmosphere, it is difficult to estimate the cost of the carbon in the future. This motivates to redefine the SCC as "the present value of the monetized damage caused by each period of emitting one extra ton of $CO_2$ today as compared to the baseline." Another challenge for assessing SCC is in estimating the discount rate of the future social cost of $CO_2$.

The estimation of the SCC will always suffer from uncertainty, speculation, and lack of information [30]. This can be noticed, for example, in (1) estimating future emissions of greenhouse gases, (2) monetizing the effects of past and future emissions on the climate system, (3) assessing the impact of changes in climate on the physical and biological environment, and (4) translating environmental impacts into economic damages. Therefore, any effort to quantify and monetize the harms associated with climate change is bound to raise serious questions of science, economics, and ethics, and thus should be viewed as provisional [30]. Avato et al. [31] consider the carbon emissions as one of the main barriers to the development and deployment of clean energy technologies. They argue that emissions (a negative externality) is not valued and therefore not included into investment decisions by energy providers. Hence, by considering the monetary effects of emissions, i.e., the SCC, an increase in development and deployment of green technologies can be achieved.

Mandell [32] summarized the result of 211 SCC estimates from 47 different studies using an integrated assessment model (IAM). The SCC was estimated to have a mean value of $€19.70/tCO_2$, a median of $€5.45/tCO_2$ and an estimated range from $€1.24/tCO_2$ to $€451/tCO_2$. Using the shadow price approach, the estimated value of SCC has a range of $€32/tCO_2$ to $€205/tCO_2$ among the countries in the European Union. Hope [33] estimated SCC considering two scenarios: low emissions case, and a business as usual (BAU) emissions scenario. This study concluded that the median SCC for the BAU scenario is $\$100/tCO_2$ with a range of $\$10/tCO_2$—$\$270/tCO_2$, and a median of $\$50/tCO_2$ for the low emission scenario with a range of $\$5/tCO_2 - \$130/tCO_2$. The U.S. government, through the interagency working group (IWG), calculated the cost imposed on the global society by each additional ton of $CO_2$. They included health impact, economic dislocation, agricultural changes and other effects that climate change can impose on humanity. They estimated the SCC to have a range from $\$5/tCO_2$ to $\$65/tCO_2$. The IWG suggests setting the SCC to $\$21/tCO_2$. The IWG also propose to utilize a discount rate of 2.5–5% to address future SCC [34].

## 3. A model for developing Pareto optimal C&T policies

In this section, we present the complete methodology for designing Pareto optimal cap-and-trade policies for a fixed planning horizon. The methodology comprises a 2-layer model and a detailed solution approach.

### 3.1. A 2-layer model

The mathematical–statistical model for obtaining Pareto optimal C&T policy designs has two broad layers, which we call the top and the bottom layers.

The bottom layer (also referred to in this paper as the *policy evaluation* layer) involves obtaining equilibrium bidding strategies of the competing generators as a function of the C&T and network parameters, while maximizing social welfare via a DC-OPF. The network performance measures (emissions, electricity price, and consumption level) corresponding to the equilibrium bidding strategy, for a given C&T policy, are fed to the top layer (*policy optimization* layer) that obtains the Pareto optimal C&T policy designs. The top layer model first performs an analysis of variance (ANOVA) using the C&T and network parameters as factors, and the values of the network performance measures from the bottom layer as the responses. The ANOVA results are used to formulate regression equations for the network performance measures as functions of the C&T and network parameters. The Pareto optimal policy designs are then obtained by optimizing the regression equations via a multi-objective optimization model. The 2-layer model is given as follows.

$$\begin{aligned} &\text{Top layer}\{ \quad \text{Optimize } f(c,r,p,b,\pi,l) \\ &\text{Bottom layer}\begin{cases} \text{Maximize } \ g_i(\alpha_i,\omega_i), \quad \forall i \in I \\ \text{s.t.} \quad \text{Maximize } \ W(Q,\Theta) \\ \text{s.t.} \quad \text{Network and policy constraints.} \end{cases} \end{aligned} \tag{1}$$

In the top layer, $f(c,r,p,b,\pi,l)$ represents the objective function of the multi-objective optimization model, where $c$ is the cap size representing the maximum tons of $CO_2$ allowed per year ($tCO_2/yr$), $r$ is the yearly cap reduction rate (% of c) which goes into effect after a preset number of initial years, $p$ is the penalty for exceeding the emissions limit per allocated allowances ($\$/tCO_2$), $b$ represents the demand price sensitivity (slope of the demand curve), $\pi$ is the social cost of carbon ($\$/tCO_2$), and $l$ denotes the vector of line

# Appendix C (continued)



capacities (MW h) in the network (a determinant for network congestion). The bottom layer is formulated, for each generator $i \in I = \{1, 2, \ldots, n\}$, as a bi-level optimization model, where $g_i(\alpha_i, \omega_i)$ denotes the profit of generator $i$, and $\alpha_i$ (intercept of supply function) and $\omega_i$ (allowance price) are the generator bids in the electricity and allowances markets, respectively. $W(Q, \Theta)$ denotes the social welfare objective function for the DC optimal power flow problem, where $Q = (q_1, \ldots, q_i, \ldots, q_n)$ is the electricity dispatch and $\Theta = (\theta_1, \ldots, \theta_i, \ldots, \theta_n)$ is the allowances allocation. For each generator $i$, the bi-level model is solved as a mathematical problem with equilibrium constraints (MPEC). The equilibrium bidding strategies for all generators in both electricity and allowances markets are obtained by solving an equilibrium problem with equilibrium constraints (EPEC).

A schematic of the solution methodology for the 2-layer model is shown in Fig. 1. The methodology begins by designing a factorial experiment with all C&T and network related parameters as factors at two or more levels, and enumerating all possible factor level combinations [box (1)]. Factor level combinations, one at a time, while yet to be evaluated [box (2)], are forwarded as input to the bottom layer [box (3)]. In the bottom layer, after the cap is adjusted, MPEC/EPEC are solved to obtain equilibrium bidding strategies of the generators for each year of the planning horizon $T$ [boxes (6) and (7)]. The cap is considered to remain constant for the first $d$ years [box (4)] and decreasing thereafter [box (5)]. For a given factor level combination, once the equilibrium strategies are obtained for each year of the planning horizon $T$, the performance measures are updated [box (8)]. Once all years of the planning horizon are considered [box (9)], performance measures for the complete horizon for the current factor level combination are sent to ANOVA [box (10)] and the next combination is drawn for evaluation. When all factor combinations are exhausted [box (2)], ANOVA is performed [box (10)]. Regression equations (one for each measure of performance) are developed using ANOVA results and are sent as input for the multi-objective optimization [box (11)], which yields the Pareto optimal C&T policies. In what follows, we present the bi-level optimization model and discuss its solution using the MPEC approach. Thereafter, we explain how EPEC approach is used in obtaining the equilibrium bidding strategies for all generators in the electricity and allowance markets.

### 3.2. A bi-level model for joint allowance and electricity settlement

We adopt the bi-level framework that is commonly used in modeling generator bidding behavior in deregulated electricity markets [35–37]. We extend the objective functions of both levels by incorporating emissions penalty cost in the upper level (see (2)) and both allowances revenue and social cost of carbon in the lower level (see (6)). We also expand the constraints set in the lower level (DC-OPF) to accommodate a C&T policy, which are explained later. The solution of the modified DC-OPF yields both the electricity dispatch and the allowances allocation.

We consider that the generators and the consumers bid with their linear supply and demand functions, respectively. ISO determines energy dispatch and allowances allocation by maximizing social welfare while satisfying network and C&T constraints. The flow in the network is controlled by the Kirchhoff's law represented by the power transfer distribution factors (PTDFs). Capacity limit constraints on the lines are also considered. The supply cost of the generators, indexed by $i$, are assumed to be quadratic convex functions given by $C_i(q_i) = \alpha_i q_i + \beta_i q_i^2$, where $\alpha_i$ and $\beta_i$ represent the intercept and the slope of the supply function, respectively. Consumers, indexed by $j$, are considered to have negative benefit functions given by $-D_j(q_j) = -d_j q_j - b_j q_j^2,\ q_j \leq 0$ [38]. Generators are paid at their marginal cost, $\frac{dC_i(q_i)}{\partial q_i} = \alpha_i + 2\beta_i q_i$. Therefore, the profit of a generator $i$ is given as $(\alpha_i + 2\beta_i q_i)q_i - (A_i q_i + B_i q_i^2)$, where $A_i$ and $B_i$ are the true cost parameters of generator $i$ estimated through a standard Brownian motion model as follows. For any year $t$, $A_i^t$ is obtained as $A_i^t = \tau A_i^{t-1} + \sigma A_i^{t-1}\theta$, where $\tau$ represent a trend parameter, $\sigma$ represent the standard deviation of the process, and $\theta$ is a standard normal random variable. Our DC-OPF model is similar to that presented by Hu and Ralph [38], which showed that the use of the above functions ensure a unique solution. For some other variants of the OPF model, readers are referred to Berry et al. [39], Borenstein et al. [40] and Limpaitoon et al. [2].

Without loss of generality, we assume that the generators pass on the cost of allowance to the consumers by modifying (shifting up) the intercept ($\alpha_i$) of their supply functions as $\hat{\alpha}_i = \alpha_i + \gamma_i \omega_i$, where $\gamma_i$ is the $CO_2$ emissions factor and $\omega_i$ is the allowance bid (cost) of generator $i$. Hence, the cost of allowance ($\omega_i$) does not

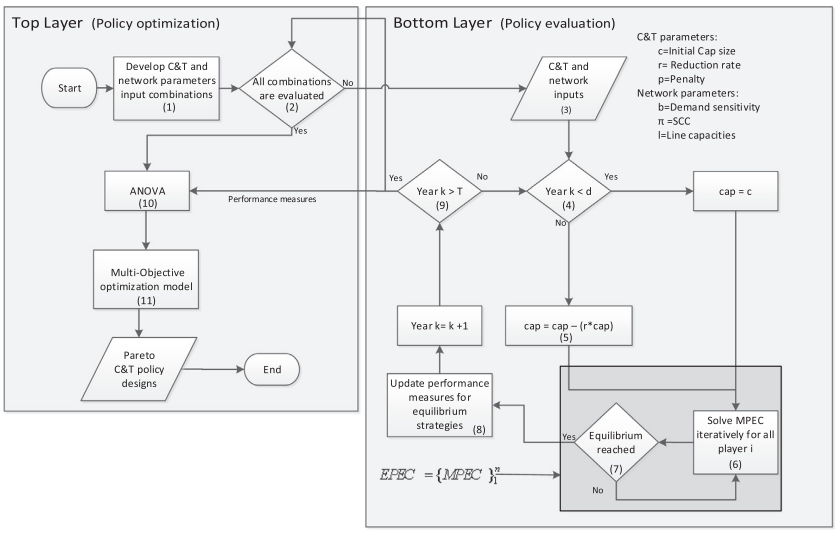


**Fig. 1.** A schematic of the solution methodology for the two-layer model.

# Appendix C (continued)



explicitly appear in the generator's (upper level) objective function. Note that, shifting of the supply function results in a new equilibrium point, where consumption (dispatch) is reduced and electricity price is increased (see Fig. 2). Hence, $\omega_i$ implicitly impacts the generator's profit through quantity dispatch $q_i$ and excess emissions penalty paid by the generators.

Social welfare is commonly considered in the literature to be total benefit to the consumers $D_j(\cdot)$ minus total cost to the generators $C_i(\cdot)$. Since allowances cost is passed onto the consumers, we include the cost of allowance as part of generators cost (i.e., use $\hat{\alpha}_i$ as the intercept of the supply cost function). We also add the allowance revenue to social welfare based on the assumption that it is recycled back as credits to consumers (to mitigate economic impacts of increased electricity prices) and subsidies to green generators. Revenue recycling has been widely discussed and recommended by many economists [e.g., 41–43]. We also subtract from the welfare function the social cost of the emissions, which is obtained by adding for all generators the product of the emissions quantities and the social cost of carbon.

Let $I = \{1,\ldots,n\}$ be the set of generator, and $J = \{1,\ldots,m\}$ be the set of consumers on the network. Let $\Phi = (\phi_1,\ldots,\phi_n)$ be the vector of generators' electricity bids, where $\phi_i = (\alpha_i, \beta_i)$ represents the bid of generator $i$, and $\Omega = (\omega_1,\ldots,\omega_n)$ be the vector of allowance bids. Let $Q = (q_1,\ldots,q_N)$, where $N = |(I \cup J)|$, be the electricity dispatch response vector obtained from the DC-OPF. Let $\Gamma = (\gamma_1,\ldots,\gamma_n)$ be the vector of $CO_2$ emissions factor ($tCO_2$/MW h) of the generators. Then the yearly emissions of generator $i$ is given by $\gamma_i * q_i$. Let $\Theta = (\theta_1,\ldots,\theta_n)$ be the vector of yearly allowance allocation to the generators. Therefore, given the supply function bids and the allowance bids of all other generators, $\Phi_{-i}$ and $\Omega_{-i}$, respectively, the bi-level optimization model for generator $i$ is given as follows.

$$\underset{\alpha_i,\omega_i}{\text{Max}}\ (\alpha_i + 2\beta_i q_i)q_i - (A_i q_i + B_i q_i^2) - p(\gamma_i q_i - \theta_i) \tag{2}$$

$$\text{s.t. } \alpha_i \in [\underline{A}, \overline{A}], \tag{3}$$

$$\omega_i \in [\underline{W}, \overline{W}], \tag{4}$$

$$\alpha_i + \gamma_i \omega_i \leqslant d_j, \quad \forall j,\ j = 1,\ldots,J, \tag{5}$$

$$Q, \Theta = \underset{q,\theta}{\text{Max}} \left[\sum_j D_j(q) - \sum_i C_i(q) + \sum_i \omega_i \theta_i - \sum_i q_i \gamma_i \pi\right] \tag{6}$$

$$\text{s.t } -C_l \leqslant \sum_{k\in(i,j)} q_i \varphi_{kl} \leqslant C_l, \quad l = 1,\ldots,L, \ (\epsilon_l^-, \epsilon_l^+) \tag{7}$$

$$\sum_i q_i + \sum_j q_j = 0, \quad (\mu) \tag{8}$$

$$c - \sum_i \theta_i \geqslant 0, \quad (\lambda) \tag{9}$$

$$\gamma_i q_i - \theta_i \geqslant 0, \quad \forall i \in I, \ (\rho_i) \tag{10}$$

$$q_i - R_{lo} \geqslant 0, \quad \forall i \in I, \ (\tau_i) \tag{11}$$

$$R_{up} - q_i \geqslant 0, \quad \forall i \in I, \ (\upsilon_i) \tag{12}$$

$$q_i \geqslant 0, \quad \forall i \in I, \ (\pi_i) \tag{13}$$

$$-q_j \geqslant 0, \quad \forall j \in J, \ (\kappa_i) \tag{14}$$

$$\theta_i \geqslant 0, \quad \forall i \in I. \ (\zeta_i) \tag{15}$$

In the formulation, the elements within parentheses in constraints (7)–(15) represent the corresponding dual variables or shadow prices. Our attention is focused primarily on $\mu$, which represents the system marginal energy price (cost) of the network [2]. Constraints (3) and (4) incorporate the bounds for electricity and allowance bids, respectively. Constraint (5) ensures that the supply function intersects with the demand curve. Objective function (6) represent the social welfare where $C_i(q)$ is the cost to the generators obtained using the shifted supply function $(\hat{\alpha}_i, \beta_i)$, $D_j(q)$ is the benefit to the consumers, and $\pi$ denotes to the SCC. Flow constraints are given in (7), where $C_l$ is the line capacity and $\varphi_{kl}$ is the PTDF for node $k$ and line $l$. Energy balance is maintained by constraint (8). Constraint (9) ensures that the allocation of allowances does not violate the cap. Since we do not consider banking of allowances, constraint Eq. (10) ensures that a generator is not allocated with more allowances than the emissions emitted. Maximum and minimum production level for each generator are controlled by constraints (11) and (12) respectively. Finally, (13)–(15) are non-negativity constraints for electricity dispatch and allowance allocation.

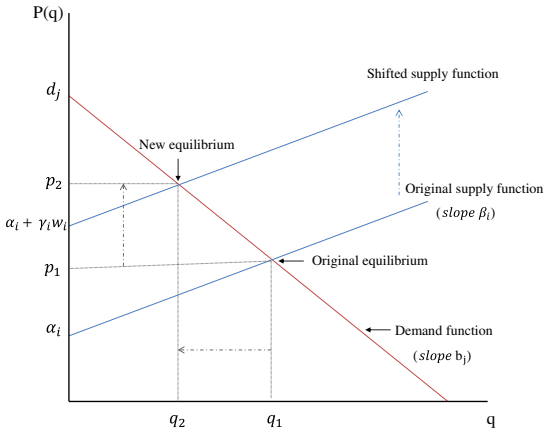


**Fig. 2.** Electricity market equilibrium with supply function shifted by allowance cost.

### 3.3. Model solution for equilibrium bidding strategies: A MPEC/EPEC approach

Bi-level optimization models have been widely studied in the literature [44,45]. Bi-level models include two mathematical programs, where one serves as a constraint for the other. For the lower level problem, with a convex objective function and non-empty feasible set, the first order necessary conditions for a solution to be optimal are given (under some regularity conditions) by the *Karush Kuhn Tucker* (KKT) equations. Hence, replacing the lower level problem in Section 3.2 by the set of optimality conditions, yields what is known as a mathematical program with equilibrium constraints (MPEC). Further details on the MPEC models can be found in [46–48].

In the other hand, an equilibrium program with equilibrium constraint (EPEC) is defined as a game, EPEC $= \{(\text{MPEC})\}_1^n$, among competing generators. Typically, MPECs have non-convex feasible sets (due to the complementarity constraints), therefore the resulting games are likely to have non-convex feasible strategy sets. Since a global equilibrium for this type of games is difficult to identify, a *local Nash equilibrium* concept is presented in [38]. The local Nash equilibrium is comprised of stationary points of the MPEC problem for each player $i$ in the game EPEC $= \{(\text{MPEC})\}_1^n$. Lack of knowledge of other players' exact strategies, which might also be changing with time, along with other uncertainties may minimize the value of the effort required to seek global optimal strategies.

Literature presents different strategies to solve EPECs, of which linear and non-linear complementarity (LCP/NCP) formulation [49] and diagonalization methods [50,51] are the most discussed. In this paper we consider a diagonalization method algorithm as presented in [52]. In the diagonalization method, MPECs for all generators are solved, for which we use a regularization method in

# Appendix C (continued)



conjunction with NLP solvers [53,54]. For other techniques to solve MPECs, readers are refers to [55,47].

### 3.4. Multi-objective optimization for Pareto optimal designs

In a complex system with multiple performance measures and the set of significant design factors that affect them, the nature of the relationship could vary widely among the performance measures. That is, a set of factor values (levels) that are optimal for a particular performance measure may not be optimal for other measures. For example, the C&T and network parameters that minimizes $CO_2$ emissions may not yield lowest electricity prices, when both reduced emissions and lower prices may be among the priorities. Therefore, a design approach that can balances among multiple priorities must be considered. Multi-objective optimization models, that yield Pareto fronts, provide such an approach.

A Pareto front is a set of points representing factor level combinations where all points are Pareto efficient. A Pareto efficient point indicates that no measure of performance can be further improved without worsening one or more of the other performance measures. Similarly, for any point outside of the Pareto front, by moving the point onto the front, one or more measures can be improved without worsening the others. In order to obtain these points, we formulate the multi-objective optimization problem (16). We used the NSGA-II genetic algorithm [57] to solve the model and obtain the Pareto envelope. Equations CL (consumption level), TE (total emissions), and AMP (average marginal price) are explained in detail in Section 4.3.1.

$$\begin{aligned} &\text{Min } TE(c,r,p,b,\pi,l),\\ &\text{Max } CL(c,r,p,b,\pi,l),\\ &\text{Min } AMP(c,r,p,b,\pi,l),\\ &\text{s.t. bounds on } c,r,p,b,\pi,l. \end{aligned} \tag{16}$$

## 4. C&T policy development for a sample network

In this section, we demonstrate, using a sample electricity network, how our model can be used to develop Pareto optimal C&T policies. We conduct the numerical study in two phases. We first implement the bottom layer of the model for evaluating a number of different ad hoc C&T policy scenarios, as shown in Table 1. In the ad hoc policies, penalty and the cap vary within their corresponding ranges (per RGGI), and SCC varies according to the IWG recommendations (see Section 2). The above variations coupled with different levels of demand-price sensitivity (slope of the demand curve) are captured as the three main scenarios SN1, SN2, and SN3 (see Table 1). Samples of results obtained by evaluating these scenarios are presented to demonstrate the impact of both C&T policy and network parameters. In phase 2, we implement the complete two layer model. We first develop a factorial experiment and conduct ANOVA. Response surfaces derived from ANOVA are used to obtain Pareto optimal C&T policies via multi-objective optimization model.

### 4.1. Sample electricity network

We consider a sample network with 4-nodes and 5-lines (see Fig. 3). Similar sample networks were considered in numerical studies in [58–62]. The network operates under a $CO_2$ C&T policy with three generation nodes and one load node. The network has two fossil fuel (coal) generators (GENCO1 and GENCO3) and one green generator (GENCO2). The green generator does not participate in the allowance auction. Emissions factor for both coal generators is assume to be one (i.e., 1 ton of $CO_2$ emission per MW h of electricity production). Allowances are distributed among competing generators using a discriminatory (pay-as-bid) auction pricing strategy. The cap is considered to decrease at a yearly rate of 2.5% starting the sixth year of implementation (this is similar to the policy implemented by the RGGI). Line capacities for C1 and C4 are set to 80 MW h, while the rest of the lines have a capacity of 120 MW h. The model is implemented for a thirty year planning horizon. Demand is considered to increase at a yearly rate of 1.1%, which is implemented in our model by raising the intercept of the demand function.

For supply functions, we consider that the generators bid only on the intercept parameter $\alpha$. Intercept parameter $A_i$ of the true cost function of the generators is estimated using a Brownian motion model (BMM) as explained in Section 3.2. The trend parameter ($\tau$) of the BMM model is set to 0.0059 for green generator and 0.0662 for coal generators. The standard deviation ($\sigma$) of the BMM model is set to 0.081 for green generator and 0.0714 for coal generators. The above numerical values were obtained from the Electric Power Annual Data 2009 ([63]). For year $t = 1$, $A_i^1$ is set to 2011 cost given in the above data. For all generators, we set the value of $B_i$ to 0.05.

### 4.2. Analysis of ad hoc C&T policies

We implemented the policy evaluation part of our model in GAMS using MPEC and CONOPT3 solvers. For each scenario in Table 1, we obtained the equilibrium bidding strategies for the complete planning horizon. For each year of the planning horizon, we recorded performance measures such as production levels of each generator (sum of which is the consumption level), marginal electricity price, generator profits, emission levels, and market share of the green generator. These yearly measures are used in calculating the network performance measures for the complete horizon.

#### 4.2.1. Impact of C&T and network parameters on performance measures

In this section we examine the effect (sensitivity) of some of the policy and network parameters on the performance measures. A more comprehensive analysis of the impact of the C&T and network parameters on the network performance is conducted in Section 4.3.1 using the analysis of variance (ANOVA) technique.

Tables 2–4 summarize the performance measures for various ad hoc C&T policies belonging to SN1, SN2, and SN3 with a cap of 80 $tCO_2$. It can be observed that a higher sensitivity in the price reduces production (or consumption) and emission levels. Social cost of carbon further contributes to this reduction. Along with the reduction of emissions, the percentage of market share of green

**Table 1**
Ad hoc C&T policies.

| Scenario designation | Demand ($b$) (slope) | Penalty ($p$) ($/$tCO_2$) | SCC ($\pi$) ($/$tCO_2$) | Cap ($c$) ($tCO_2$) |
|---|---|---|---|---|
| SN1 | 0.025 | 10–50 | 0–21 | 80–120 |
| SN2 | 0.05 | 10–50 | 0–21 | 80–120 |
| SN3 | 0.075 | 10–50 | 0–21 | 80–120 |

# Appendix C (continued)



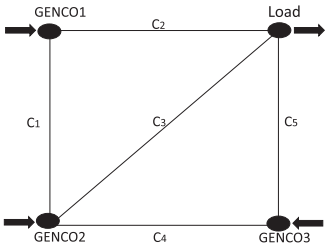


**Fig. 3.** A 4-node sample network for numerical study.

sources is in general higher when consumers are more sensitive, and their profits are slightly reduced. Electricity prices suffer a significant reduction of almost $10/MW h on average.

*4.2.1.1. Generators behavior.* Fig. 4 shows all three generators' yearly production levels for the scenario SN1 under two different penalty levels ($30/tCO$_2$ and $50/tCO$_2$) and zero SCC. Recall that we considered the emissions factor $\gamma = 1$, which means each MW h of coal based electricity production results in one unit (ton) of $CO_2$ emission. Hence, sum of the production levels of GENCO1 and GENCO3 represents the total emission in the network. GENCO2 is the green generator with zero emissions. The thicker solid lines in the figures represent the total emissions cap for the network.

In the low penalty cost scenario ($p = \$30/tCO_2$), as the demand grows over the years and the cap reduces, the coal generators still find it profitable to increase their share of production (above green generation) while paying more in penalties. Whereas, in the high penalty cost scenario ($p = \$50/tCO_2$), the coal generators control their bids to significantly lower their production. In fact, till year 22, the combined emissions from GENCO 1 and 3 remain below the cap. The green generator maintains a high level of production.

**Table 2**
Performance of ad hoc C&T policies belonging to SN1 (demand slope 0.025).

| | SCC-0 | | | SCC-21 | | |
|---|---|---|---|---|---|---|
| | 10 | 30 | 50 | 10 | 30 | 50 |
| Production (MW h) | 8021 | 8023 | 7483 | 8026 | 7397 | 5893 |
| Emissions ($tCO_2$) | 5633 | 5641 | 4038 | 5636 | 4018 | 2057 |
| Market share (%) | 32 | 36 | 45 | 38 | 55 | 57 |
| AMP ($/MW h) | 66.7 | 67.9 | 67.4 | 67.8 | 68.2 | 69.8 |
| Profit ($) | 129,436 | 128,290 | 165,259 | 128,470 | 167,445 | 203,593 |

**Table 3**
Performance of ad hoc C&T policies belonging to SN2 (demand slope 0.05).

| | SCC-0 | | | SCC- 21 | | |
|---|---|---|---|---|---|---|
| | 10 | 30 | 50 | 10 | 30 | 50 |
| Production (MW h) | 7742 | 7617 | 6155 | 7738 | 6305 | 5942 |
| Emissions ($tCO_2$) | 5094 | 5060 | 2580 | 4917 | 2415 | 2016 |
| Market share (%) | 34 | 34 | 58 | 36 | 62 | 66 |
| AMP ($/MW h) | 55.6 | 57.01 | 60.98 | 56.39 | 60.04 | 62.15 |
| Profit ($) | 103,740 | 97,776 | 155,773 | 1,067,733 | 161,307 | 176,520 |

**Table 4**
Performance of ad hoc C&T policies belonging to SN3 (demand slope 0.075).

| | SCC-0 | | | SCC- 21 | | |
|---|---|---|---|---|---|---|
| | 10 | 30 | 50 | 10 | 30 | 50 |
| Production (MW h) | 7983 | 6754 | 5575 | 6672 | 5694 | 5641 |
| Emissions ($tCO_2$) | 5772 | 3472 | 1905 | 3362 | 2052 | 1982 |
| Market share (%) | 28 | 49 | 66 | 50 | 64 | 65 |
| AMP ($/MW h) | 42.37 | 48.19 | 54.47 | 48.65 | 53.82 | 54.12 |
| Profit ($) | 64,193 | 103,425 | 142,079 | 107,056 | 139,902 | 141,322 |

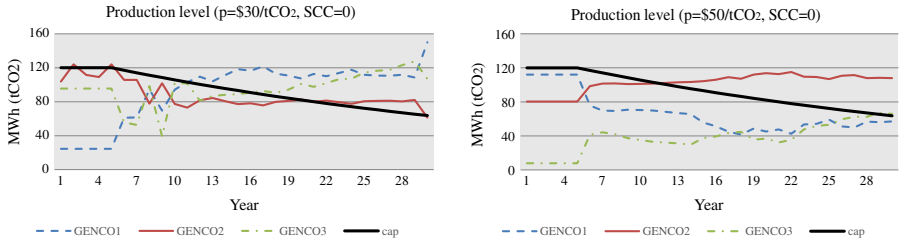


**Fig. 4.** Production level comparison for SN1 under different penalty levels.

# Appendix C (continued)



A higher cost of penalty causes the total electricity consumption over the horizon to fall from 8256 MW h to 6213 MW h (a 23% reduction) and the total emissions for the horizon to reduce from 5635 $tCO_2$ to 2795 $tCO_2$ (a 50% reduction). The share of green generation in the two penalty levels are 32% and 49%, respectively. The average marginal electricity price rises from \$52.7/ MW h to \$60.8/ MW h (a 15.4% increase).

The penalty level choice varies for different markets. California's C&T set a penalty of 4 allowances per ton not covered by allowances, and the reserve allowance price was set to \$10.71 in 2013, which is set to increase to \$11.34 for 2014 [64]. In the case of EU ETS, the penalty was set to 40 euros in the phase I, and increased to 100 euros during phase II [25]. The effectiveness of penalty is affected by allowance prices and quantity (cap), among others. For example, if allowance prices drop, as was the case in phase I in the EU ETS, a low level of penalty will unlikely generate emissions reduction since generators can either afford to buy allowances, and/or pay a penalty for non-compliance.

*4.2.1.2. Generation and emission levels.* Fig. 5 shows the effect of SCC on total coal-based generation (or, equivalently, total emissions) as well as total green generation over the horizon for increasing values of penalty cost and demand-price sensitivity. As expected, at higher values of penalty and demand-price sensitivity, the coal-based generation decreases. At higher SCC, the reduction in coal-based generation is sharper (plot b). Also at higher SCC and penalty costs, the effect of increased demand-price sensitivity is reduced (plot b). As far as green generation is concerned, it can be observed (plot a) that higher demand-price sensitivity compounds the effect of penalty in increasing generation. This effect is further pronounced when SCC is higher (plot b).

*4.2.1.3. Electricity prices.* Fig. 6 depicts the average marginal prices under the same parameter combinations as in Fig. 5. It can be seen that higher penalty produces higher price, which increases further with increased SCC, as expected. We also note that, higher demand-price sensitivity significantly lowers the price at all levels of penalty and SCC.

*4.2.1.4. Generators market share.* Fig. 7 shows the market share of green and coal based energy, aggregated over the complete horizon. As expected, an increase in penalty (from \$10/$CO_2$ to \$50/$tCO_2$) raises the share of green energy from 32% to 45%. The increase in green energy is further noticeable when the SCC is included. By considering SCC (Plot (b)) the share of green based energy achieves a 57% versus a 43% of coal share for a penalty of \$50/$tCO_2$. Note that adding a SCC produces the share of green based energy to be higher than coal based energy share (which is not the case when SCC = 0). As mentioned in Section 2, SCC could accelerate the transition to green technologies. Results presented in this section helps to quantify the assertion.

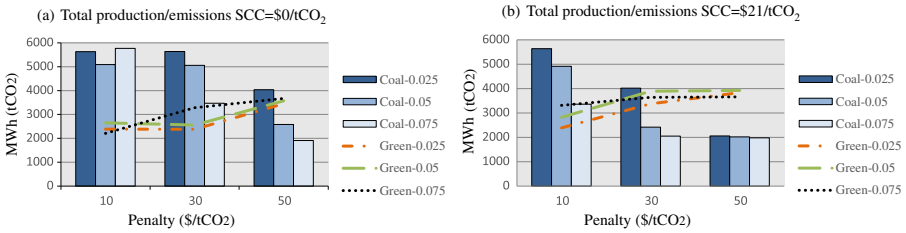


**Fig. 5.** Impact of penalty and demand-price sensitivity on $CO_2$ emissions (for different values of SCC).

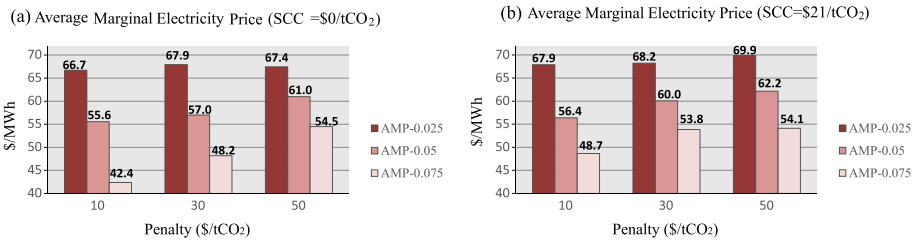


**Fig. 6.** Impact of penalty and demand-price sensitivity on average marginal price of electricity (for different values of SCC).

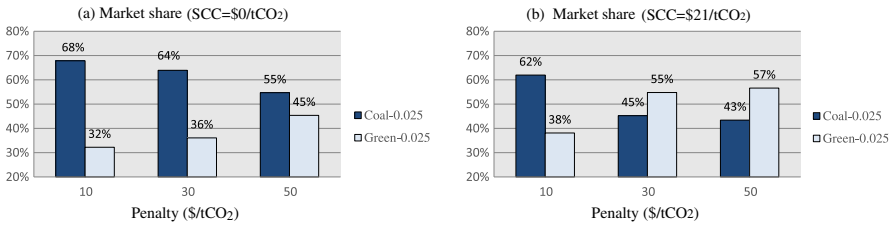


**Fig. 7.** Impact of penalty and SCC on market share of green generation.

# Appendix C (continued)



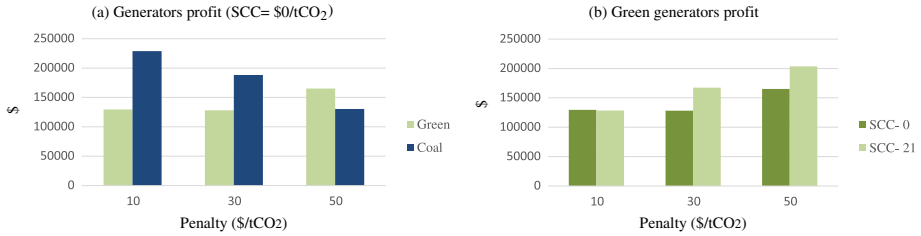


**Fig. 8.** Generator profits for different penalties and SCC.

*4.2.1.5. Generators profit.* Fig. 8(a) shows the cumulative generator profits (coal generators are combined as one) for different penalty levels and zero SCC. When higher penalty for non-compliance is considered, coal generators see their profit to be reduced (approximately 43%). Coal based generators reduce their electricity production in order to maintain emissions according with the allowances allocated. It was also observed in Figs. 5 and 7 that the increase of penalty reduces the emissions (and hence production) and coal market share, resulting in lower profits for coal based generators. Green generators observe an increase in profit as we consider higher penalties (approximately 21%). It can be observed that including SCC (Plot (b)) further increases the cumulative profit of the green generator. These results show that C&T policies will likely have conflicting implications. On one hand, the environment and society may benefit from a reduction in emissions and increase in green power. On the other hand, coal-based generators do not have incentives to participate in the market because of profit loses. This is one of the major concerns, for example in the U.S., where fossil fuel energy sources are still a major portion of the energy portfolio.

### 4.3. Development of Pareto optimal C&T policies

In this section, we first develop response surface equations for each performance measure using a factorial design and ANOVA. We then demonstrate how those equations can be used to obtain Pareto optimal C&T designs.

#### 4.3.1. Performance response surface generation

In order to obtain the response surfaces for the network performance measures, we adopt a designed factorial experiment comprising six factors: penalty, cap size, cap reduction rate, SCC, demand-price sensitivity, and line capacities (congestion). We consider each factor at three levels resulting in a $3^6$ factorial experiment. The numerical levels of the factors are given in Table 5. All 729 factor combinations were evaluated using the bottom layer model, and the resulting performance measures were used to conduct ANOVA (with type I error $\alpha = 0.05$) utilizing the R software (version 2.15.1). Results from ANOVA conducted separately for each of the three performance measures (total $CO_2$ emissions (TE), total electricity consumption (CL), and average marginal price (AMP)) are presented below. For more detailed information about factorial design of experiments and ANOVA, we refer the readers to [56].

**Table 5**
Factor levels for $3^6$ experiment.

| Factors | Coded values | | |
|---|---|---|---|
| | −1 | 0 | 1 |
| Cap reduction ($r$) (%) | 2.5 | 5 | 7.5 |
| Initial cap size ($c$) | 80 | 120 | 160 |
| Penalty ($p$) | 10 | 30 | 50 |
| Demand-price sensitivity ($b$) | 0.075 | 0.05 | 0.025 |
| Congestion ($l$) | 120 | 100 | 80 |
| SCC ($\pi$) | 0 | 21 | 42 |

*4.3.1.1. Total $CO_2$ Emissions Level: TE.* When TE was used as the response variable, all main factors and some two level interactions were found to be statistically significant. Using the significant factors and interactions, a second order regression model was developed. The model has a multiple $R$-squared value of 0.839 and an adjusted $R$-squared value of 0.833.

$$\begin{aligned} TE = {} & 3696.63 - 1186.03\pi - 989.66p + 618.84b + 683.56c \\ & - 322.92l - 316.37r + 270.66\pi^2 + 353.8p^2 - 253.34b^2 \\ & + 648.22p\pi + 340.81c\pi + 256.36pc - 219.83bl - 217.25pb \\ & + 194.49pl + 184.02l\pi - 142.89r\pi - 141.85pr - 128.33bc \\ & - 124.11b\pi + 259.39p^2\pi - 312.67\pi^2p^2 + 161.21p\pi^2 \\ & - 150.1cp^2 + 234.56\pi^2b^2 + 61.19cr. \end{aligned}$$

Factor effect plots for the six significant main factors are presented in Fig. 9. All the factors exhibit approximately linear behavior over the three levels, indicating that their impact on TE are either *higher the better* or *lower the better*.

*4.3.1.2. Total Consumption Level: CL.* As in the case for TE, all six main factors and some two level interactions were found to be statistically significant. A second order regression model incorporating the significant factors and interactions was developed. The model has a multiple $R$-squared value of 0.842 and an adjusted $R$-squared value of 0.835. Plots of the factor effects at various levels are presented in Fig. 10. Non-linearity in the factor effects can be observed to be a bit higher than in the case of TE, which can also be seen in the regression equation that has more non-linear terms.

$$\begin{aligned} CL = {} & 7315.88 - 1237.44\pi + 689.52b - 758.85p + 425.21c \\ & - 263.04l - 521.34\pi^2 - 344.16b^2 - 232.83r + 86.63l^2 \\ & + 84.57c^2 + 67.39p^2 + 304.15p\pi - 216.74bl + 167.3pl \\ & - 166.88bp + 157.77pc + 156.99b\pi + 146.67l\pi + 128.88c\pi \\ & + 128.26cr + 292.63\pi^2b^2 - 91.97pr + 112.51p\pi^2 \\ & - 111.2c\pi^2 - 60.14r\pi + 144.98rc^2 + 55.24cl + 95.2bl^2 \\ & + 92.89cl^2 - 52.3bc + 90.43pl^2 + 84.05rl^2 + 244.67p^2\pi \\ & - 89.2cp^2. \end{aligned}$$

*4.3.1.3. Average Marginal System Price: AMP.* For AMP as the response variable, the only main factor that was not statistically significant was the cap reduction rate. Some of the two level interactions were significant. The regression model has a multiple $R$-squared value of 0.637 and an adjusted $R$-squared value of 0.621. Lower $R$-squared value is, perhaps, indicative of the fact that

# Appendix C (continued)



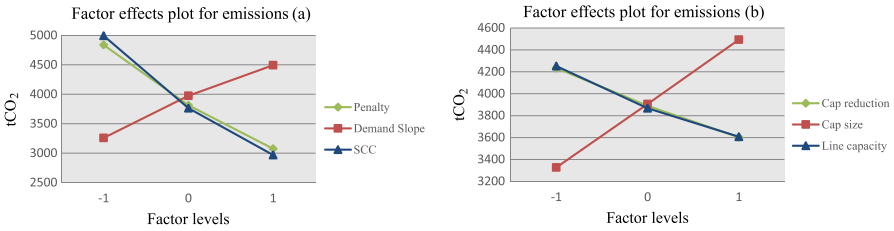


**Fig. 9.** Factor effect plots for total emissions.

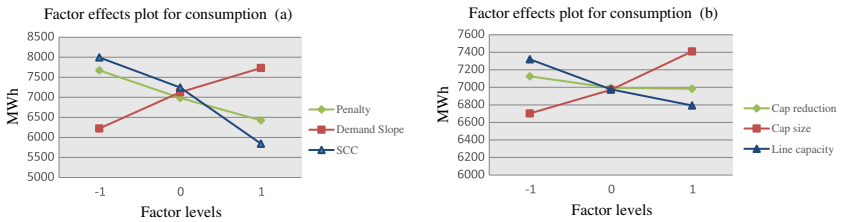


**Fig. 10.** Factor effect plots for consumption level.

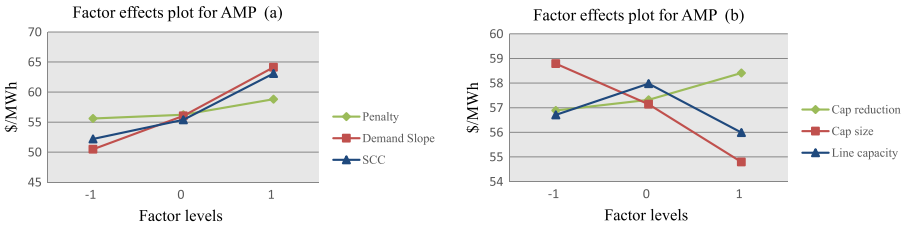


**Fig. 11.** Factor effect plots for average electricity marginal price.

the factor effects have a higher order (>2) of non-linearity (see Fig. 11), which could not be captured from a 3-level factorial experiment.

$$\begin{aligned} AMP = {} & 55.1717 + 6.809\pi + 2.9673\pi^2 + 1.6172p + 0.9829p^2 \\ & + 5.2204b + 3.6239b^2 - 1.1398c - 0.3786l - 3.2884l^2 \\ & - 0.2442r - 0.6737r^2 - 0.3548c^2 - 0.8224p\pi - 1.0853b\pi \\ & + 0.8359r\pi + 0.7443l\pi - 3.5386\pi^2 b^2 + 2.4959\pi^2 l^2 \\ & - 2.0189p^2\pi + 2.3979p^2 b + 1.2676p^2 r - 0.7284pc \\ & - 0.7782pl - 0.8208br - 1.1743cr - 0.7409lr - 1.3341cr^2 \\ & - 1.2651rc^2 - 1.3376cl. \end{aligned}$$

### 4.4. Design of Pareto optimal C&T policies

We first demonstrate the need for Pareto optimal designs to simultaneously accommodate multiple performance measures.

**Table 6**
Performance measures of C&T policies optimized for individual measures.

| Optimized measure | Consumption (MW h) | Emissions ($tCO_2$) | AMP ($/MW h) |
|---|---|---|---|
| CL | 8950 | 7272 | 35.8 |
| TE | 5606 | 765 | 54.7 |
| AMP | 7747 | 4274 | 21.9 |

Thereafter, we discuss how to obtain the Pareto optimal C&T policy designs.

The need for Pareto designs is motivated by the results presented in Table 6, which shows that a C&T policy optimized for a particular performance measure tends to produce poor outcomes for the other measures. Notice from the table that, a design optimized for TE yields a consumption level of 5606 MW h whereas the design optimized for CL has a consumption level of 8950 MW h. Similarly, a design optimized for CL yields an AMP of $35.8/MW h, which is much higher than $21.9/MW h which is attained by a design optimizing AMP.

We formulated a multi-objective optimization model, as presented earlier in (16), using the equations developed above for TE, CL, and AMP. Of the six variables in these equations, SCC ($\pi$) and demand-price sensitivity ($b$) are not controlled by a C&T policy maker, and hence each of those variables were considered at three different fixed values, resulting in nine possible combinations. For each of these nine combinations, the multi-objective model was solved and the optimal settings for the other four variables (cap reduction rate, cap size, penalty, and congestion level) were obtained.

Before presenting the complete Pareto envelopes for all three measures, parts (a), (b), and (c) of Fig. 12 show the Pareto fronts for each pair of performance measures. Each front is plotted for three combinations of coded values of $(\pi, b)$ $(0,-1)$, $(0,0)$, and $(0,1)$. It may be noted that, for a fixed SCC value of 21 (coded value of 0), lower values of demand-price sensitivity result in higher Par-

# Appendix C (continued)



**Table 7**
Average values of performance measures from Pareto envelopes.

| $\pi$ | $b$ | CL | TE | AMP |
|---|---|---|---|---|
| −1 | −1 | 7125.03 | 3921.19 | 43.79 |
| −1 | 0 | 7850.56 | 4788.07 | 50.18 |
| −1 | 1 | 8505.91 | 5689.47 | 57.51 |
| 0 | −1 | 6314.70 | 2907.43 | 50.17 |
| 0 | 0 | 7425.11 | 3760.65 | 52.41 |
| 0 | 1 | 7774.23 | 4007.63 | 61.64 |
| 0 | −1 | 4942.74 | 2620.05 | 57.53 |
| 0 | 0 | 5888.57 | 2883.47 | 63.02 |
| 0 | 1 | 6699.43 | 3232.42 | 67.95 |

eto fronts and therefore increases the levels of consumption, emissions, and AMP.

We obtained the Pareto envelopes (considering all three measures) for all nine combinations of $\pi$ and $b$. For each envelope, we computed the average values of the measures over all the Pareto efficient points. In the solution of the multi-objective model, we chose to obtain 100 Pareto efficient points. The results are presented in Table 7. As observed earlier in Fig. 12, for fixed value of $\pi$, decrease in demand-price sensitivity (from −1 to 1) results in increase in CL, TE, and AMP. For a fixed value of $b$, increase in SCC results in decreases in CL and TE and an increase in AMP.

To illustrate further, we present in Fig. 13 two complete Pareto envelopes for two arbitrarily chosen combination of $(\pi, b)$ of (0,0) and (0,1). It can be observed that Pareto efficient designs that minimize emissions yield lower consumption levels and higher average marginal prices. Allowing higher emissions results in increase in consumption and decrease in price. This shows that stricter emissions policies will increase electricity prices. For sixty of the one hundred efficient points on the Pareto envelope (0,1), the corresponding values of the four C&T design parameters are shown in Table 8. We picked a subset of the designs (instead of all 100) for reasons of space. In what follows, we describe how an envelope can be used to select an appropriate design for a C&T policy.

Consider the scenario with $\pi = 0$ and $b = 1$. Say that it is desired to have an aggregated consumption level above 9000 MW h and the total emissions below 6000 $tCO_2$ over the complete planning horizon. It can be seen from the Table 8 that the Pareto efficient designs 85, 86, 87, 90, and 91 are those that meet both the consumption and emissions conditions. Since AMP is lower the better, the Pareto efficient design with the lowest AMP should be chosen. The design 86 happens to be the one with lowest AMP of $56.17/MW h, for which the actual consumption level is 9017.7 MW h and the emissions is 5211.57 $tCO_2$. The values of the C&T design parameters for the Pareto efficient point 86 are $p = \$28.2/tCO_2$, $r = 0.075$, $c = 159.05$ $tCO_2$, and $l = 120$ MW h.

## 5. Concluding remarks

In this paper, we have developed a mathematical–statistical model that allows us to obtain Pareto optimal C&T policies. The model has two broad layers. The bottom (policy evaluation) layer evaluates the impact of C&T and network parameters on the performance measures of an electricity network. The top (policy optimization) layer obtains the Pareto optimal designs using the results of the bottom layer. The existing literature, containing both empirical studies [8] and mathematical models [2,12], helps to effectively evaluate the impact of given C&T policies. Our research extends the literature from evaluation of C&T policies to design of Pareto optimal policies that accommodate different interests of the network constituents (e.g., higher consumption, lower emissions, lower electricity prices). We have demonstrated that a Pareto envelope generated by our model can serve as an useful tool for policy makers to select alternative C&T policies satisfying various interests of the electricity network constituents. Results presented in the paper also examine the sensitivity of important factors affecting electricity markets such as social cost of carbon and demand-price sensitivity. Electricity generators can benefit from this model by using the bottom layer to assess impact of given C&T policies on their bidding strategies and capacity expansion planning.

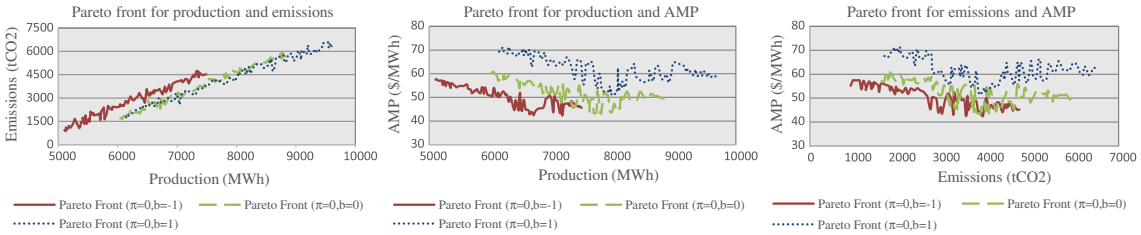


**Fig. 12.** Pareto fronts for each possible performance pair.

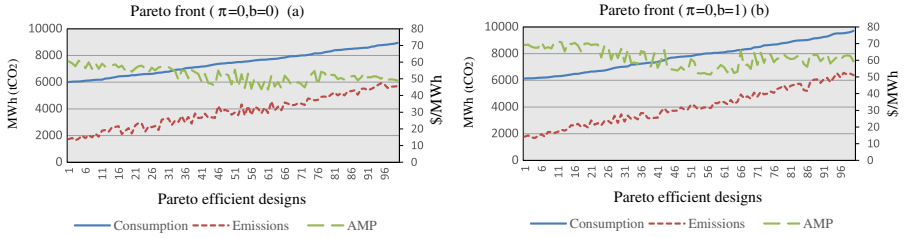


**Fig. 13.** Pareto envelopes.

# Appendix C (continued)



**Table 8**
Pareto C&T designs for $\pi$=0 and $b$ = 1.

| Design | Coded values | | | | Real values | | | | Performance measures | | |
|---|---|---|---|---|---|---|---|---|---|---|---|
| | *p* | *r* | *c* | *l* | Penalty | Cap red. | Cap | Lines cap | Consumption | Emissions | AMP |
| 1 | 1.00 | 1.00 | −1.00 | 0.71 | 50.00 | 0.075 | 80.00 | 85.80 | 6137.88 | 1780.92 | 69.25 |
| 2 | 1.00 | 1.00 | −0.91 | 0.65 | 50.00 | 0.075 | 83.76 | 87.06 | 6145.92 | 1870.79 | 69.36 |
| 3 | 1.00 | 1.00 | −1.00 | 0.90 | 50.00 | 0.075 | 80.00 | 82.04 | 6148.38 | 1715.37 | 68.14 |
| 4 | 1.00 | 1.00 | −1.00 | 0.99 | 50.00 | 0.075 | 80.00 | 80.16 | 6160.64 | 1682.59 | 67.51 |
| 5 | 1.00 | 0.75 | −1.00 | 0.96 | 50.00 | 0.069 | 80.00 | 80.78 | 6181.69 | 1823.88 | 67.59 |
| 6 | 1.00 | 1.00 | −1.00 | 0.21 | 50.00 | 0.075 | 80.00 | 95.84 | 6201.12 | 1955.74 | 71.04 |
| 7 | 0.91 | 0.96 | −1.00 | 0.90 | 48.12 | 0.074 | 80.00 | 82.04 | 6213.98 | 1779.46 | 67.14 |
| 8 | 1.00 | 1.00 | −0.51 | 0.71 | 50.00 | 0.075 | 99.45 | 85.80 | 6225.41 | 2132.34 | 67.85 |
| 9 | 0.97 | 1.00 | −0.51 | 0.77 | 49.37 | 0.075 | 99.45 | 84.55 | 6254.46 | 2125.61 | 67.14 |
| 10 | 1.00 | 1.00 | −1.00 | −0.07 | 50.00 | 0.075 | 80.00 | 101.49 | 6295.03 | 2054.07 | 71.32 |
| 11 | 1.00 | 0.91 | −0.92 | −0.07 | 50.00 | 0.073 | 83.14 | 101.49 | 6313.72 | 2159.18 | 71.11 |
| 12 | 1.00 | 0.97 | −0.72 | −0.11 | 50.00 | 0.074 | 91.29 | 102.12 | 6327.84 | 2284.80 | 70.88 |
| 13 | 1.00 | 0.94 | −0.31 | 0.96 | 50.00 | 0.073 | 107.61 | 80.78 | 6363.68 | 2222.25 | 65.33 |
| 14 | 1.00 | 0.40 | −1.00 | −0.07 | 50.00 | 0.060 | 80.00 | 101.49 | 6401.94 | 2363.68 | 70.67 |
| 15 | 1.00 | 0.91 | −0.25 | −0.07 | 50.00 | 0.073 | 110.12 | 101.49 | 6438.88 | 2642.75 | 69.64 |
| 16 | 1.00 | 0.00 | −0.96 | −0.07 | 50.00 | 0.050 | 81.57 | 101.49 | 6485.80 | 2601.45 | 70.45 |
| 17 | 1.00 | 1.00 | −0.06 | −0.11 | 50.00 | 0.075 | 117.65 | 102.12 | 6490.29 | 2745.16 | 68.95 |
| 18 | 0.91 | 0.49 | −0.28 | 0.90 | 48.12 | 0.062 | 108.86 | 82.04 | 6528.29 | 2518.58 | 65.14 |
| 19 | 1.00 | 0.91 | −0.45 | −0.48 | 50.00 | 0.073 | 101.96 | 109.65 | 6587.54 | 2638.59 | 69.98 |
| 20 | 1.00 | 0.97 | −0.72 | −0.61 | 50.00 | 0.074 | 91.29 | 112.16 | 6607.42 | 2459.61 | 70.16 |
| 21 | 1.00 | 0.50 | −0.03 | −0.07 | 50.00 | 0.062 | 118.90 | 101.49 | 6654.26 | 2987.76 | 69.12 |
| 22 | 0.98 | 0.91 | −0.45 | −0.58 | 49.69 | 0.073 | 101.96 | 111.53 | 6664.47 | 2682.77 | 69.59 |
| 23 | 1.00 | 0.91 | −0.28 | −0.58 | 50.00 | 0.073 | 108.86 | 111.53 | 6698.67 | 2795.07 | 69.40 |
| 24 | 1.00 | 0.97 | 0.29 | 0.99 | 50.00 | 0.074 | 131.45 | 80.16 | 6713.10 | 2625.98 | 61.75 |
| 25 | 1.00 | 0.91 | −0.01 | −0.48 | 50.00 | 0.073 | 119.53 | 109.65 | 6735.35 | 2953.48 | 68.80 |
| 26 | 1.00 | 0.91 | −0.03 | −0.58 | 50.00 | 0.073 | 118.90 | 111.53 | 6792.65 | 2975.01 | 68.69 |
| 27 | 1.00 | 1.00 | 0.51 | 0.97 | 50.00 | 0.075 | 140.24 | 80.63 | 6862.97 | 2779.06 | 60.34 |
| 28 | 1.00 | 0.78 | 0.63 | −0.10 | 50.00 | 0.070 | 145.25 | 101.96 | 6938.01 | 3333.37 | 66.18 |
| 29 | 0.00 | 0.97 | −0.75 | 0.90 | 29.92 | 0.074 | 90.04 | 82.04 | 6974.37 | 2813.35 | 61.37 |
| 30 | 1.00 | 0.50 | 0.65 | −0.07 | 50.00 | 0.062 | 145.88 | 101.33 | 7012.55 | 3451.77 | 66.88 |
| 71 | −0.07 | 1.00 | 1.00 | −0.60 | 28.67 | 0.075 | 160.00 | 112.00 | 8476.50 | 4769.34 | 57.23 |
| 72 | −0.79 | 0.79 | −0.64 | −0.37 | 14.24 | 0.070 | 94.43 | 107.45 | 8521.54 | 5134.39 | 64.49 |
| 73 | −0.25 | 1.00 | 0.62 | −0.85 | 24.90 | 0.075 | 144.94 | 117.02 | 8618.33 | 4954.14 | 58.49 |
| 74 | −0.76 | 0.95 | −1.00 | −0.51 | 14.86 | 0.074 | 80.00 | 110.27 | 8631.73 | 5000.01 | 63.85 |
| 75 | −0.76 | 0.93 | −0.72 | −0.61 | 14.86 | 0.073 | 91.29 | 112.16 | 8655.31 | 5165.07 | 63.57 |
| 76 | −0.35 | 1.00 | 0.56 | −0.85 | 23.02 | 0.075 | 142.43 | 117.02 | 8675.17 | 5064.49 | 58.84 |
| 77 | −0.65 | 0.94 | 0.49 | −0.58 | 17.06 | 0.073 | 139.61 | 111.53 | 8699.10 | 5354.30 | 61.09 |
| 78 | −0.79 | 0.79 | 0.99 | −0.11 | 14.24 | 0.070 | 159.69 | 102.12 | 8755.75 | 5451.45 | 60.71 |
| 79 | −0.76 | −0.58 | −0.15 | −0.51 | 14.86 | 0.036 | 114.20 | 110.27 | 8794.46 | 5618.38 | 63.46 |
| 80 | −0.69 | 0.96 | −0.56 | −0.92 | 16.12 | 0.074 | 97.57 | 118.43 | 8823.88 | 5281.57 | 61.67 |
| 81 | −0.76 | 0.93 | 0.75 | −0.51 | 14.86 | 0.073 | 149.96 | 110.27 | 8882.61 | 5587.20 | 60.74 |
| 82 | −0.79 | 0.94 | 0.71 | −0.57 | 14.24 | 0.073 | 148.39 | 111.37 | 8938.72 | 5662.54 | 60.94 |
| 83 | −0.76 | 0.43 | 0.76 | −0.60 | 14.86 | 0.061 | 150.27 | 112.00 | 8985.68 | 5730.99 | 62.43 |
| 84 | −0.76 | 0.43 | 0.76 | −0.61 | 14.86 | 0.061 | 150.27 | 112.16 | 8992.19 | 5736.41 | 62.40 |
| 85 | −0.24 | 0.75 | 0.98 | −0.99 | 25.22 | 0.069 | 159.06 | 119.84 | 9006.27 | 5262.84 | 57.73 |
| 86 | −0.24 | 1.00 | 0.98 | −1.00 | 25.22 | 0.075 | 159.06 | 120.00 | 9017.70 | 5211.57 | 56.17 |
| 87 | −0.99 | 0.99 | −0.33 | −0.75 | 10.16 | 0.075 | 106.98 | 114.98 | 9066.58 | 5915.05 | 64.11 |
| 88 | −0.99 | 0.99 | 0.27 | −0.75 | 10.16 | 0.075 | 130.82 | 114.98 | 9142.15 | 6042.52 | 63.04 |
| 89 | −0.99 | 0.84 | 0.27 | −0.75 | 10.16 | 0.071 | 130.82 | 114.98 | 9155.30 | 6067.47 | 63.28 |
| 90 | −0.76 | 1.00 | 0.74 | −0.85 | 14.86 | 0.075 | 149.65 | 117.02 | 9187.42 | 5805.73 | 59.44 |
| 91 | −0.99 | 0.93 | 0.88 | −0.61 | 10.16 | 0.073 | 155.29 | 112.16 | 9254.73 | 6077.10 | 61.47 |
| 92 | −0.96 | 0.13 | 0.76 | −0.73 | 10.78 | 0.053 | 150.27 | 114.51 | 9285.63 | 6189.26 | 63.63 |
| 93 | −0.69 | 0.96 | 0.88 | −1.00 | 16.12 | 0.074 | 155.29 | 120.00 | 9371.63 | 5859.68 | 58.04 |
| 94 | −0.93 | 0.93 | 0.77 | −0.95 | 11.41 | 0.073 | 150.90 | 119.06 | 9478.67 | 6196.06 | 60.20 |
| 95 | −0.98 | −0.87 | 0.78 | −0.98 | 10.47 | 0.028 | 151.22 | 119.69 | 9513.49 | 6539.19 | 61.98 |
| 96 | −0.93 | 0.93 | 0.76 | −1.00 | 11.41 | 0.073 | 150.27 | 120.00 | 9521.13 | 6226.28 | 60.02 |
| 97 | −0.98 | −0.87 | 0.98 | −0.98 | 10.47 | 0.028 | 159.06 | 119.53 | 9525.84 | 6554.68 | 62.46 |
| 98 | −0.99 | −0.01 | 0.99 | −0.94 | 10.16 | 0.050 | 159.69 | 118.75 | 9571.73 | 6450.68 | 62.98 |
| 99 | −0.99 | −0.01 | 0.96 | −1.00 | 10.16 | 0.050 | 158.43 | 120.00 | 9620.80 | 6492.06 | 62.63 |
| 100 | −0.99 | 0.99 | 0.99 | −1.00 | 10.16 | 0.075 | 159.69 | 120.00 | 9716.60 | 6381.46 | 59.18 |

Computational challenges associated with our model are limited to the bottom layer (in particular, solving the EPEC problem), especially when a network has a large number of generators [38]. The number of time periods in the planning horizon also adds to the computational burden as EPEC needs to be solved for each period. However, the computation time for the top layer model is independent of the size of the network, number of generators, and the time periods of the planning horizon.

**Acknowledgements**

Authors acknowledge the useful comments and suggestions provided by the reviewers which have significantly improved the quality of the manuscript.

**References**

[1] Stavins R. A us cap-and-trade system to address global climate change. The Brookings Institution, The Hamilton Project; 2007.

# Appendix C (continued)




[2] Limpaitoon T, Chen Y, Oren S. The impact of carbon cap and trade regulation on congested electricity market equilibrium. J Regul Econ 2011:1–24.
[3] Cummins Mark. EU ETS market interactions: the case for multiple hypothesis testing approaches. Appl Energy 2013;111:701–9.
[4] European Commission. An EU budget for low-carbon growth. Technical Report; 2013. <http://ec.europa.eu/clima/policies/finance/budget/docs/pr_2012_03_15_en.pdf> (released 19.11.13, accessed 12.12.13).
[5] Shammin M, Bullard C. Impact of cap-and-trade policies for reducing greenhouse gas emissions on us households. Ecol Econ 2009;68:2432–8.
[6] Linn J. The effect of cap-and-trade programs on firms profits: evidence from the nitrogen oxides budget trading program. J Environ Econ Manage 2010;59:1–14.
[7] Chen Y, Hobbs B, Leyffer S, Munson T. Leader-follower equilibria for electric power and NOx allowances markets. Comput Manage Sci 2006;3:307–30.
[8] Ruth M, Gabriel S, Palmer K, Burtraw D, Paul A, Chen Y, et al. Economic and energy impacts from participation in the regional greenhouse gas initiative: a case study of the state of Maryland. Energy Policy 2008;36:2279–89.
[9] Bird L, Holt E, Levenstein Carroll G. Implications of carbon cap-and-trade for U.S. voluntary renewable energy markets. Energy Policy 2008;36:2063–73.
[10] Goettle R, Fawcett A. The structural effects of cap and trade climate policy. Energy Econ 2009;31:S244–53.
[11] Parmesano H, Kury T. Implications of carbon cap-and-trade for electricity rate design, with examples from Florida. Electr J 2010;23:27–36.
[12] Linares P, Javier Santos F, Ventosa M, Lapiedra L. Incorporating oligopoly, $CO_2$ emissions trading and green certificates into a power generation expansion model. Automatica 2008;44:1608–20.
[13] Fullerton D, Metcalf G. Cap and trade policies in the presence of monopoly and distortionary taxation. Resource Energy Econ 2002;24:327–47.
[14] Rocha P, Das TK. Finding joint bidding strategies for day-ahead electricity and related markets. In: Handbook of networks in power systems I. Springer; 2012. p. 61–88.
[15] Rocha P, Das T, Nanduri V, Botternd A. Impact of $CO_2$ cap-and-trade programs on restructured power markets with generation capacity investments. In preparation; 2013.
[16] Goulder L, Hafstead M, Dworsky M. Impacts of alternative emissions allowance allocation methods under a federal cap-and-trade program. J Environ Econ Manage 2010;60:161–81.
[17] Nanduri V, Otieno W. Assessing the impact of different auction-based $CO_2$ allowance allocation mechanisms. In: Power and energy society general meeting, 2011 IEEE. IEEE; 2011. p. 1–7.
[18] Bushnell J, Chen Y. Allocation and leakage in regional cap-and-trade markets for $CO_2$. Resource Energy Econ 2010.
[19] California Market Advisory Committee and others. Recommendations for designing a greenhouse gas cap-and-trade system for California recommendations of the Market Advisory Committee to the California Air Resources Board. Technical Report; 2007.
[20] Nanduri Vishnu, Kazemzadeh Narges. Economic impact assessment and operational decision making in emission and transmission constrained electricity markets. Appl Energy 2012;96:212–21.
[21] Hobbs B, Bushnell J, Wolak F. Upstream vs. downstream $CO_2$ trading: a comparison for the electricity context. Energy Policy 2012;7:3632–43.
[22] Mansur, Erin. Upstream versus downstream implementation of climate policy. Technical Report. National Bureau of Economic Research; 2010. <http://www.nber.org/papers/w16116.pdf?new_window=1> (accessed 17.12.13).
[23] Hong Taehoon, Koo Choongwan, Lee Sungug. Benchmarks as a tool for free allocation through comparison with similar projects: focused on multi-family housing complex. Appl Energy 2014;114:663–75.
[24] Pan Xunzhang, Teng Fei, Wang Gehua. Sharing emission space at an equitable basis: allocation scheme based on the equal cumulative emission per capita principle. Appl Energy 2014;113:1810–8.
[25] Crossland Jarrod, Li Bin, Roca Eduardo. Is the European Union Emissions Trading Scheme (EU ETS) informationally efficient? Evidence from momentum-based trading strategies. Appl Energy 2013;109:10–23.
[26] European Commision. EU Action against climate change. Technical Report. The EU Emissions Trading Scheme; 2009. <http://ec.europa.eu/clima/publications/> (accessed 31.07.13).
[27] International Emissions Trading Association. IETA response on CARB cap-and-trade program rules. Technical Report. IETA; 2010. <http://www.ieta.org> (accessed 31.07.13).
[28] Center for Climate and Energy Solutions. Climate change 101: understanding and responding to global climate change. Technical Report. C2ES; 2011. <http://www.c2es.org/docUploads/climate101-fullbook.pdf> (accessed 31.07.13).
[29] Rocha P. Cap-and-trade modeling and analysis for electric power generation systems. Ph.D. thesis. University of South Florida; 2011.
[30] U.S. Department of Energy. Monetization of emissions reduction benefits. Technical Report. U.S. Department of Energy. <https://www1.eere.energy.gov/buildings/appliance_standards/commercial/pdfs/dt_prelim_tsdch16.pdf> (chapter 16, accessed 18.12.13).
[31] Avato M, Barroso L, Candal Patrick, Coony Jonathan. Accelerating clean energy technology research, development, and deployment: lessons from non-energy sectors. The World Bank 2008;138:121–42.
[32] Mandell S. Carbon emission values in cost benefit analyses. Transport Policy 2011;18:888–92.
[33] Hope C. The social cost of $CO_2$ from the page09 model. Economics Discussion Paper; 2011.
[34] Bell RG, Callan D. More than meets the eye: the social cost of carbon in us climate policy, in plain English. Policy Brief 2011.
[35] Fampa M, Barroso L, Candal D, Simonetti L. Bilevel optimization applied to strategic pricing in competitive electricity markets. Comput Optimiz Appl 2008;39:121–42.
[36] Hobbs B, Metzler C, Pang J. Strategic gaming analysis for electric power systems: an MPEC approach. IEEE Trans Power Syst 2000;15:638–45.
[37] Gabriel S, Leuthold F. Solving discretely-constrained MPEC problems with applications in electric power markets. Energy Econ 2010;32:3–14.
[38] Hu X, Ralph D. Using EPECS to model bilevel games in restructured electricity markets with locational prices. Oper Res 2007;55:809–27.
[39] Berry C, Hobbs B, Meroney W, O'Neill R, Stewart Jr W. Understanding how market power can arise in network competition: a game theoretic approach. Utilities Policy 1999;8:139–58.
[40] Borenstein S, Bushnell J, Stoft S. The competitive effects of transmission capacity in a deregulated electricity industry. Technical Report. National Bureau of Economic Research; 1997.
[41] Parry I, Bento A. Tax deductions, environmental policy, and the double dividend hypothesis. J Environ Econ Manage 2000;39:67–96.
[42] Barnes P, Breslow M. Pie in the sky: the battle for atmospheric scarcity rent. Corp Enterprise Dev 2000.
[43] Metcalf G, Weisbach D. The design of a carbon tax. Law School. University of Chicago; 2009.
[44] Dempe S. Annotated bibliography on bilevel programming and mathematical programs with equilibrium constraints. Optimiz: A J Math Program Oper Res 2003.
[45] Colson B, Marcotte P, Savard G. An overview of bilevel optimization. Ann Oper Res 2007;153:235–56.
[46] Outrata J. Optimality conditions for a class of mathematical programs with equilibrium constraints. Math Oper Res 1999:627–44.
[47] Scheel H, Scholtes S. Mathematical programs with complementarity constraints: stationarity, optimality, and sensitivity. Math Oper Res 2000:1–22.
[48] Mordukhovich B. Optimization and equilibrium problems with equilibrium constraints. Omega 2005;33:379–84.
[49] Ferris M, Munson T. Complementarity problems in games and the path solver1. J Econ Dyn Contr 2000;24:165–88.
[50] Dafermos S. An iterative scheme for variational inequalities. Math Program 1983;26:40–7.
[51] Pang J, Chan D. Iterative methods for variational and complementarity problems. Math Program 1982;24:284–313.
[52] Su C, Cottle R. Equilibrium problems with equilibrium constraints: stationarities, algorithms, and applications. Ph.D. thesis. Stanford University; 2005.
[53] Birbil S, Fang S, Han J, et al. An entropic regularization approach for mathematical programs with equilibrium constraints. Comput Oper Res 2004;31:2249–62.
[54] Kanzow C, Schwartz A. A new regularization method for mathematical programs with complementarity constraints with strong convergence properties. Inst Math 2010.
[55] Andreani R, Martí nez J. On the solution of mathematical programming problems with equilibrium constraints. Math Methods Oper Res 2001;54:345–58.
[56] Wu CJ, Hamada MS. Experiments: planning, analysis, and optimization. John Wiley and Sons; 2011. Vol. 552.
[57] Deb K, Pratap A, Agarwal S, Meyarivan T. A fast and elitist multiobjective genetic algorithm: NSGA-II. IEEE Trans Evol Comput 2002;6:182–97.
[58] Baringo L, Conejo A. Wind power investment within a market environment. Appl Energy 2011;88:3239–47.
[59] Das TK, Rocha P, Babayigit C. A matrix game model for analyzing FTR bidding strategies in deregulated electric power markets. Int J Electr Power Energy Syst 2010;32:760–8.
[60] Chen Y, Wang L. A power market model with renewable portfolio standards, green pricing and GHG emissions trading programs. In: Energy 2030 conference 2008. Energy 2008 IEEE. IEEE; 2008. p. 1–7.
[61] Baldick R. Electricity market equilibrium models: the effect of parametrization. IEEE Trans Power Syst 2002;17:1170–6.
[62] Hobbs B. Linear complementarity models of Nash-Cournot competition in bilateral and POOLCO power markets. IEEE Trans Power Syst 2001;16:194–202.
[63] U.S. Energy Information Administrationy. Electric power annual 2009. Technical Report. U.S. Energy Information Administrationy; 2011. <http://www.eia.gov/electricity/annual/> (accessed 31.07.13).
[64] Air Resources Board. 2014 Annual auction reserve price notice, California cap-and-trade program greenhouse gas allowance auctions. Technical Report; 2013. <http://www.arb.ca.gov/cc/capandtrade/auction/2014_annual_reserve_price_notice.pdf> (accessed 12.12.13).

## Appendix D: Published Material in Journal *Energy*

**Appendix D (continued)**

# Emissions control via carbon policies and microgrid generation: A bilevel model and Pareto analysis

Felipe Feijoo[a,1], Tapas K. Das[b,2]

[a] *Johns Hopkins University, 3400 N. Charles Street, Latrobe Hall 205, Baltimore, MD 21218*

[b] *University of South Florida, 4202 E. Fowler Avenue, ENB118, Tampa, FL 33620*

**Abstract**

Economic models are needed to analyze the impact of policies adopted for controlling carbon emissions and increasing distributed renewable generation in microgrids (green penetration). The impacts are manifested in performance measures like emissions, electricity prices, and electricity consumption. This paper presents an economic model comprising bi-level optimization and Pareto analysis. In the bi-level framework, the upper level models the operation of the microgrids and the lower level deals with electricity dispatch in the grid. The economic model is applied on a sample network in two steps. In step1, the bi-level model yields operational strategies for the microgrids and the corresponding values of the grid performance measures. In step2, a statistical analysis of variance combined with Pareto optimization attains guidelines for setting policies for emissions reduction and green penetration without adversely impacting electricity prices and demand. We conclude that renewable generation from microgrids can significantly reduce the negative impacts of the policies. Our economic model is novel as it 1) integrates operational strategies of microgrids and the grid under an emissions control regime, 2) explicitly considers social cost of carbon in the electricity dispatch, and 3) balances multiple objectives of emissions reduction, green penetration, and electricity consumption using a Pareto analysis.

*Keywords:* Smartgrid, microgrid, emissions control, renewable energy,

*Email addresses:* ffeijoo@jhu.edu (Felipe Feijoo), das@usf.edu (Tapas K. Das)

[1] Postdoctoral researcher, Department of Civil Engineering, Johns Hopkins University

[2] Professor and Chair of Industrial and Management Systems Engineering, University of South Florida

MPEC.

---

## 1. Introduction

Many countries around the world have adopted stricter carbon emissions reduction targets. For instance, the EU has established an emissions trading system (EU ETS) that seeks to reduce the greenhouse gas (GHG) emissions by 21% by 2020 from the 2005 level. In a recent declaration, the Environmental Protection Agency (EPA) in the U.S. has set carbon emissions reduction targets for each state with an overall goal of reducing 30% below 2005 level by 2030 [1]. Among the various means of emissions reduction, implementation of a carbon cap, assessment of the true social cost of carbon, and transformation of the power grid to a smart grid to allow distributed renewable generation via microgrids will play key roles. The U.S. Department of Energy (DOE) envisions that by 2030 many of the current electricity grids will upgrade their operations into smart grids [2]. It is anticipated that part of the distributed renewable (green) generation will be provided by a growing number of microgrids operating under the smart grids. Microgrids (with renewable generation, storage devices, and smart meters) will develop cost efficient operating strategies, which will determine their interactions with the smart grid including buy and sell decisions of electricity. Economic models need to be developed to assess the true impact of carbon cap, social cost of carbon (SCC), and green penetration via microgrids on grid performance measures such as carbon emissions reduction, electricity prices, and electricity consumption. This paper presents such an economic model, part of which accounts for the interaction between the microgrids and the independent system operator (ISO) of a smart grid using a bi-level optimization framework. The remaining part of the model processes the results of the bi-level optimization using a statistical analysis of variance and Pareto analysis to develop policy guidelines that attain a desirable balance among emissions reduction, green penetration, and electricity price and consumption.

Literature contains a number of models that address the issue of operational planning of microgrids (e.g., [3], [4],[5], and [6]) without accounting for the dispatch by the main (smart) grid. These microgrid models consider the main grid as a buffer, i.e., a microgrid can buy or sell electricity from or to the grid at any time and in any quantity. This assumption may not hold as the number and sizes of the microgrids grow in a network resulting in an increase in the proportion of grid electricity produced and consumed by the

microgrids. Therefore, the ISOs must consider microgrids' influence on the optimal dispatch of electricity. The need for such joint control of operations of microgrids and smart grid was emphasized in [7].

Commonly expected benefits of microgrids in smart grids, such as reduction of congestion and transmission losses, efficient utilization of electricity and heat, and reduction of emissions, were studied in [8]. Since microgrid energy production is associated with high uncertainty, incorporation of efficient and large scale energy storage facilities, for a large deployment, was recommended in [9]. It was also suggested in [10] that the efficiency of microgrid operation strongly depends on the battery scheduling process. A microgrid-based planning model considering the power system reliability and economic criteria has recently appeared in [11]. A multi-objective intelligent energy management system for microgrids to minimize their operation cost and the environmental impact is proposed in [10]. A bi-level model in [12], similar in spirit to our model, examined the competition between microgrids and a large central generation unit. The societal impact of carbon emissions is known as the social cost of carbon (SCC). A detailed discussion and various definitions of SCC can be found in [13]. Estimation of SCC suffers from uncertainties associated with the future levels of green house gas emissions, the monetized effects of past and future emissions, and methods of translating the environmental effects into economic measures [14]. An interagency working group (IWG), in the U.S., has suggested setting the SCC to $\$21/tCO_2$ [15]. It is asserted in [16] that consideration of the monetary effects of emissions via SCC will increase the development and deployment of green technologies. In the remaining part of this section, we provide a brief outline of the network topology, assumptions and approach for the bi-level optimization model, result of which are further analyzed using a statistical and Pareto analysis technique for developing policy guidelines.

It is considered that the electricity network is a smart grid and it is controlled by an independent system operator. Microgrids are grid-connected and are widely distributed among different buses. The smart grid covers a large area such that the microgrids are likely to be subjected to different solar, wind, and demand patterns. Microgrids are considered as distributed green energy resources with storage, which produce and trade electricity to satisfy demand. The microgrids develop efficient operational strategies over a planning horizon (say, 24 hours) and participates in the hourly market with supply bid only. An operational strategy includes green energy production quantity, charge/discharge of batteries, and electricity buy or sell quantity

bids to ISO. Microgrids are assumed to be price takers. To obtain operational strategies, microgrids consider forecasted values of solar irradiance, wind speed, electricity demand, and the locational marginal price (LMP). The ISO develops the optimal hourly dispatch via DC OPF considering the microgrids' bid, environmental constraints (e.g., emissions cap and SCC), supply functions of the other generators, demand curves of the consumers, and network system constraints.

The objectives of the microgrids and the ISO are attained via a bi-level optimization model where the upper level model minimizes the operation (production) cost of the microgrids and the lower level model develops an optimal electricity dispatch. The solution of the bi-level model also yields the carbon emissions level, green energy penetration, electricity price, and electricity consumption. Thus, the optimization model offers a tool to asses overall impact of microgrids on the smart grid. It is known that network performance measures (emissions level, green penetration, price, and consumption) are negatively correlated. For example, a consumers concern is price increase, a generators concern is profit/revenue reduction, and a policy makers concerns include inadequate emissions reduction and reduced electricity consumption. A high reduction in emissions (environmentally desirable) is likely to increase the cost of electricity (hurting consumers), reduce electricity consumption (lowering economic activity), and reduce market share and profits of fossil fuel generators [13]. Hence, we develop a designed statistical experiment to first measure the effects of cap, SCC, and green penetration via microgrids on the market performance measures. Results of the statistical study are used to develop a Pareto analysis, which yields choices for emissions cap, SCC, and microgrid generation capacities to support policies for emissions reduction, green penetration, and economic activity (electricity consumption).

The contributions of this paper can be summarized are as follows. 1) We model the game between microgrids and the ISO to obtain operational equilibrium strategies. 2) We analyze the impact of microgrid generation, SCC, and carbon cap on carbon emissions, electricity prices, electricity consumption, and green penetration. 3) We develop a statistical sensitivity analysis using analysis of variance to study the true impact of SCC, carbon cap, and microgrid penetration. 4) Finally, we develop policies for emissions control and green penetration by balancing multiple objectives of emissions reduction, green penetration, and electricity consumption using a Pareto analysis.

The rest of the paper is organized as follows. Section 2 presents the de-

tails of the bi-level model. Section 3 presents the model solution approach. Section 4 provides the details of the bi-level model implementation on a sample electricity network with 82 buses and 37 microgrids. Section 5 describes the results obtained from the mode implementation. Section 6 presents the designed experiment and the Pareto analysis. The concluding remarks are given in Section 7.

## 2. Microgrid and Smartgrid interaction: A bi-level model approach

Our adoption of a bi-level modeling framework is motivated by its common use in modeling interaction among participants in deregulated electricity markets (e.g., [17], [18], and [19]). The bi-level framework (leader-follower or Stackelberg game) allows us to study how the ISO (lower level model) reacts to the microgrids decisions (upper level model) and, consequently guides the operational strategies of the microgrids. Figure 1 shows a schematic of the interaction between the microgrids and the smart grid.

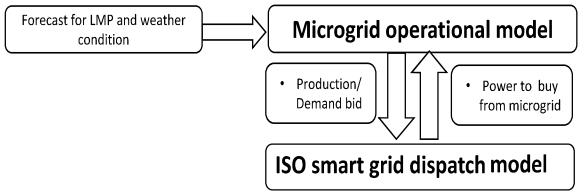


Figure 1: A bi-level optimization framework for smartgrid with microgrids

The upper level model considers all microgrids in the network, and obtains their individual operational strategies. It considers the current values of the hourly forecasts for electricity prices, electricity demand, and weather conditions for all hours of the planning horizon. These forecasts are specific to each microgrid location. Literature contains several microgrid operational models that are based on forecasted parameters with no uncertainty (e.g., [9], [20], [21], and [12]). We also do not consider forecast uncertainties in our model. However, if uncertainties are to be accommodated, a stochastic bi-level model will have to be developed. The stochastic model will consider a set of forecast scenarios and their probabilities. The upper level model will minimize the expected operational cost of the microgrids, where, for each scenario, a lower level model will be solved [22]. Also, since a carbon cap is assumed to be in place, a secondary market for emissions allowances

auction can also be incorporated in the model. Modeling bidding strategies for allowances and an auction-based settlement were considered in [13] and [23].

The upper level objective function of our model minimizes the sum of the costs of operation and maintenance, start up, storage, and electricity trade with the grid, for all microgrids. Note that, as each microgrid has a different forecast, the solution of the upper level model obtains the individualized strategies for production, storage, and electricity trade with the grid. The combination of these strategies minimizes the total operating cost of all microgrids. As a result, these strategies may not be optimal for each of the microgrids. To obtain an optimal strategy for each microgrid, the model will have to be formulated as a non-cooperative game with all microgrids as independent players, and an equilibrium solution will have to be obtained. This can be accomplished by formulating each microgrid's decision problem as a separate bi-level model, where the upper level considers its operation and the lower level considers the ISO's problem. The equilibrium strategy for each microgrid can be found by solving an equilibrium problem with equilibrium constraints (EPEC) [24] and [25]. Though an EPEC approach seems logical, as each microgrid's influence (market power) in the network is small, benefits of computational effort required in solving a large game with all microgrids as individual players may not be appreciable.

The operational strategies of the microgrids are updated every hour of the planning horizon as follows. At the beginning of any hour, the upper level model uses the current forecasts to develop the operational plans for all remaining hours of the horizon. The lower level model, on the other hand, obtains the dispatch for the current hour only. Detail formulation of the upper and lower level models are presented next. Table 1 shows the definition of the variables and parameters of the upper level model (note that o/w stands for otherwise).

*2.1. Upper level model: Operational planning for microgrids*

The operational model (also refer to as an energy management system, EMS) minimizes a community microgrid's operation cost. Similar to the studies presented in [10] and [26], the cost includes production and maintenance cost of green generators (levelized cost), the cost of trading power with the smartgrid, and the battery storage cost.

It is assumed that each microgrid in the smartgrid is comprised of a community of households (hence refer to as community microgrid) with a

**Appendix D (continued)**

Table 1: Notation for variables and parameters

| Variable | Definition | Unit |
|---|---|---|
| $P_{im}^{h}$ | Production level of generator $i \in Gm$ at hour $h$ ($Gm$ : set of generation units in microgrid $m$) | [kWh] |
| $P_{gm}^{h}$ | Power sold from grid to microgrid $m$ at hour $h$ | [kWh] |
| $\hat{P}_{mg}^{h}$ | Quantity bid of microgrid $m$ to the grid at hour $h$ | [kWh] |
| $P_{sm}^{h}$ | Power stored by microgrid $m$ at end of hour $h$ | [kWh] |
| $P_{bm}^{h,out}$ | Output from battery at microgrid $m$ at hour $h$ | [kWh] |
| $P_{bm}^{h,in}$ | Input to battery at microgrid $m$ at hour $h$ | [kWh] |
| $Y_{im}^{h}$ | 1, if generator $i \in Gm$ is used at hour $h$, 0 o/w | – |
| $Y_{dm}^{h}$ | 1, if battery in $m \in M$ is discharged at $h$, 0 o/w ($M$ : total number of microgrid) | – |
| $Y_{cm}^{h}$ | 1, if battery in $m \in M$ is charged at $h$, 0 o/w | – |
| $Y_{mg}^{h}$ | 1, if microgrid $m \in M$ sells power at $h$, 0 o/w | – |
| $Y_{gm}^{h}$ | 1, if microgrid $m \in M$ buys power at $h$, 0 o/w | – |
| **Parameter** | **Definition** | **Unit** |
| $P_{lm}^{h}$ | Load of household $l$ in microgrid $m$ at hour $h$ | [kWh] |
| $P_{im}^{h,min}$ | Min. production of generator $i \in Gm$ at hour $h$ | [kWh] |
| $P_{im}^{h,max}$ | Max. production of generator $i \in Gm$ at hour $h$ | [kWh] |
| $P_{sm}^{max}$ | Max. storage capacity of microgrid $m$ | [kWh] |
| $\beta_{m}^{out}$ | Battery discharge loss factor of microgrid $m$ | [%] |
| $\beta_{m}^{in}$ | Battery charge loss factor of microgrid $m$ | [%] |
| $\beta_{m}$ | Battery storage decay factor of microgrid $m$ | [%] |

number of green generating units (solar panels and wind turbines), and some battery storage capacity with related decay and charging/discharging efficiencies. Given the forecast of the electricity prices (LMP) and the weather conditions (solar irradiance and wind speed) for every hour, a microgrid in the network decides on the amount of energy to produce and buy/sell from/to the smartgrid in a horizon of 24 hours. The energy produced and/or purchased from the smartgrid is used to either satisfy demand in the microgrid, or raise storage level of the batteries for future periods, or for sale to the smartgrid. Microgrids are assumed to bid with quantity only to the ISO, and act as price takers. Microgrids have the ability to switch off generating units for either balancing supply and demand or other economic reasons. The model is formulated as a mixed-integer optimization problem and it is

**Appendix D (continued)**

similar to those presented in [10] and [26]. Let $M$ denotes the set of community microgrids in the network, and $Gm$ denotes the set of generation units in microgrid $m \in M$. Let $OM_i^h$ denote the operation and maintenance cost per KWh of unit $i \in Gm$ at hour $h$, $STC_i^h$ denote start up cost of unit $i \in Gm$ at hour $h$. The battery storage cost per KWh of microgrid $m \in M$ is denoted by $BSC_m$, and $\mu_m^h$ denotes the forecasted electricity price (nodal price) of microgrid $m$ at hour $h$. The operational planing model is presented in equations (1)-(13).

$$\begin{aligned}\min_P \sum_h \sum_{m\in M} \sum_{i\in Gm} & OM_i^h[P_{im}^h] + STC_i^h Y_{im}^h + \\ & \mu_m^h(P_{gm}^h - \hat{P}_{mg}^h) + BSC_m[P_{sm}^h] \end{aligned} \tag{1}$$

$$\begin{aligned} s.t. \sum_{i\in Gm} P_{im}^h + P_{gm}^h + \beta_m^{out} P_{bm}^{h,out} = \\ \sum_{l\in m} P_{lm}^h + P_{bm}^{h,in} + \hat{P}_{mg}^h \quad \forall m \in M, h, \end{aligned} \tag{2}$$

$$P_{bm}^{h,out} \le \beta_m P_{sm}^{h-1} \qquad \forall m \in M, h, \tag{3}$$

$$P_{sm}^h = \beta_m P_{sm}^{h-1} - P_{bm}^{h,out} + \beta_m^{in} P_{bm}^{h,in} \quad \forall m \in M, h, \tag{4}$$

$$Y_{im}^h P_{im}^{h,min} \le P_{im}^h \le P_{im}^{h,max} Y_{im}^h \forall i \in Gm, m \in M, h, \tag{5}$$

$$\hat{P}_{mg}^h \le \sum_i P_{im}^h + \beta_m P_{sm}^{h-1} \qquad \forall m \in M, h, \tag{6}$$

$$P_{sm}^h \le P_{sm}^{max} \quad \forall m \in M, h, \tag{7}$$

$$P_{bm}^{h,out} \le \beta_m P_{sm}^{max} Y_{dm}^h \quad \forall m \in M, h, \tag{8}$$

$$P_{bm}^{h,in} \le \beta_m P_{sm}^{max} Y_{cm}^h \quad \forall m \in M, h, \tag{9}$$

$$Y_{dm}^h + Y_{cm}^h \le 1 \quad \forall m \in M, h, \tag{10}$$

$$\hat{P}_{mg}^h \le (P_{sm}^{max} + \sum_{i\in m} P_{im}^{h,max}) Y_{mg}^h \quad \forall m \in M, h, \tag{11}$$

$$P_{gm}^h \le (P_{sm}^{max} + \sum_{l\in m} P_{lm}^h) Y_{gm}^h \quad \forall m \in M, h, \tag{12}$$

$$Y_{gm}^h + Y_{mg}^h \le 1 \quad \forall m \in M, h. \tag{13}$$

The objective function (1) represents the total operational and maintenance cost. The cost function is composed of the operational and maintenance cost (OM), start-up cost (STC) battery storage cost (BSC), and the cost or benefit of electricity trade with the main grid. All the cost com-

ponents (OM, STC, and BSC) are considered to be linear functions. The operational decisions of microgrids at any time of the horizon depend on the forecasted demand, weather conditions, and electricity price of future periods. Since the market is cleared only for the current hour (e.g., beginning of the time horizon), microgrids consider their bids for energy sold to the gird for future periods as operational planning strategies.

Constraint (2) ensures the power balance for every microgrid and for each hour of the horizon. In order to ensure the power balance in each microgrid, the total input of electricity has to equal the total output, hence the power produced from microgrid energy sources, power discharged from batteries, and power purchased from the grid must equal microgrid demand, charge of batteries, and energy sold to the grid.

Constraint (3) sets the maximum amount of stored energy available to withdraw at hour $h$, which is affected by the battery storage decay factor $\beta_m$, and depends on the stored energy at the end of period $h-1$ (previous period). The withdrawal of energy from batteries may be used to satisfy demand or to be sold to the grid.

The battery storage level of every microgrid at the end of each hour $h$, shown in (4), is calculated as the energy available (storage level) at the end of the previous hour $(h-1)$ minus the output (discharge) in hour $h$ plus the input (modified by the battery charge loss factor $\beta_m^{in}$) of electricity in hour $h$. The battery charge loss factor represent the amount of electricity (percentage) that is lost when charging a battery. In practice, this factor depend on the temperature, age, and depth of discharge, among others, and ranges from 10% to 20%.

Minimum and maximum production levels of generation units in each microgrids are controlled by (5). Estimates for $P_{im}^{h,max}$ in equation (5) are based on the weather (solar and wind) data presented in Section 4. The theoretical available power for wind sources is given by $P = 1/2\rho A v^3$, where $v$ represent the wind speed, $A$ is the area of the wind turbine, $\rho$ is the density of air, and $P$ is the wind energy output. For solar generating units, the maximum power output depends on the area of the solar panels and their efficiency.

Equation (6) represents the maximum amount of energy available to be sold to the grid for each microgrid at any hour. The available energy corresponds to the wind and solar electricity production in hour $h$ plus the energy available in the storage device at the end of the period $h-1$ (or beginning of period $h$). Strategic decisions of microgrids may results in storing electricity

in periods in which prices are lower, and then use this electricity when prices rise.

The limit for the amount of energy that can be stored in the batteries (maximum battery capacity) is given by constraint (7). It is assumed that at each hour, microgrids can only either charge or discharge batteries. Storage capacity decay is not considered in our model since the time horizon considered to be only 24 hours (as described in Section 4), for which the decay is minimal.

Constraints (8)-(10) determine whether to charge or discharge batteries (10) and the quantity of energy to draw or to supply to the batteries (8)-(9). It is assumed that microgrids cannot charge and discharge batteries in the same period, but they are allowed to do nothing.

Finally, constraints (11)-(13) determine, for each hour, if a microgrid sells to or buy electricity from the smartgrid. The terms withing parenthesis in (11) and (12) play the role of big M and are logical limit for the amount of energy that microgrids can sell or buy from the grid, respectively. Similarly, the terms in the right hand side of the constraints (8) and (9) also play the role of big M in optimization literature. Guidelines to obtain the values of M are found in [19].

*2.2. Lower level model: Electricity dispatch via modified DC-OPF*

Electricity dispatch by an independent system operators (ISO) seeks to minimize the social cost of generating the power required by the demand nodes in the network. To do so, there are different strategies that the ISOs use for electricity dispatch (e.g., DC-OPF model, merit order, flat dispatch, among others). Authors have adopted a standard DC-OPF model (similar to those presented in [17], [19], and [27]) for dispatch of all generators (e.g., fossil fuel and green generators), and modified it by introducing carbon emissions constraints and adding a social cost of carbon to the objective function. A similar DC-OPF that incorporates carbon policies is presented in our previous work [13]. Also, electric vehicles (PHEVs) are assumed to act as small generators in the network [28]. Microgrids are considered as a generator (when selling electricity to the smartgrid) or a load (when buying electricity from the smartgrid). The modified DC-OPF model (dispatch for a particular hour) is given as follows. Let $P = \{P_i\}$ denote the dispatch vector. The bid supply cost of the generators (fossil fuel generators), indexed by $i$, are assumed to be quadratic convex functions $C_i(P_i) = \alpha_i P_i + \beta_i P_i^2$, where $\alpha_i$ and $\beta_i$ represent the intercept and the slope of the bid supply function (not

**Appendix D (continued)**

true cost of generators), respectively. Loads, indexed by $j$, are considered to have negative benefit functions (consumers' benefit treated as negative cost) given by $-D_j(P_j) = -d_j P_j - b_j P_j^2$, $P_j \leq 0$ [27]. The cost of obtaining power from electric vehicles at node $k$ is given by $PHEV_k(\alpha_k)$. $P_i \gamma_i \pi$ represents the cost associated to the emissions, where $\gamma_i$ is the emissions factor (tons of $CO_2$ per MWh produced) of generator $i$ (assumed to be 1 for all generators), and $\pi$ denotes SCC. The cost and benefit of the microgrids are denoted by the linear functions $MC_m(P_{mg}^g)$, and $MD_m(P_{gm}^h)$, respectively. Then, the modified DC-OPF for any hour is presented in equations (14)-(23).

$$\sum \underset{P}{\text{Min}} \quad \sum_i C_i(P_i) + \sum_j D_j(P_j) + \sum_k PHEV_k(a_k) \tag{14}$$
$$+ \sum_i P_i \gamma_i \pi + \sum_m MC_m(P_{mg}^g) - MD_m(P_{gm}^h)$$
$$s.t. \quad -C_l^{min} \leq \sum_n P_n \varphi_{nl} \leq C_l^{max}, \forall l \quad (\epsilon_l^-, \epsilon_l^+) \tag{15}$$
$$\sum_i P_i + \sum_j P_j + \sum_k a_k + \sum_m (P_{mg}^g - P_{gm}^h) = 0, (\mu) \tag{16}$$
$$\sum_i \gamma_i P_i \leq Cap, \quad (\lambda) \tag{17}$$
$$a_k \leq \beta_k (C_k^{max} - D_k), \quad (\rho_k) \tag{18}$$
$$P_i - R_i^{lo} \geq 0, \quad \forall i \quad (\tau_i) \tag{19}$$
$$R_i^{up} - P_i \geq 0, \quad \forall i \quad (\upsilon_i) \tag{20}$$
$$0 \leq P_{mg}^g \leq \hat{P}_{mg}^h, \quad \forall m \quad (\upsilon_m) \tag{21}$$
$$P_i \geq 0, \quad \forall i \quad (\pi_i) \tag{22}$$
$$-P_j \geq 0. \quad \forall j \quad (\kappa_i) \tag{23}$$

The objective function (14) represents the total social cost (or, maximization of social welfare) which is defined as the total cost of producing electricity (generators cost) minus the benefit of the consumers. We have added to the standard social cost function the concept of social cost of carbon ($\pi$, SCC) and the benefit/cost of microgrids. The social cost increases as more carbon emissions are generated since the SCC acts as a penalty for emissions. A detail discussion on SCC can be found in [13].

Constraint (15) controls the flow of electricity in the network via the power transfer distribution factors ($\varphi_{nl}$), where $n$ denotes a node in the

**Appendix D (continued)**

network and $l$ a transmission line. The power transfer distribution factor describes the mega-watts flowing in line $l$ if 1 mega-watt is injected at node $n$. The lower and upper limit of the transmission line $l$ are given by $C_l^{min}$ and $C_l^{max}$, respectively.

The power balance in the network (the total demand is equated to the total production) is controlled by (16). Microgrids can behave as either generators ($P_{mg}^g$) or loads ($P_{gm}^h$), by supplying or consuming electricity from the grid. This operational decision is taken in the upper level model that was presented earlier in Section 2.1. The supply of energy from PHEV is represented by $\alpha_k$. $P_i$ and $P_j$ represent the electricity supplied by generator $i$ and consumed by the demand load (node) $j$, respectively.

A cap to the carbon emissions in the network is set by (17), where $\gamma_i$ is the carbon emissions factor for generator $i$, and $P_i$ its power output. Therefore, $\gamma_i P_i$ accounts for the amount of emissions that generator $i$ produces by dispatching $P_i$ mega-watts of electricity.

Constraint (18) monitors the maximum power available at PHEV nodes ($C_k^{max} - D_k$), where $C_k^{max}$ is the power available at node $k$, and $D_k$ is the demand at node $k$. The percentage of energy lost at PHEV nodes due to transformer losses is given by $\beta_k$.

Constraints (19) and (20) control the lower ($R_i^{lo}$) and upper ($R_i^{up}$) limits of the energy that generators can supply. A minimum level of generation is normally considered (as in constraint 20) to maintain operational reliability of generators. The upper limit ($R_i^{up}$) is set by the installed capacity of generator (power plant) $i$.

The maximum amount of electricity that the ISO can buy from each microgrid is given by (21), where $\hat{P}_{mg}^h$ is the decision from the upper level model (microgrids quantity bid) and $P_{mg}^g$ correspond to the decision of the ISO. Hence, the mega-watts of electricity that the ISO can purchase ($P_{mg}^g$) is limited by the electricity bid ($\hat{P}_{mg}^h$) of microgrid $i$. Remember that the ISO must consider microgrids supply of electricity in the network power balance, as described in constraint (16).

Non-negativity constraints are given by (22) and (23). The variables in parenthesis in the right hand side of each constraint correspond to the dual variables or shadow prices. Our attention is primarily focused on $\mu$, which represents the system marginal price of electricity.

**Appendix D (continued)**

### 3. Bi-level Optimization model

Bi-level models include two mathematical programs, where one serves as a constraint for the other. A generic description of the bi-level model can be presented as follows.

$$\begin{aligned} &\underset{x_i}{\text{Max}}\ f_i(x,y) \\ &s.t\ \ d_i(x_i,y) \geq 0, \quad g_i(x_i,y) = 0, \\ &y = \underset{y}{\text{Min}}\, F(x,y) \\ &\qquad s.t\ \ D(x,y) \geq 0, \quad G(x,y) = 0. \end{aligned} \tag{24}$$

For the lower level problem, with a convex objective function and non-empty feasible set, the first order necessary conditions for a solution to be optimal are given (under some regularity conditions) by the *Karush Kuhn Tucker* (KKT) conditions. Hence, replacing the lower level problem in (24) by the set of KKT conditions yields what is known as a mathematical program with equilibrium constraints (MPEC), as given below.

$$\begin{aligned} &\underset{x_i}{\text{Max}}\ f_i(x,y) \\ &s.t\ \ d_i(x_i,y) \geq 0, \quad g_i(x_i,y) = 0, \\ &\nabla_y F(x,y) - \nabla_y D(x,y)^t \delta + \nabla_y G(x,y)^t \eta = 0, \\ &G(x,y) = 0, \quad D(x,y) \geq 0, \quad D(x,y)^t \perp \delta, \quad \delta \geq 0. \end{aligned} \tag{25}$$

The non-linearity due to the complementarity constraints $(D(x,y)^t \perp \delta)$ in (25) is linearized using the constraints $D(x,y)^t \leq YM$, and $\delta \leq (1-Y)M$, where $Y$ is a binary variable and $M$ is a sufficiently big number. The final model after transformations is a mixed integer programming model. Further details on bi-level models and MPECs can be found in [17], [18], and [19].

### 4. Model Implementation

The model was implemented on a sample smartgrid network with 82 buses including 37 microgrids, 30 demand nodes (or loads), 5 traditional (fossil fuel) generators, and 10 PHEV nodes. The smartgrid has 100 transmission lines. The weather conditions (hourly solar irradiance and wind speed) are modeled using the data provided by The Pacific Northwest Cooperative Agricultural

**Appendix D (continued)**

Weather Network[3] (AgriMet) for 2012-2013. To keep our model simple, we assumed that the microgrids produce energy using solar and wind sources only. The total levelized cost for energy production is based on the data provided by U.S. Energy Information Administration[4] (EIA). Since the current production costs for renewable energy sources are higher than fossil fuel based energy, it is assumed that there exist rebate and incentive programs which make the renewable energy production costs competitive. The total levelized costs (after rebates and incentives) for the renewable sources of each community microgrid are obtained from triangular distributions with parameters $(min, median, max)$ given as (0.028,0.059,0.083) for wind, and (0.046,0.059,0.093) for solar energy, respectively, in 2010 \$/KWh. Figure 2 depicts the approximate hourly average electricity price (LMP) in comparison to the levelized costs. The hourly LMP is calibrated by solving the lower level DC-OPF model by assuming that the microgrids do not have generation and storage capacity and are subject to emissions cap and SCC. The assumption of having rebates and incentives programs minimizes the impact of choosing levelized cost instead of the marginal cost. However, this paper does not attempt to look into this issue and hence, without loss of generality, the levelized cost is considered. The operation cost for energy storage devices are according the International Renewable Energy Agency[5] (IRENA)

The electricity demand data for each household in the community microgrids was obtained from the study presented in [29]. Generators in the smartgrid were considered to have a quadratic cost function, and consumers were modeled via a negative quadratic benefit function. The parameters for the generator cost function and consumers benefit function were considered to be random variables with uniform distributions [27]. A number of ad hoc emissions control scenarios with different values of social cost of carbon (SCC) and emissions cap were considered to be in effect for the sample network (see Table 2). The model was solved for a planning horizon of 24 hours, though the model can accommodate time horizons of any length. The model was implemented in GAMS platform and solved using CPLEX (GAMS code

[3]AgriMet provides hourly weather conditions data. The information can be obtain in http://www.usbr.gov/pn/agrimet/wxdata.html.

[4]Further details on energy cost, as well as the data considered in this study, can be found in http://www.eia.gov/forecasts/aeo/er/index.cfm. (Last accessed on January 2014)

[5]Details can be found in http://www.irena.org/DocumentDownloads/Publications. (Last accessed on August 2014)

**Appendix D (continued)**

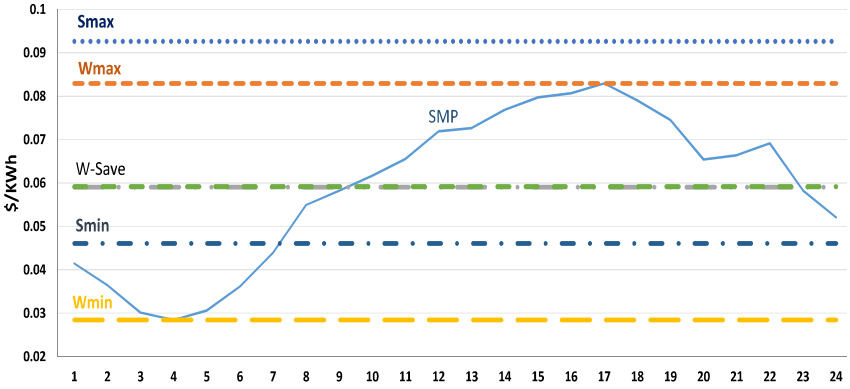


Figure 2: Levelized costs for wind and solar operation in relation to the appropriate average hourly LMPs in the sample network

is available upon request to authors). Details about the model computational time are not presented here, since GAMS/CPLEX was able to solve the model in a couple of seconds.

Table 2: Emissions control scenarios

| | SCN1 | SCN2 | SCN3 | SCN4 |
|---|---|---|---|---|
| SCC ($\$/tCO_2$) | 20 | 20 | 40 | 40 |
| Cap ($tCO_2$) | 600 | 1000 | 600 | 1000 |

## 5. Results

In this section, we present the results obtained from the application of our model on the sample network subject to the four different emissions control scenarios.

### *5.1. Operational decisions for community microgrids*

Figure 3 shows the cumulative operational decisions of the 37 microgrid communities with household sizes of 50 for the 24 hour planning horizon. It can be seen that microgrids purchase most of the energy early in the morning when electricity prices are low (see Figure 2) and green generation is at a minimum (due to low solar irradiance and wind speed). This energy is used to satisfy their demand as well as to charge the batteries (see battery level

with red-squared label in Figure 3) for future hours with higher electricity prices. Energy production at the community microgrids increases during the day reaching its maximum in the afternoon, when both wind speed and solar irradiance are at their maximum levels. During this increased energy production, microgrids are able to satisfy their demand (production higher than microgrid demand) and, at the same time, sell excess of electricity to the smartgrid. This is also observed in the amount of electricity purchased by microgrids (green-triangular label), which achieves a minimum level when the production is at its maximum. Increased supply of green energy (with no SCC) during afternoon hours helps to lower the fossil fuel generation and thus reduce the system marginal price (SMP) resulting in an increased overall demand in the smartgrid. The impacts of community microgrids is examined in detail in the rest of the paper.

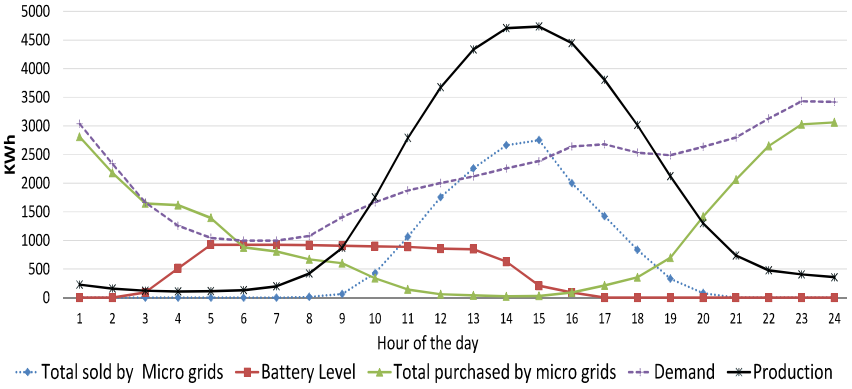


Figure 3: Daily operational plan for the community microgrids

*5.2. Impact of cap, SCC, and microgrids on electricity prices*

Figure 4 shows the average reduction in SMP of electricity during peak hours (10:00 to 18:00) for the four emissions control scenarios and all microgrid sizes. The price reduction for each emissions control scenario is in comparison with the corresponding baseline when microgrids are loads only and have no generation and storage capacity. When microgrid sizes are small (community microgrids of 50 or 100 households), low reductions in SMP are observed due to the low green energy injection to the main grid from microgrids. Also, for smaller microgrid sizes, there is no significant difference among the four emissions control scenarios. As microgrids become larger, the

maximum reduction is achieved under SCN1, which amounts to $\$1.6/MWh$ (2.53%) reduction. A stricter carbon policy with a lower cap and high SCC (as in SCN3) is likely to affect standard fossil fuel generators, and allow the green generators to assume higher market power. However, since the model presented here does not consider generators' bidding strategies, effects of such market power can not be ascertained. The green energy supplied by microgrids (free of SCC) reduces the need for fossil fuel sources, thus reducing the overall price increase induced by environmental policies (SCC and cap). This aspect is explained further in the explanation of Figure 6.

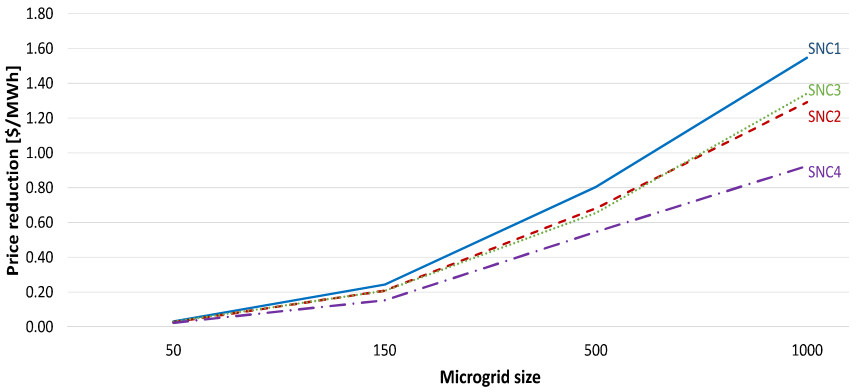


Figure 4: Reduction of electricity price (SMP) during peak hours for different sizes of community microgrids and emissions control scenario

### *5.3. Impact of cap, SCC, and microgrids on market demand*

We compare the main grid demand for electricity (demand for load nodes only, not microgrids) during the peak hours with that of the baseline scenario. The increases in demand when microgrids have generation and storage capacity for all emissions control scenarios and sizes are shown in Figure 5. A prediction/expectation that is commonly found in the literature is that microgrids are likely to reduce demand in the main grid during peak hours (peak shaving) and thus reduce congestion. Here, we observe that in the presence of environmental constraints and consumption guided by a demand curve, green generation by microgrids will help to lower price and actually increase energy demand during peak hours. Since SCC and emissions cap are considered, the original market equilibrium (with no SCC and cap) is modified and results in a new equilibrium point with increased electricity prices

and reduced demand. Green energy from microgrids help to restore the original market equilibrium point. Notice that a higher SCC tends to produce lower increase in demand, as higher SCC drives up the cost of fossil fuel based electricity, and hence the percentage reduction of SMP resulting from green generation in the community microgrids is lower. Likewise, a higher emissions cap allows higher fossil fuel based electricity generation, hence the relative increase in demand due to microgrids' green generation is smaller (see lines for SCN3 and SCN4). However, from the graphs for SCN1 and SCN2, it is clear that SCC has a more dominant impact on demand than the emissions cap. The observations made from Figure 5 are further explained by the market equilibrium diagram in Figure 6.

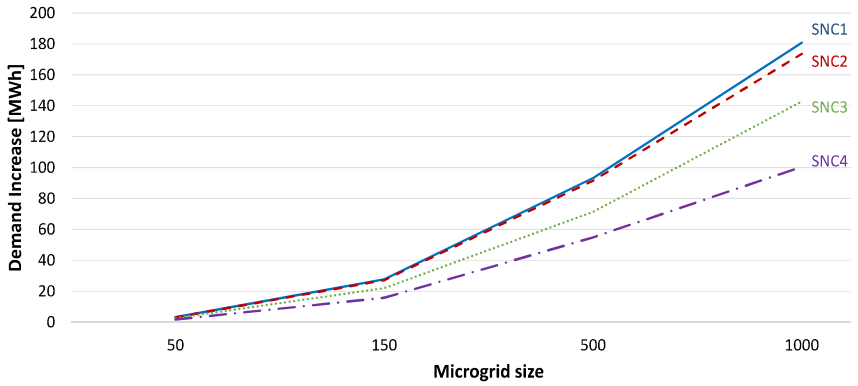


Figure 5: Total demand increase during peak (10:00-18:00) hours due to SMP reduction by green generation in the microgrids

Let the original market equilibrium be at $Q$ when the supply function does not take into account SCC and green generation in the microgrids. Two different scenarios of SCC and microgrid generation are superimposed. SCC1 is considered to be lower than SCC2, and the quantity of green generation by microgrids are considered identical in both. Clearly, adding SCC2 raises the original supply function to a higher level compared to that for SCC1 (since SSC1 $\leq$ SSC2). When green generation is supplied by the community microgrids, the overall supply cost drops (recall that we had assumed that in the presence of rebates and incentives the green generation cost will be comparable to fossil fuel based generation). Clearly the drop in supply function with SCC2 will be less than for the function with SCC1 ($\Delta SMP_2 \leq \Delta SMP_1$) due to the nature of demand nodes represented by quadratic (non-linear) demand functions. Hence, the increased demand caused by introduction of

green generation for SCC2 would be smaller than for SCC1 ($\Delta Q_2 \leq \Delta Q_1$). Note that, to keep this exposition simple, we did not impose the emissions cap on this diagram, although a similar analysis can be performed.

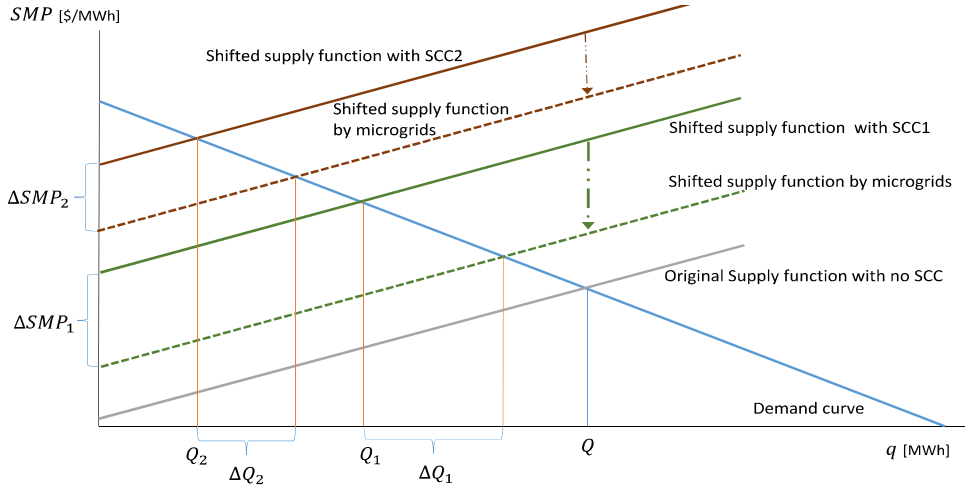


Figure 6: Impact of SCC and green generation by microgrids on market equilibrium

*5.4. Impact of cap, SCC, and microgrids on emissions and green penetration*

Table 3 shows the emissions reduction achieved (in $tCO_2$ per 24 hours) for different sizes of microgrids and four scenarios of emissions control. Emissions reduction is calculated for each scenario as the difference between the emissions level of the baseline scenario (with no green energy from microgrids) and the emissions level of the scenarios when green microgrid generation is considered. Hence, the emissions reduction measures the impact that green energy from microgrids has for different combinations of emissions cap and SCC. Note that, each scenario has a different equilibrium solution resulting in different demand, electricity dispatch, price, and emissions. Clearly, small microgrid communities (each with 50 households) did not create a significant impact on emissions due to their limited generation capacity. Higher emissions reductions were obtained for larger microgrid communities.

A higher value of SCC (SCN3 and SCN4) resulted in higher emission reductions as it was more expensive to provide energy from fossil-fuel generators whose supply cost functions were shifted up by SCC (see Figure 6) resulting in higher equilibrium points with increased price and reduced demand. This can be explained as follows. Microgrids help to lower electricity prices and

**Appendix D (continued)**

Table 3: Emissions reduction [$tCO_2/24hours$]

| Microgrid size | SCN1 | SCN2 | SCN3 | SCN4 |
|---|---|---|---|---|
| 50 | 0.24 | 1.46 | 6.72 | 14.96 |
| 150 | 1.3 | 8.56 | 52.76 | 108.84 |
| 500 | 4.58 | 28.42 | 195.47 | 351.98 |
| 1000 | 9.4 | 56.65 | 393.7 | 688.88 |

increase demand (as observed earlier in Figures 4 and 5). Since SCN4 has the lowest increase in demand (due to lowest price reduction through introduction of microgrids), it yields the highest reduction in emissions as microgrid generation satisfies a higher proportion of the demand. Though SCN3 and SCN4 have the same SCC, higher cap of SCN4 results in lower increase in demand relative to SCN3 and thus relatively higher emissions reduction.

Recall from Figure 6 that, introduction of microgrids lowers the supply curve and thus increases demand. If the level of such a demand increase is close to the level of green electricity supplied by the microgrids, the emissions reduction will not be significant (as observed for SCN1 and SCN2). The emissions reduction in percentage for SCN4 is equal to 11.69% considering community microgrids of size 1000. The corresponding percentages for the other scenarios are 0.095%, 0.35%, and 7.94% for SCN1, SNC2, and SCN3, respectively. Also, note that the highest emissions reduction achieved in SCN4 did not result in the lowest emissions level, which was achieved in SCN3 that has a lower cap. Emissions level for the four scenarios (with microgrid size of 1000) were as follows: SCN1=9933$tCO_2$, SCN2=15085$tCO_2$, SCN3=4564$tCO_2$, and SCN4=5051$tCO_2$. Clearly, SCN2 has the highest level of emissions as it has the lowest SCC (\$20$tCO_2$) and highest cap (1000$tCO_2$).

As the emissions factor is considered to be $\gamma = 1\ tCO_2/MWh$, the emissions reduction percentages are also the measures by which fossil fuel based generation is reduced. The U.S. department of energy states that the deployment of microgrid should achieve (at least) a 20% reduction in emissions, and improvement of energy efficiencies via reduction in energy provided by fossil fuel based generators [30].

Table 4 shows the penetration of green energy (in percentage of total consumption) in the network for all combinations of microgrid sizes and emissions control scenarios. The percentage of energy supplied by green sources increases with the size of community microgrids, which reaches a

maximum of 27.96% for SCN3. Green energy penetration can be increased by raising the assessment of the social cost of carbon (see SCN3-4). Also, it can be seen that the percentage of green energy penetration is reduced with the increase in emissions cap for same SCC (SCN4 vs. SCN3).

Table 4: Green energy penetration [%]

| Microgrid size | SCN1 | SCN2 | SCN3 | SCN4 |
|---|---|---|---|---|
| 50 | 0.31 | 0.2 | 0.63 | 0.55 |
| 150 | 2.67 | 1.77 | 5.14 | 4.54 |
| 500 | 8.48 | 5.74 | 15.52 | 14.32 |
| 1000 | 15.29 | 10.44 | 27.96 | 24.8 |

## 6. Supporting emissions policies using a Pareto analysis

In this section, we present a Pareto analysis driven approach to support emissions policy issues for smartgrids. A broad policy question that we address here is; what should be the recommended levels of green penetration and emissions reduction that will sustain adequate market demand for electricity needed to spur economic growth? To address this question, we first develop response surface equations for three different market performance measures (emissions reduction (EM), green energy penetration (GP), and market demand (MD) for electricity in the smartgrid) as a function of emissions cap, SCC, and microgrid size. We first use these equations to examine the sensitivity of the impact of SCC, Cap, and microgrid size on the market performances measures. Also, as the performance measures are conflicting, i.e., the optimal choice of parameters for one measure could be highly non-optimal for another, we develop a Pareto analysis approach to answer the policy question regarding green penetration, emissions reduction, and market demand for electricity.

### *6.1. Response surface equations*

A response surface equation for each of the performance measures was obtained via a factorial designed experiment and analysis of variance (ANOVA) of the experimental data. The factorial experiment comprised three factors (SCC, emissions cap, and microgrid size). Each of the three factors was set at four levels resulting in a $4^3$ full factorial experiment. The numerical levels

considered for the factors are given in Table 5. The 64 experiments involve solving the bi-level model for each factor combinations. Three performance measures for each experiment were recorded. A separate analysis of variance (ANOVA) was performed for each performance measure (with type I error $\alpha = 0.05$) utilizing the R software (version 2.15.1). The ANOVA results were used to identify the significant factors and interactions, which were then used to formulate the response surface equations, presented below. See [31] for a discussion about factorial experiments and ANOVA analysis.

Table 5: Factor levels for the $4^3$ factorial experiment

| Factor | L1 | L2 | L3 | L4 |
|---|---|---|---|---|
| SCC ($\pi$) | 20 | 30 | 40 | 50 |
| Cap ($C$) | 400 | 600 | 800 | 1000 |
| Microgrid size ($M$) | 50 | 150 | 500 | 1000 |

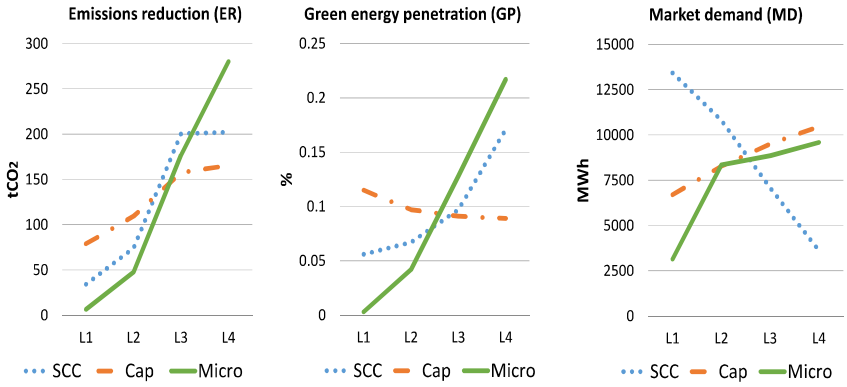


Figure 7: Effects of SCC, cap, and microgrid size on ER, GP, and MD

*6.1.1. Emissions reduction (ER)*

For ER as the response variable, all three main factors and some of the interactions were found to be statistically significant. Using these significant factors and interactions, a third order regression model was developed. The model has a multiple R-squared value of 0.859 and an adjust R-squared value of 0.836. The response surface equation is as follows.

$ER = 1.062\text{E}3 - 2.861\text{E}\text{-}1M - 1.813\text{E}\text{-}4M^2 + 2.09\text{E}\text{-}1C$
$- 1.404\text{E}\text{-}4C^2 - 1.150\text{E}2\pi + 3.582\pi^2 - 3.503\text{E}\text{-}2\pi^3 +$

**Appendix D (continued)**

$3.327\text{E-}4MC - 1.522e\text{E-}2M\pi$.

Effect plots for the three main factors are presented in Figure 7 (left). Microgrid size and emissions cap exhibit approximately linear behavior over the four levels, indicating that higher ER is achieved at higher values of M and C (see notation in Table 5). SCC exhibits a nonlinear behavior where ER increases with SCC until a certain point before leveling off. The impact of SCC (higher levels, higher reductions) is expected. The increase of ER as emissions cap increases is explained and exemplified in Section 5 with Figures 4, 5, and 6.

*6.1.2. Green penetration (GP)*

As in the case for ER, all three main factors were found to be statistically significant. Three of the two factor interactions were also found to be significant. A second order regression model incorporating all the significant factors and interactions was developed. The model has a multiple R-squared of 0.976 and an adjusted R-squared of 0.972. The main factor effects are shown on Figure 7 (middle). Emissions cap and microgrid size exhibit approximately linear effects on green penetration, whereas the SCC exhibits a more prominent quadratic effect on GP, resulting in the following equation

$GP = 2.39\text{E-}1 + 1.27\text{E-}4M - 1.008\text{E-}7M^2 - 2.095\text{E-}4C + 1.023\text{E-}7C^2 - 1.18\text{E-}2\pi + 1.582\text{E-}4\pi^2 + 7.56\text{E-}6M\pi - 9.46\text{E-}8MC + 1.831\text{E-}6C\pi$.

*6.1.3. Market demand of electricity (MD)*

For MD as the response variable, all main factors where found to be statistically significant, but only the interaction effect among cap (C) and SCC was statistically significant. Using these, a second order regression model was developed. The mode has a multiple R-squared of 0.994 and an adjust R-squared value of 0.993. The effects plot of the main factors is shown in Figure 7 (right). The response surface equation is obtain as

$MD = 1441.85 + 1.498M + 22.746C + 146.716\pi - 2.120\pi^2 - 0.471C\pi$.

The effects plot for MD corroborates the results seen earlier in Section 5. That is, higher levels of both cap and microgrid size achieve higher market demand. A higher value of SCC results in a significant reduction in the MD.

**Appendix D (continued)**

*6.2. A Pareto analysis approach*

It may be noted from the effect plots in Figure 7 that SCC affects MD in a manner completely opposite to its impact on ER and GP. Higher cap (C) increases ER and MD while decreasing GP. An increase in microgrid size (M) has a strictly increasing impact on ER and GP, while for MD, the increase levels off quickly. It is clear from the observation above that a Pareto analysis offers a viable tool for addressing the policy design question raised earlier. A Pareto front is a set of points representing 3 tuples $(\pi, C, M)$ where all points are Pareto efficient. A Pareto efficient point indicates that no individual measure of performance can be further improved without worsening one or more of the other performance measures. The Pareto front was developed by optimizing $ER, GP$, and $MD$ subject to bounds of the design parameters $(\pi, C, M)$. The Pareto front is shown in Figure 8.

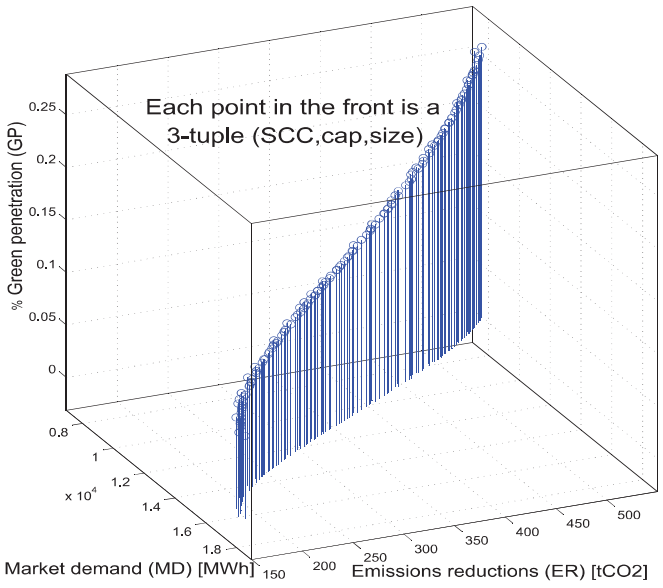


Figure 8: A Pareto front for ER,GP, and MD

It may be noticed from Figure 8 that a higher percentage of green energy penetration yields higher emissions reduction and a decrease in market demand for electricity. If we move southwest along the front, we obtain designs with higher market demands but at the cost of reduced GP and ER. Hence, the Pareto front can guide the choice of a policy by the decision makers. A small sample set of Pareto efficient points in the front are presented in

**Appendix D (continued)**

Table 6 for illustration purposes. A method for choosing a Pareto efficient strategy for smartgrid design can be developed using the approach described in [13], where it is shown that a level for emissions cap, SCC, and microgrid community size can be found if targets for emissions reduction are settled. Furthermore, levels for cap and SCC that comply with a target can be found such that the negative impacts are minimized (e.g., increase in electricity price).

Table 6: Sample set of Pareto efficient points from Figure 8

| M | C | $\pi$ | GP | ER | MD |
|---|---|---|---|---|---|
| 1000 | 1000 | 20 | 0.091 | 168.3 | 17147 |
| 1000 | 434.8 | 42.2 | 0.282 | 355.93 | 6709.3 |
| 1000 | 624.9 | 42.3 | 0.266 | 416.1 | 7103 |

Since the SCC ($\pi$) is not controlled by the policy makers but only assessed, Pareto fronts for different levels of assessed values of $\pi$ ($20, $30, $40, and $50 per $tCO_2$) were developed (see Figure 9). Each point on these Pareto fronts is a two-tuple (C, M). Notice that as the SCC increases, the Pareto fronts move towards higher values of GP and ER, with a significant reduction in MD.

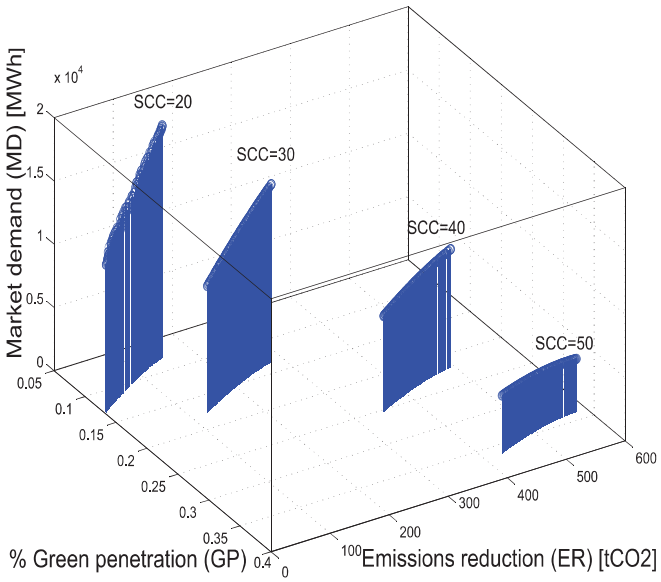


Figure 9: Pareto fronts for different values of SCC

## 7. Conclusions

Stricter carbon emissions reduction targets have been established worldwide. Broad emissions reduction policies will have to consider implementation of strategies like cap-and-trade, take into account the social cost of carbon (SCC), and increase green energy penetration via microgrids. However, selection of policy parameters, e.g., carbon cap, estimate of SCC, and green penetration target, that are not well supported by a comprehensive model, may adversely impact electricity prices and consumption. This paper develops a mathematical-statistical methodology to support the policy makers to strike a balance among carbon emissions reduction, green penetration, and electricity consumption. The results from the model provide critical insights on how combinations of social cost of carbon, emissions cap, and green generation capacities of the community microgrids (which dictates green penetration) impact the electricity prices and the demand in the smart grid. In the presence of emissions control (SCC and cap), higher green penetration by the microgrids reduces the average electricity price and increases the demand in the smart grid, even in the peak hours. (Note that, when SCC is considered, the costs of electricity from fossil fuel generators, in our example problem, are considered to be higher than green electricity from the microgrids.) As alluded in the paper, the estimate of SCC varies widely in the literature. We show that, if higher estimates of SCC are considered, available green generation capacity in the network may not be able to fully compensate for the reduction in demand due to high increase in electricity price from the fossil fuel generators. This may result in a net reduction of consumption in the network. To address this issue, the proposed methodology considers a Pareto analysis, which allows the public (policy makers) to set targets for emissions reduction, percent green penetration, and market demand. A key limitation of the optimization model in our methodology is that it does not consider the stochastic hourly variations of solar irradiance and wind speed. It only considers the average values. Also, our model considers solar and wind as the only possible sources of generation in the community microgrids. In practice, microgrids often have other generation sources like fuel cells, combined heat and power (CHP), and biomass. The model also ignores the ramp up/down constraints for fossil fuel generators.

## References

[1] U.S. Environmental Protection Agency, NRDC summary of EPA

**Appendix D (continued)**

clean power plan. carbon pollution standards for existing power plants, Tech. rep., U.S. Environmental Protection Agency, available at http://www.nrdc.org/air/pollution-standards/files/pollution-standards-epa-plan-summary.pdf. Accessed on November 18, 2014 (2014).

[2] U.S. Department of Energy, Smart grid research and developoment. Multy-year program plan (2010-2014)- september 2012 update, Tech. rep., U.S. Department of Energy, available at http://energy.gov/sites/prod/files/SG_MYPP_2012%20Update.pdf. Last accessed on December 5, 2013 (2012).

[3] A. Hawkes, M. Leach, Modelling high level system design and unit commitment for a microgrid, Applied energy 86 (7) (2009) 1253–1265.

[4] G.-C. Liao, Solve environmental economic dispatch of smart microgrid containing distributed generation system–using chaotic quantum genetic algorithm, International Journal of Electrical Power & Energy Systems 43 (1) (2012) 779–787.

[5] G. Kyriakarakos, D. D. Piromalis, A. I. Dounis, K. G. Arvanitis, G. Papadakis, Intelligent demand side energy management system for autonomous polygeneration microgrids, Applied Energy 103 (0) (2013) 39 – 51. doi:http://dx.doi.org/10.1016/j.apenergy.2012.10.011.

[6] O. Hafez, K. Bhattacharya, Optimal planning and design of a renewable energy based supply system for microgrids, Renewable Energy 45 (0) (2012) 7 – 15.

[7] W. Saad, Z. Han, H. V. Poor, T. Basar, Game-theoretic methods for the smart grid: an overview of microgrid systems, demand-side management, and smart grid communications, Signal Processing Magazine, IEEE 29 (5) (2012) 86–105.

[8] Y.-H. Chen, S.-Y. Lu, Y.-R. Chang, T.-T. Lee, M.-C. Hu, Economic analysis and optimal energy management models for microgrid systems: A case study in taiwan, Applied Energy.

[9] A. Del Real, A. Arce, C. Bordons, Combined environmental and economic dispatch of smart grids using distributed model predictive con-

**Appendix D (continued)**

trol, International Journal of Electrical Power & Energy Systems 54 (0) (2014) 65 – 76.

[10] A. Chaouachi, R. M. Kamel, R. Andoulsi, K. Nagasaka, Multiobjective intelligent energy management for a microgrid, IEEE Transactions on Industrial Electronics 60 (4) (2013) 1688–1699.

[11] A. Khodaei, M. Shahidehpour, Microgrid-based co-optimization of generation and transmission planning in power systems, IEEE Transactions on Power Systems 28 (2) (2013) 1582–1590.

[12] G. E. Asimakopoulou, A. L. Dimeas, N. D. Hatziargyriou, Leader-follower strategies for energy management of multi-microgrids, IEEE Transactions on Smart Grid 4 (4) (2013) 1909–1916.

[13] F. Feijoo, T. K. Das, Design of pareto optimal CO2 cap-and-trade policies for deregulated electricity networks, Applied Energy 119 (2014) 371–383.

[14] U.S. Department of Energy, Monetization of emissions reduction benefits, Tech. rep., U.S. DOE., available at https://www1.eere.energy.gov/buildings/appliance_standards /commercial/pdfs/dt_prelim_tsdch16.pdf. Accessed on December 18, 2013.

[15] R. G. Bell, D. Callan, More than meets the eye: The social cost of carbon in US climate policy, in plain english, Policy Brief.

[16] P. Avato, J. Coony, Accelerating clean energy technology research, development, and deployment: lessons from non-energy sectors, no. 138, World Bank-free PDF, 2008.

[17] M. Fampa, L. Barroso, D. Candal, L. Simonetti, Bilevel optimization applied to strategic pricing in competitive electricity markets, Computational Optimization and Applications 39 (2) (2008) 121–142.

[18] B. Hobbs, C. Metzler, J. Pang, Strategic gaming analysis for electric power systems: An MPEC approach, Power Systems, IEEE Transactions on 15 (2) (2000) 638–645.

[19] S. A. Gabriel, F. U. Leuthold, Solving discretely-constrained MPEC problems with applications in electric power markets, Energy Economics 32 (1) (2010) 3–14.

**Appendix D (continued)**


[20] R. Palma-Behnke, C. Benavides, E. Aranda, J. Llanos, D. Saez, Energy management system for a renewable based microgrid with a demand side management mechanism, in: Computational Intelligence Applications In Smart Grid (CIASG), 2011 IEEE Symposium on, IEEE, 2011, pp. 1–8.

[21] C. Battistelli, A. Conejo, Optimal management of the automatic generation control service in smart user grids including electric vehicles and distributed resources, Electric Power Systems Research 111 (0) (2014) 22 – 31. doi:http://dx.doi.org/10.1016/j.epsr.2014.01.008.

[22] L. Baringo, A. J. Conejo, Wind power investment: A benders decomposition approach, Power Systems, IEEE Transactions on 27 (1) (2012) 433–441.

[23] V. Nanduri, W. Otieno, Assessing the impact of different auction-based CO2 allowance allocation mechanisms, in: Power and Energy Society General Meeting, 2011 IEEE, IEEE, 2011, pp. 1–7.

[24] Z.-Q. Luo, J.-S. Pang, D. Ralph, Mathematical programs with equilibrium constraints, Cambridge University Press, 1996.

[25] D. Ralph, Y. Smeers, EPECs as models for electricity markets, in: Power Systems Conference and Exposition, 2006. PSCE'06. 2006 IEEE PES, IEEE, 2006, pp. 74–80.

[26] F. A. Mohamed, H. N. Koivo, Multiobjective optimization using mesh adaptive direct search for power dispatch problem of microgrid, International Journal of Electrical Power & Energy Systems 42 (1) (2012) 728–735.

[27] X. Hu, D. Ralph, Using EPECs to model bilevel games in restructured electricity markets with locational prices, Operations research 55 (5) (2007) 809–827.

[28] Y. Li, R. Kaewpuang, P. Wang, D. Niyato, Z. Han, An energy efficient solution: Integrating plug-in hybrid electric vehicle in smart grid with renewable energy, in: Computer Communications Workshops (INFOCOM WKSHPS), 2012 IEEE Conference on, IEEE, 2012, pp. 73–78.

**Appendix D (continued)**


[29] A. Colmenar-Santos, S. Campíñez-Romero, C. Pérez-Molina, M. Castro-Gil, Profitability analysis of grid-connected photovoltaic facilities for household electricity self-sufficiency, Energy Policy.

[30] U.S. Department of Energy, Financial assistance funding opportunity announcement, microgrid research, development, and system design, Tech. rep., U.S. Department of Energy, http://www.floridaenergy.ufl.edu/wp-content/uploads/DE-FOA-0000997-Microgrid.pdf. Last accessed on March 6, 2014 (2014).

[31] D. C. Montgomery, Design and analysis of experiments, John Wiley & Sons, 2008.

[32] European Commission, An EU budget for low-carbon growth, Tech. rep., U.S. Department of Energy, available at http://ec.europa.eu/clima/policies/finance/budget/docs/pr_2012_03_15_en.pdf. Released on November 19, 2013. Accessed on December 12, 2013 (2013).

[33] S. Abu-Sharkh, R. Arnold, J. Kohler, R. Li, T. Markvart, J. Ross, K. Steemers, P. Wilson, R. Yao, Can microgrids make a major contribution to UK energy supply?, Renewable and Sustainable Energy Reviews 10 (2) (2006) 78–127.

[34] O. Alsayegh, S. Alhajraf, H. Albusairi, Grid-connected renewable energy source systems: challenges and proposed management schemes, Energy Conversion and Management 51 (8) (2010) 1690–1693.

[35] H. Ren, W. Gao, A MILP model for integrated plan and evaluation of distributed energy systems, applied energy 87 (3) (2010) 1001–1014.

[36] M. Ruth, S. Gabriel, K. Palmer, D. Burtraw, A. Paul, Y. Chen, B. Hobbs, D. Irani, J. Michael, K. Ross, et al., Economic and energy impacts from participation in the regional greenhouse gas initiative: A case study of the state of maryland, Energy Policy 36 (6) (2008) 2279–2289.

[37] T. Limpaitoon, Y. Chen, S. Oren, The impact of carbon cap and trade regulation on congested electricity market equilibrium, Journal of Regulatory Economics (2011) 1–24.